Combination treatment effects of
BRAF (B-RAF proto-oncogene, serine/threonine kinase) inhibitors
and HSP90 (heat shock protein 90) inhibitors in BRAF-mutated colorectal cancer cell lines

Dissertation
zur Erlangung des akademischen Grades
Doktor der Medizin (Dr. med.)

vorgelegt
der Medizinischen Fakultät
der Martin-Luther-Universität Halle-Wittenberg

von Georg Heinrich Klose

Betreuer: Prof. Dr. Stephan Michael Feller, Halle (Saale)

Gutachter:
Prof. Dr. Stephan Michael Feller, Halle (Saale)
Prof. Dr. Karl-Heinz-Friedrich, Jena
Prof. Dr. Daniel Stange, Dresden

Eröffnung des Promotionsverfahrens: 04.07.2023
Verteidigung der Promotion: 10.04.2024

Abstract

In advanced colorectal cancer, frequently occurring BRAFV600 mutations are associated with an exceptionally bad prognosis and chemotherapy resistance. Unfortunately, because of many resistance mechanisms and in contrast to BRAFV600-mutated malignant melanoma, BRAF-mutated colorectal cancers escape from BRAF inhibition under monotherapy as well as combination therapy with another targeted agent or chemotherapy. A major part of known BRAF inhibitor resistance mechanisms are dependent on sufficient HSP90 function, which indicates HSP90 as a promising target in combination with BRAF inhibition for the treatment of BRAFV600-mutated colorectal cancer. However, preclinical data of combinational treatment of HSP90 inhibitors with BRAF inhibitors in BRAFV600-mutated colorectal cancer are still very scarce and clinical evidence for beneficial activity is missing.

To investigate, whether HSP90 inhibitors are potential partners in combination therapy with BRAF inhibitors, this thesis studies combination treatment effects of BRAF inhibitors and HSP90 inhibitors in BRAFV600-mutated colorectal cancer cells. Therefore, different compounds, different cell lines and different preclinical approaches such as two-dimensional monolayer cell culture resazurin assay, three-dimensional soft agar anchorage-independent growth assay and finally, mouse xenografts were used. The latter were performed as a collaboration.

All in all, BRAF inhibitors and HSP90 inhibitors were shown to act in a synergistic or additive manner. The synergistic or additive combination treatment effects were almost consistent in all used BRAFV600-mutated colorectal cancer cell lines through all used approaches. This confirms HSP90 as potential target for combination treatment in BRAFV600-mutated colorectal cancer.

Thus, this thesis contributes to preclinical evidence for the approach combining HSP90 inhibitors with BRAF inhibitors in BRAFV600-mutated colorectal cancer treatment, which is a prerequisite for future clinical trials. Simultaneously, it encourages to further investigate HSP90 inhibitors and BRAF inhibitors combination treatment effects at the proteomic level for a deeper understanding of the underlying mechanisms.

Klose, Georg Heinrich: Combination treatment effects of BRAF (B-RAF proto-oncogene, serine/threonine kinase) inhibitors and HSP90 (heat shock protein 90) inhibitors in BRAF-mutated colorectal cancer cell lines, Halle (Saale), Univ., Med. Fak., Doc. Thesis, 68 pages, 2023

Referat

Kolorektale Karzinome zeigen häufig BRAFV600 Mutationen. In fortgeschrittenen Stadien sind diese assoziiert mit einer äußerst ungünstigen Prognose und mit schlechtem Ansprechen auf Chemotherapie. In Patienten mit BRAFV600 mutiertem malignen Melanom konnte die Prognose durch Mono- beziehungsweise Kombinationstherapie mit BRAF-Inhibitoren wesentlich verbessert werden. Aufgrund verschiedenster Resistenzmechanismen ist dies beim BRAFV600 mutierten kolorektalen Karzinom bisher nicht gelungen. Da ein Großteil der BRAF Inhibitor-Resistenzmechanismen von einer regelhaften HSP90-Funktion abhängig ist, könnte die Inhibition von HSP90 in Kombination mit BRAF Inhibitoren einen wertvollen therapeutischen Ansatz darstellen. Allerdings ist die präklinische Datenlage bislang ungenügend und klinische Daten fehlen völlig.

Daher wurden im Rahmen dieser Dissertation die Behandlungseffekte von verschiedenen BRAF- und HSP90-Inhibitoren in Kombination an verschiedenen kolorektalen Karzinomzelllinien mit BRAFV600 Mutation mittels verschiedener experimenteller Methoden untersucht, z.B. im zweidimensionalen Einzelschicht-Zellkultur Resazurin Versuch und im dreidimensionalen Weichagar verankerungsunabhängigen Wachstumsassay. Zusätzlich wurde ein Xenotransplantatversuch an Mäusen durch eine kollaborierende Arbeitsgruppe durchgeführt.

Insgesamt konnte eine synergistische oder zumindest additive Interaktion in der Wirkung der Kombination von HSP90- und BRAF-Inhibitoren gezeigt werden. Dabei zeigten sich die synergistischen bzw. additiven Effekte nahezu durchgängig in allen untersuchten BRAFV600 mutierten Zelllinien in den verschiedenen experimentellen Methoden und mit verschiedenen Inhibitoren. Dies bestätigt eine HSP90-Inhibition in Kombination mit BRAF-Inhibition als potentiellen Therapieansatz im BRAFV600 mutierten kolorektalen Karzinom.

Somit trägt diese Dissertation dazu bei, die Kombination von HSP90- und BRAF-Inhibitoren im BRAFV600 mutierten kolorektalen Karzinom einen Schritt weiter in Richtung klinischer Erprobung zu führen. Gleichzeitig regt sie eine weiterführende und vertiefende Forschung auf proteomischer Ebene an, um die Wirkungsmechanismen in der Kombinationstherapie besser zu verstehen.

Klose, Georg Heinrich: Combination treatment effects of BRAF (B-RAF proto-oncogene, serine/threonine kinase) inhibitors and HSP90 (heat shock protein 90) inhibitors in BRAF-mutated colorectal cancer cell lines, Halle (Saale), Univ., Med. Fak., Diss., 68 Seiten, 2023

Contents

Abbreviations

14-3-3	14-3-3 protein, member of phosphoserine-/phosphothreonine-binding proteins
2D	two-dimensional
3D	three-dimensional
5YOS	five year overall survival
A	17-(Allylamino)-17-demethoxygeldanamycin
ACF	aberrant crypt foci
AKT	protein kinase B
AMPK	AMP-activated protein kinase
APC	adenomatous polyposis coli
ATP	adenosine triphosphate
ARAF	A-RAF proto-oncogene, serine/threonine kinase
Bliss-CI	Bliss-combination index
BMF	BCL2 modifying factor
BRAF	B-RAF proto-oncogene, serine/threonine kinase
BRAFi	BRAF inhibitor, plural: BRAFis
BRAFV600E	mutant BRAF at site 600 with glutamic acid instead of valine
Caco-2	BRAFwt CRC cell line
CI	confidence interval
CIMP	CpG island methylator phenotype
CIN	chromosomal instability
CK2	casein kinase 2
CO_2	carbon dioxide
COLO 201	BRAFmut CRC cell line
COT	mitogen-activated protein kinase kinase kinase 8
CpG	5'—cytosine—phosphate—guanine—3'
CR	conserved region
CRAF	RAF-1 proto-oncogene, serine/threonine kinase
CRC	colorectal cancer
Ctrl	control
D	dabrafenib
DFG-motif	aspartic acid-phenylalanine-glycine-motif
DMEM	Dulbecco's modified eagle medium
DNA	deoxyribonucleic acid
E	treatment effect
EDTA	ethylenediaminetetraacetic acid
EGF	epidermal growth factor
EGFR	epidermal growth factor receptor
EGFRi	EGFR inhibitor, plural: EGFRis
EIF4F	eukaryotic translation initiation factor 4F
ELK1	ETS transcription factor ELK1
EMT	epithelial-mesenchymal transformation
ERK	extracellular signal-regulated kinase

FBS	fetal bovine serum
FDA	food and drug administration
FGFR	fibroblast growth factor receptor
FOS	Finkel–Biskis–Jinkins murine osteosarcoma viral oncogene homolog
GCHP	goblet cell rich hyperplastic polyp
GDP	guanosine diphosphate
GRB2	growth factor receptor-bound protein 2
GSK3β	glycogen synthase kinase 3 β
GTP	guanosine triphosphate
H	HSP990
HER2/3	human epidermal growth factor receptor 2/3
HGF	hepatocyte growth factor
HGFR	hepatocyte growth factor receptor
HNPCC	hereditary nonpolyposis colorectal cancer
HRAS	Harvey rat sarcoma viral oncogene homolog
HSA	highest single agent
HSP70	heat shock protein 70
HSP90	heat shock protein 90
HSP90i	HSP90 inhibitor, plural: HSP90is
HT-29	BRAFmut CRC cell line
IC_{50}	half effective inhibitory concentration
IGF1R	insulin like growth factor 1 receptor
IGFBP7	insulin-like growth factor-binding protein 7
JNK	c-Jun N-terminal kinase
KIT	proto-oncogene KIT
KRAS	Kirsten rat sarcoma viral oncogene homolog
LOH	loss of heterozygosity
M	metastasis stage
MAPK	mitogen-activated protein kinase
MEK	MAPK/ERK kinase
MEKi	MEK inhibitor, plural: MEKis
MLH1	mutL homolog 1
MMR	mismatch repair
MSH2	mutS homolog 2
MSH6	mutS homolog 6
MSI	microsatellite instability
MSS	microsatellite stability
mTOR	mechanistic target of rapamycin (a kinase)
mut	mutated
MVHP	micro vesicular hyperplastic polyp
MYC	avian myelocytomatosis viral oncogene homolog
N	lymph node metastasis stage

OS	overall survival
OX-CO-1	BRAFmut CRC cell line
p16	cyclin dependent kinase inhibitor 2A
p53	tumour protein p53
PBS	phosphate buffered saline
PD1	programmed cell death protein 1
PDGFR	platelet-derived growth factor receptor
Pen-Strep	penicillin-streptomycin
PI3K	phosphatidylinositol-4,5-bisphosphate 3-kinase
PKC	protein kinase C
PMS2	post meiotic segregation increased 2
PP5	protein phosphatase 5
PTEN	phosphatase and tensin homolog
RAS	rat sarcoma viral oncogene homolog
RBD	RAS-binding domain
RET	RET-proto-oncogene
RKIP	RAF kinase inhibitor protein
RKO	BRAFmut CRC cell line
RNF43	ring finger protein 43
RTK	receptor tyrosine kinase
SH	protooncogene SRC homolog
SHP2	SH2 domain-containing protein tyrosine phosphatase 2
SMAD2/4	mothers against decapentaplegic homolog 2/4
SOS	son of sevenless
SRC	SRC proto-oncogene
SSL	sessile serrated lesion
T	tumour stage
TGFβ	transforming growth factor beta
TIE2	tunica interna endothelial cell kinase 2
TNM	tumour-nodes-metastasis
TSA	traditional serrated adenoma
UICC	Union for International Cancer Control
V	vemurafenib
VEGF	vascular epithelial growth factor
VEGFR	VEGF receptor
WHO	World Health Organisation
WNT	wingless-type mouse mammary tumour virus integration site family
wt	wild type

1 Introduction

1.1 Epidemiology and risk factors of CRC

Colorectal cancer (CRC) is one of the most frequent and most lethal cancer entities in humans. More than 61.000 new cases and over 25.000 CRC-related deaths per year make CRC the third most common cancer type among men, the second most common among women and the third most lethal cancer in both sexes in Germany (Robert Koch-Institut and Gesellschaft der epidemiologischen Krebsregister in Deutschland e.V. 2017). Approximately 1.8 million patients worldwide develop CRC and each year 860.000 patients die suffering from CRC (Bray et al. 2018). Evitable risk factors are alcohol intake (Fedirko et al. 2011), obesity (Renehan et al. 2008), physical inactivity (Shaw et al. 2018), poor diet with low fibre intake (Dahm et al. 2010; Park et al. 2005) and excessive consumption of red and processed meat (Bouvard et al. 2015), low Vitamin D levels (McCullough et al. 2019) and smoking (Walter et al. 2014). Besides evitable risk factors, sporadic CRCs show family clustering as inevitable risk factor: 20-30% of CRC patients have a positive family history (Testa et al. 2018). Additionally, several inherited syndromes leading to hereditary CRC are known. They represent 2-5% of all CRC cases (Jasperson et al. 2010). The most common syndromes are hereditary nonpolyposis colorectal cancer (HNPCC) syndrome on the one hand, synonymously called Lynch syndrome, with a germ line mutation in the mismatch repair (MMR) system leading to a lifetime CRC risk of 50-80%. On the other hand, familial adenomatous polyposis leads to 100% lifetime CRC risk, because of a germ line mutation in the APC (adenomatous polyposis coli) gene (Jasperson et al. 2010).

1.2 Cancerogenesis of CRC

1.2.1 Histological classification

CRCs are believed to develop from precursor lesions. The World Health Organisation (WHO) classification of non-malignant epithelial colorectal lesions distinguishes between adenomas and serrated lesions. To avoid confusion between adenomas and different subtypes of serrated lesions, adenomas are also named conventional adenomas. Conventional adenomas are non-malignant polypous lesions of the colon mucosa showing at least low-grade dysplasia and a tubular, villous or tubulovillous architecture with lacking 'saw-tooth' patterns. Conventional adenomas represent approximately 90% of non-malignant polypous colonic lesions (Mirzaie et al. 2016). In contrast, serrated lesions show 'saw tooth' patterns of their epithelium with or without dysplasia (International Agency for Research on Cancer 2019). They are subtyped into hyperplastic polyps, sessile serrated lesions (SSL) with or without dysplasia (previously termed sessile serrated adenoma/polyp) and traditional serrated adenomas (TSA), representing 60-75%, 20-30% and < 1% of all serrated polyps, respectively (IJspeert et al. 2015).

According to their histology, hyperplastic polyps are further subtyped into microvesicular hyperplastic polyps (MVHP) (60%), goblet cell rich hyperplastic polyps (30%) and mucin poor hyperplastic polyps (rare) (IJspeert et al. 2015). The earliest known precursor lesions are aberrant crypt foci, which bear initial molecular alterations and which show very focal morphological anomalies of single crypts (Takayama et al. 1998). According to current WHO classification from 2019, CRCs are graded, using a two-tiered grading system (low- and high-grade), which replaces the formerly three-tiered system (grade 1, grade 2 and grade 3). Low-grade CRCs (formerly grade 1 and 2) are characterised by a retained glandular differentiation, whereas high-grade CRCs show complex histoarchitectural features, like solid growth or signet ring differentiation (International Agency for Research on Cancer 2019).

1.2.2 Adenoma-carcinoma sequence/CIN-pathway

Since Wolff and Shinya developed the fibre optic flexible colonoscope with interventional ability in 1969 (Wolff and Shinya 1973), colonoscopy and polypectomy of the entire colon became feasible. This led to deeper understanding of colorectal cancerogenesis. Observing precancerous lesions and CRCs at different levels of progression, conventional adenomas could be considered to be the common precancerous lesion, which turns to CRC (Muto et al. 1975). However, the mechanisms of cancerogenesis at molecular level were almost unknown. 1988 Vogelstein and colleagues introduced a revolutionary model: the adenoma-carcinoma sequence (***Figure 1***). They describe the stepwise accumulation of different mutations in enterocytes at different points of adenoma and CRC development. The first step is the loss of function of APC, a tumour suppressor gene of the WNT-pathway (wingless-type mouse mammary tumour virus integration site family) (Vogelstein et al. 1988). It is consensus that isolated loss of APC can initiate conventional adenoma growth, but not CRC. Therefore, additional mutations were required. Since APC is also involved in chromosome segregation, loss of APC is thought to induce chromosomal instability (CIN), which makes cell genome more susceptible to the development of aneuploidy, loss of heterozygosity and subchromosomal genomic alterations (Pino and Chung 2010). Therefore, further mutations can easily occur. The major genes affected are KRAS (Kirsten rat sarcoma viral oncogene homolog), p53 (tumour protein p53) and PI3K (phosphatidylinositol-4,5-bisphosphate 3-kinase) with almost 50%, 65% and 15% in all CRCs respectively (Loree et al. 2018). With an increasing number of mutations, CIN increases as well and more and more mutations accumulate in affected cells (Pino and Chung 2010). Mutations of KRAS, p53, PI3K and many more drive the precancerous lesion into cancer. Because of the major importance of CIN, the term 'CIN pathway' is used synonymously for the classical adenoma-carcinoma-sequence pathway.

1.2.3 Serrated pathway

Most CRCs follow the CIN-pathway, typically developing from conventional adenomas (Muto et al. 1975). Therefore, this type of adenoma was considered to be the only precancerous type for decades, while serrated lesions like hyperplastic polyps were believed to stay benign with no need of excision (IJspeert et al. 2015). This belief has radically changed in the past two decades (IJspeert et al. 2015). It is now known, that up to 30% of CRC develop from serrated lesions (International Agency for Research on Cancer 2019). Since serrated lesions usually do not follow CIN pathway, another major pathway of cancerogenesis in CRC was postulated: the serrated pathway (***Figure 1***). In contrast to the CIN pathway, BRAF (murine sarcoma viral oncogene homolog B) mutations rather than APC or KRAS mutations seem to play the major role in serrated lesions (Clancy et al. 2013). They were found in up to 85% of MVHPs and in up to 100% of SSLs, suggesting to initiate the serrated pathway (IJspeert et al. 2015). However, similar to APC loss in the CIN pathway, more events are required to drive the lesion into cancer. One key mechanism is epigenetic silencing by deoxyribonucleic acid (DNA) hypermethylation of 5'—cytosine—phosphate—guanine—3' (CpG) rich promoter regions of crucial tumour suppressor genes resulting in CpG island methylator phenotype (CIMP) (IJspeert et al. 2015). In normal cells, CpG island methylation regulates the expression of genes. Aberrant CpG island methylation of promoter regions of tumour suppressor genes causes silencing of tumour suppressor genes driving precancerous lesions into CRC and progressing CRC (IJspeert et al. 2015). Depending on the grade of hypermethylation, CIMP can be classified in CIMP-negative, CIMP-low and CIMP-high (Jia et al. 2016). The mechanism of CIMP development is not yet clear (IJspeert et al. 2015). However, mutated BRAF is associated with CIMP-high in 77% of cases, but not with CIMP-negative phenotypes. So, CIMP seems to be initiated by mutated BRAF (Fang et al. 2014). If members of the MMR system, such as MLH1 (mutL homolog 1), MSH2 (mutS homolog 2), MSH6 (mutS homolog 6) or PMS2 (postmeiotic segregation increased 2), were silenced, the MMR becomes insufficient (Zoratto et al. 2014). Then, DNA damage, typically occurring in microsatellites during DNA replication, cannot be repaired anymore. Microsatellites are short tandem repeats of one to six nucleotides, which are interindividually different, but intraindividually uniform (Zoratto et al. 2014). During DNA replication, microsatellites get mutated very frequently, because polymerases tend to slip on them, producing prolonged or shortened replicates, and thus resulting in frame shift mutations (Zoratto et al. 2014). Without sufficient MMR, these replication failures remain uncorrected, leading to microsatellites varying in length, so called microsatellite instability (MSI) (Zoratto et al. 2014). Like CIMP, MSI is graded in MSI-high, MSI-low and microsatellite stability (MSS) depending on the number of affected microsatellite loci in PCR or the lack of MLH1, MSH2, MSH6 or PMS2 expression (Battaglin et al.

2018). MSI-high CRCs usually are right sited, poorly differentiated and they show mucinous histology and lymphocyte infiltration (Battaglin et al. 2018). Fortunately, MSI-high CRC are associated with an excellent prognosis, except in relapse (Battaglin et al. 2018). Thus, MSI testing has become implemented in clinic diagnostics already. In sporadic CRC, 80-90% of MSI cases are caused by CIMP (Battaglin et al. 2018). In up to 25% of all MSI CRCs, the MMR deficiency is caused by a germ line mutation of MLH1 as part of the HNPCC syndrome (Battaglin et al. 2018). HNPCC syndrome patients inescapably develop MSI CRC, so MSI screening and genetic diagnostics are crucial for detecting HNPCC syndrome patients and their relatives (Battaglin et al. 2018).

Since the different cancerogenesis pathways are not exclusive, CRCs may show properties of different pathways in the same tumour complicating subtyping (Testa et al. 2018). However, stepwise models lack to explain the striking intra- and intertumour heterogeneity observed in CRC. Therefore, further models of cancerogenesis have been established, like the Big-Bang-Model (Sottoriva et al. 2015) or the Punctuated Equilibrium Model (Sievers et al. 2017).

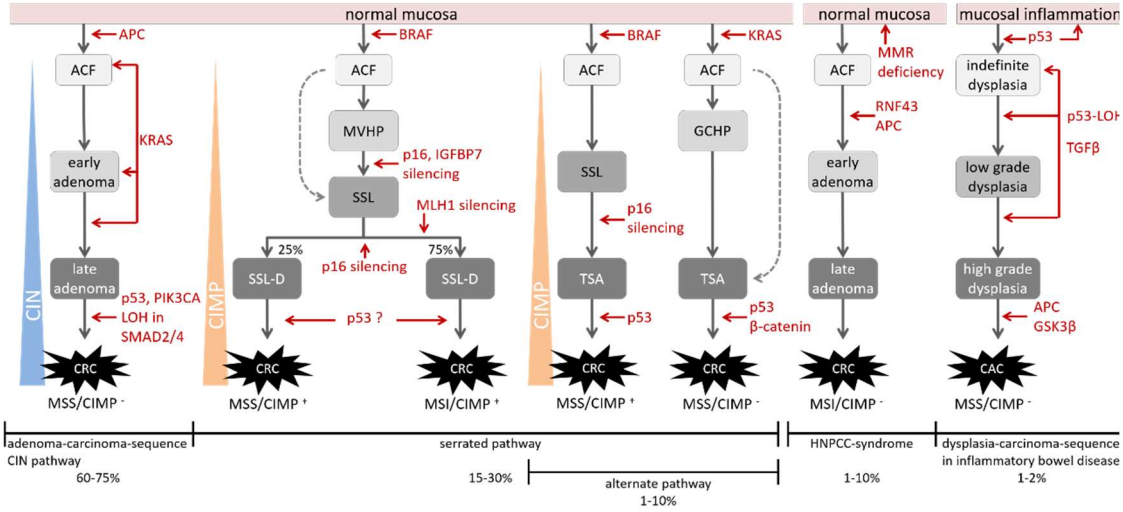

Figure 1: *Simplified schematic of stepwise cancerogenesis.*
Abbreviations: aberrant crypt foci (ACF), CpG island methylator phenotype (CIMP), chromosomal instability (CIN), colorectal carcinoma (CRC), goblet cell rich hyperplastic polyp (GCHP), hereditary nonpolyposis colorectal cancer (HNPCC), loss of heterozygosity (LOH), mismatch repair system (MMR), microsatellite instability (MSI), microsatellite stability (MSS), microvesicular hyperplastic polyp (MVHC), sessile serrated lesion without/with dysplasia (SSL/SSL-D), traditional serrated adenoma (TSA), protein names (please see section Abbreviation, pages III-V)
After Testa et al. 2018, modified, including contents from IJspeert et al. 2015 and International Agency for Research on Cancer 2019.

1.3 Molecular classification of CRC

Since CRC is a highly heterogeneous disease with different locations, different molecular alterations, different and mixed ways of cancerogenesis, different outcomes, different drug response etc., many efforts have been taken to classify CRCs regarding different criteria like histological pattern, mutational status, MSI status etc. (Jordan 2018). However, these classifications do not cover the broad spectrum of CRC sufficiently. In 2015, Guinney and colleagues developed a classification based on six independent classification systems, revealing four different consensus molecular subtypes (CMS), which are widely accepted. These four CMS groups cover 87% of all CRC, the remaining 13% are overlapping mixtures of CMS groups or indeterminate (Guinney et al. 2015). Even within the CMS groups, CRCs show heterogeneous characteristics, but, interestingly, in each group predominant properties are typical within the group.

For the most part, CMS1 CRCs are right sided, more frequent in women, BRAFV600 mutated (mut), MSI as well as CIMP high and they show mucinous histological patterns (Dienstmann et al. 2017; Guinney et al. 2015). Usually, CMS1 CRCs follow the serrated pathway, developing from SSLs as mentioned above (Jordan 2018). Patients with CMS1 CRCs commonly have a good prognosis, unless they get a relapse. In that case, the prognosis shrinks down to 9 months survival after relapse, which is the worst in all CMS groups (Guinney et al. 2015). CMS1 CRCs show high lymphocytic infiltration due to a particular high immune activation, leading to direct clinical implication (Guinney et al. 2015). So in 2017, the tumour immunologic drug pembrolizumab, which is an anti-PD1 (programmed cell death protein 1) antibody, was approved by the food and drug administration (FDA) for the treatment of metastasized MSI high CRC, commonly grouped in CMS1 (Marcus et al. 2019). Because of MSI status and immunologic activity, the term 'MSI immune subtype' can be used synonymously (Dienstmann et al. 2017). By contrast, the CIN pathway splits up into different CMS groups.

CMS2 CRCs, also known as 'canonical subtype', commonly develop from conventional adenomas following the CIN ('canonical') pathway (Dienstmann et al. 2017). They were characterized by intermediately differentiated epithelial low-grade (formerly grade 2) histological patterns, CIN, MSS, negative for CIMP, frequent APC and p53 mutations (Dienstmann et al. 2017; Guinney et al. 2015). Typically, CMS2 CRCs are left sided, more frequent in men than in women and patients have a good prognosis (Guinney et al. 2015). Up-regulation of WNT/MYC (avian myelocytomatosis viral oncogene homolog) signalling pathway is very common (Guinney et al. 2015).

CMS3 CRCs are predominantly characterised by metabolic deregulation (Guinney et al. 2015). KRAS, APC, p53 and PI3K mutations are frequent in CMS3 CRCs (Guinney et al. 2015). Especially KRAS is considered to be linked to deregulated metabolism in cancer (Yun et al. 2009). Therefore, CMS3 is also named 'metabolic subtype' (Dienstmann et al. 2017). Similar to CMS2, CMS3 CRCs seem to develop from conventional adenoma as well (Dienstmann et al. 2017). However, since 16% of CMS3 CRCs show MSI, they are not restricted to MSS (Guinney et al. 2015).

CMS4 CRCs are associated with the worst overall survival (OS) of all subgroups. The five year overall survival (5YOS) after diagnosis is reduced by more than 10% compared to the other CMS groups (Guinney et al. 2015). CMS4 CRCs are characterised by histological low-grade (formerly grade 2) patterns with high-grade desmoplasia, the stromal reaction by surrounding fibroblasts to the invasive cancer (Dienstmann et al. 2017). Tumours are usually MSS, CIN and negative for CIMP (Guinney et al. 2015). Pathways responsible for EMT (epithelial-mesenchymal transformation), such as TGFβ (transforming growth factor beta), integrins and VEGF (vascular epithelial growth factor) are frequently up-regulated in CMS4 CRCs (Guinney et al. 2015). Interestingly, TGFβ seems to determinate the further development of serrated polyps. If TGFβ signalling becomes hyperactivated, SSLs run into CMS4. Otherwise they become CMS1 CRC (Fessler et al. 2016). In contrast to immunogenic CMS1 CRCs, CMS4 evade the immune system. By up-regulation of immunosuppressive signalling pathways, such as TGFβ, the tumour surrounding leukocyte infiltration is characterised by immunosuppressive cells like regulatory T-cells protecting CMS4 CRCs from immunological attacks (Becht et al. 2016).

Currently, the CMS system is probably the most advanced characterisation of CRC. It considers the enormous heterogeneity of CRC integrating molecular, morphologic and prognostic aspects.

1.4 Physiological mechanism of BRAF action

1.4.1 The MAPK pathway

BRAF is a serine/threonine protein kinase of the RAF family and plays a major role in classical MAPK (mitogen-activated protein kinase)/ERK (extracellular signal-regulated kinase) signalling (Morrison 2012). This pathway is very important in mammalian cells for the conversion of extracellular signals, such as receptor tyrosine kinase (RTK)/RTK-ligand interactions, into potentiated and fine-tuned intracellular signals at the cytosolic and nuclear levels, which may regulate cell growth, differentiation, proliferation and/or survival (Zhang and Liu 2002). The MAPK/ERK pathway underlies many regulations and is linked to multiple other signalling pathways of the cellular signalling machinery. So far, its complexity is not entirely understood.

As an example, a RTK like EGFR (epidermal growth factor receptor) binds with its extracellular domain to its ligand like EGF (epidermal growth factor) and hence becomes oligomerised and activated by autophosphorylation at its intracellular tyrosine residues (***Figure 2***) (Dawson et al. 2005; Kozer et al. 2014). Once activated, the preformed intracellular complex of GRB2 (growth factor receptor-bound protein 2), an adaptor protein composed of SRC (SRC proto-oncogene) homology (SH) 2 and SH3 domains, and the GTP (guanosine diphosphate)/GDP (guanosine triphosphate) exchange factor SOS (son of sevenless) can bind to the phosphorylated tyrosine residues on EGFR through the GRB2 SH2 domain, thereby recruiting themselves to the plasma membrane (Margolis and Skolnik 1994). Now RAS (rat sarcoma viral oncogene homolog) can interact with SOS, which activates RAS by exchanging GDP for GTP. GTP-loaded RAS dimerises and activates RAF (Güldenhaupt et al. 2012; Lin et al. 2014; Nan et al. 2015). The detailed mechanisms of RAF activation, especially for BRAF, are explained below. Activated RAF in turn phosphorylates MEK1/2 (MAPK/ERK kinase 1/2) at serine residues to activate MEK1/2, which subsequently activates ERK1/2 (Morrison 2012). ERK1/2, also known as MAPK1/2, are the main effector serine/threonine kinases with more than 600 substrates in cytoplasm and nucleus (Maik-Rachline et al. 2019; Morrison 2012). For instance, important ERK1/2 targets are MYC, FOS (Finkel–Biskis–Jinkins murine osteosarcoma viral oncogene homolog) and cyclin D1, which are deregulated in cancer and very frequently acting as oncogenes. MYC is a transcription factor important for cell growth, proliferation, apoptosis, metabolism, stem cell renewal and differentiation (Eischen et al. 2001; Miller et al. 2012; Murphy et al. 2005). MYC phosphorylation by ERK1/2 protects MYC against degradation, so it accumulates in nucleus, leading to enhanced activity, when ERK1/2 is active (Maik-Rachline et al. 2019). FOS is also a transcription factor important for cell proliferation, differentiation, apoptosis, angiogenesis, EMT and metastasis (Ashida et al. 2005; Marconcini et al. 1999; Qu et al. 2019). ERK1/2 phosphorylates and activates ELK1 (ETS transcription factor ELK1), which acts as transcription factor, increasing FOS expression. Unless FOS becomes phosphorylated by ERK1/2, it is rapidly degraded. Since FOS is expressed only after a significant delay, long term activity of ERK1/2 is required for FOS phosphorylation, which is the case during aberrant MAPK/ERK signalling (Maik-Rachline et al. 2019). Through the suppression of cyclin D1 inhibition, ERK1/2 also regulates the cell cycle, leading to cell growth and proliferation (Fang and Richardson 2005; Maik-Rachline et al. 2019).

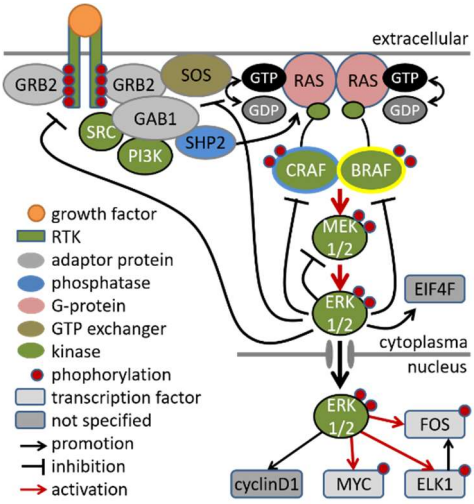

Figure 2: *Simplified MAPK pathway, after Morrison 2012, modified.*
Abbreviations: guanosine di/triphosphate (GDP/GTP), receptor tyrosine kinase (RTK), protein names (please see section Abbreviation, pages III-V)

1.4.2 BRAF regulation

All RAF family members, namely ARAF (A-RAF proto-oncogene, serine/threonine kinase), BRAF and CRAF (RAF-1 proto-oncogene, serine/threonine kinase), are structured in two domains and three conserved regions (CR): the N-terminal regulatory domain containing CR1 and CR2 and the C-terminal kinase domain containing CR3 (Terrell and Morrison 2019). CR1 contains the RAS-binding domain (RBD), which binds to RAS during its activation, and the cysteine rich domain (CRD) (Terrell and Morrison 2019). CR2 is rich in serine/threonine residues and works as a flexible hinge region between CR1 and CR3 (Dankner et al. 2018). CR3 contains a negatively charged regulatory region, the P-loop, an αC helix, the activation segment, the dimerising interface and a aspartic acid-phenylalanine-glycine-motif (DFG-motif), which are all important for the regulation of BRAF function (Dankner et al. 2018). The subsequently detailed mechanisms of RAF regulation focus on BRAF, but the regulation of ARAF and CRAF is very similar.

To avoid dangerous aberrant activation, BRAF activity is tightly regulated by several mechanisms at the levels of protein conformation, phosphorylation and interaction with other proteins. BRAF exists as monomer in an inactive conformation and dimerisation is required for its activation (Terrell and Morrison 2019). In its inactive form, the BRAF CR1 region binds with its RBD and CRD to CR3 blocking the kinase domain (Terrell and Morrison 2019). Moreover, negative regulatory sites of the kinase domain are phosphorylated, inhibiting BRAF activity (Terrell and Morrison 2019). The P-loop, important for ATP (adenosine triphosphate) binding, interacts strongly with the activation segment, so an inhibiting conformation is stabilized (Dankner et al. 2018). The αC helix also interacts with the activation segment, covering the dimerising interface.

Furthermore the DFG-motif blocks the catalytic activity (Dankner et al. 2018). In addition to this autoinhibition, several proteins bind to BRAF to protect downstream targets against accidental activation. 14-3-3 (14-3-3 protein, member of phosphoserine-/phosphothreonine-binding proteins) binds CR2 and the kinase domain of autoinhibited BRAF (McPherson et al. 1999). Interestingly, MEK1, the downstream target of BRAF, also forms a complex with inactive BRAF monomers in a 'face-to-face' manner, blocking catalytic activity of both (Haling et al. 2014). CRAF forms a similar inhibitory complex with RKIP (RAF kinase inhibitor protein) rather than MEK1, which becomes disrupted through RKIP phosphorylation by PKC (protein kinase C), activating CRAF (Corbit et al. 2003). Finally, HSP90 (heat shock protein 90) binds to inactive BRAF, stabilizing its inhibited conformation (Schulte et al. 1995; Terrell and Morrison 2019).

To fully activate RAF, all the protecting inhibition mechanisms have to be removed. BRAF activation is started by binding to activated RAS with its RBD (Herrmann et al. 1995). However, the most important mechanism appears to be the localisation of BRAF to cell membrane, rather than RAS binding itself (Terrell and Morrison 2019). The favourable position of BRAF in proximity to membrane gets stabilised by interaction of CRD with lipids bound to RAS or directly with phospholipids of the cell membrane (Travers et al. 2018). Due to the interaction with RAS and the cell membrane, 14-3-3 dissociates from CR2, exposing this region to the phosphatase activity of several relevant protein phosphatases (McPherson et al. 1999). In addition, to enable a conformational change and dimerisation, sites within the negatively charged regulatory region of CR3 need to be phosphorylated, leading to more negative charges. These are driven by CK2 (casein kinase 2) in case of BRAF, or SRC family kinases in the cases of ARAF and CRAF (Terrell and Morrison 2019). Thus, homodimerisation or heterodimerisation becomes possible, by side-to-side contact of the different RAF family members. The most common BRAF/CRAF heterodimers reach the highest catalytic activity (Cope et al. 2018; Terrell and Morrison 2019; Weber et al. 2001). The exact mechanism and the stabilisation of dimerisation remains poorly understood. However, it seems that 14-3-3, while stabilising the inactive conformation, may also stabilise the formed dimer (Weber et al. 2001). For full kinase activity, a final conformational change, exposing the catalytic cleft, is required. In BRAF, two phosphorylations in the activation segment of CR3 immediately adjacent to site 600, namely threonine 599 and serine 602, bring in the negative charges necessary to conduct this change in conformation (Cope et al. 2018; Terrell and Morrison 2019). Interestingly, despite the inhibitory effect of the MEK1/BRAF complex mentioned above, MEK1 seems to promote autophosphorylation of the activation segment of BRAF (Cope et al. 2018). Like 14-3-3, HSP90 stabilises the inactive and the active BRAF conformations as well (da Rocha Dias et al. 2005; Terrell and Morrison 2019).

Once activated, BRAF phosphorylates MEK1/2 in a very specific manner at serine residues, leading to the dissociation of MEK1/BRAF complex and to MEK1/2 activation (Cope et al. 2018; Haling et al. 2014).

To shut off signalling, several mechanisms, leading to a termination of RAF activity, can be employed. Importantly, a negative feedback loop by ERK phosphorylating RAS at serine/threonine sites interrupts the interaction of RAF and RAS. RAF dissociates into monomers and detaches from cell membrane, leading to inactivation (Terrell and Morrison 2019). Additionally, dephosphorylation of the negatively charged regulatory region by PP5 (protein phosphatase 5) and autophosphorylation of negative regulating sites abolish RAF activity. Finally, RAF becomes stepwise recycled to its initial pre-signalling conditions (Terrell and Morrison 2019).

1.5 Pathological mechanism of mutated BRAF action

More than 200 different BRAF mutations are known, leading to a more or less aberrant BRAF function (Yao et al. 2017). Some years ago, BRAFV600E (mutant BRAF at site 600 with glutamic acid instead of valine) was considered to represent more than 90% of BRAF mutations (Holderfield et al. 2014). However, since next generation sequencing became more established in clinic, the number of known BRAF mutations increased rapidly. In metastatic CRC, 22% of BRAF mutations occur at nonV600 sites (Jones et al. 2017). Recently, three distinct groups of BRAF mutations have been identified, by considering kinase activity, RAS-dependency and dimerisation-dependency compared to BRAF wild type (wt). Mutations of class 1 occur in the activation segment at V600 and are characterised by high kinase activity and constitutive RAS- and dimerisation-independent activation. Class 2 mutations typically occur in the P-loop or activation segment, leading to RAS-independent but dimerisation-dependent activation with intermediate to high kinase activity. Finally, class 3 mutations typically occur in the P-loop or the DFG-motif, leading to low or dead kinase activity and RAS- and dimerisation-dependent signalling by cross-activation of the second protomer in the dimer (Dankner et al. 2018; Yao et al. 2015; Yao et al. 2017). Since class 1 and especially BRAFV600E are still the most frequent and most important BRAF mutations in CRC (Dankner et al. 2018), the following description of mechanism of action is focused on class 1.

Position 600 is in the close proximity to the physiologically autophosphorylated threonine 599 and serine 602. The replacement of the uncharged amino acid valine at position 600 by a charged amino acid like glutamic acid, aspartic acid, lysine, or arginine, as common in class 1 BRAF mutations, mimics the phosphorylation that usually occurs during activation (Dankner et

al. 2018). In BRAFV600E, glutamic acid 600 forms a salt bridge with lysine 507 within the αC helix, which enables the active conformation of the αC helix, mimicking the conformational change during dimerisation (Lavoie and Therrien 2015). Thus BRAFV600E evades all feedback mechanisms and autoinhibition mechanisms. BRAF gets independently activated as monomer with a more than 500-fold kinase activity compared to BRAFwt, leading to strikingly increased downstream signalling (Dankner et al. 2018; Wan et al. 2004). Because of the continuous MAPK activation, ERK becomes long-term hyperactivated, which leads to oncogenic alteration of ERK target's activity driving cancerogenesis (Maik-Rachline et al. 2019).

1.6 BRAF mutation in CRC

Approximately 10% of CRCs are BRAFmut, with V600 as the most frequent mutation site (Dankner et al. 2018; Guinney et al. 2015). BRAFV600 mutations are preferentially associated with MSI-high, right-sided location, higher age at diagnosis, female sex, mucinous histological pattern, smoking (Clancy et al. 2013; Gonsalves et al. 2014) and resistance to standard chemotherapy (Ursem et al. 2018). BRAFV600mut CRC is associated with worse prognosis compared to BRAFwt CRCs (***Figure 3***) (Lochhead et al. 2013). In particular, it is considered to be an independent negative prognostic factor in MSS tumours (Sanz-Garcia et al. 2017). By contrast, in non-metastasized MSI tumours the evidence remains inconclusive, as to whether there is a negative impact on the relatively good prognosis of MSI tumours (Lochhead et al. 2013; Roth et al. 2010). In metastasized MSI and MSS CRC, BRAFV600 mutations are associated with a very poor prognosis (Samowitz et al. 2005; Shimada et al. 2019; Venderbosch et al. 2014). Because of their prognostic value, namely excellent prognosis of MSI and worse prognosis of BRAFV600mut MSS tumours, BRAFV600 mutational status and MSI status were implemented in clinical diagnosis as important prognostic biomarkers (Smeby et al. 2018). Therefore, in most clinical trials investigating BRAF or KRAS prognostic value, studies have been stratified by MSI status, usually without consideration of the potentially confounding tumour heterogeneity. However, this might change with the recent CMS classification. BRAFV600 mutations typically occur in CMS1 tumours rather than CMS2, 3 or 4 with a frequency of 42% vs. 1% vs. 7% vs. 7%, respectively (Guinney et al. 2015). Initial studies stratified by CMS subgroups suggest an enrichment of BRAFV600 mutations in CMS1, not only in MSI, but also in MSS CRCs (Smeby et al. 2018). Consistent with former evidence, BRAFV600 mutations are an independent negative prognostic factor in MSS, but not in MSI tumours. Interestingly, across the CMS subgroups, CMS1 MSS BRAFV600mut CRCs show worse prognosis than CMS2, 3 or 4 MSS BRAFV600mut CRCs, possibly because of a higher positive correlation of CMS1 MSS BRAFV600mut CRCs with metastasis (Smeby et al. 2018).

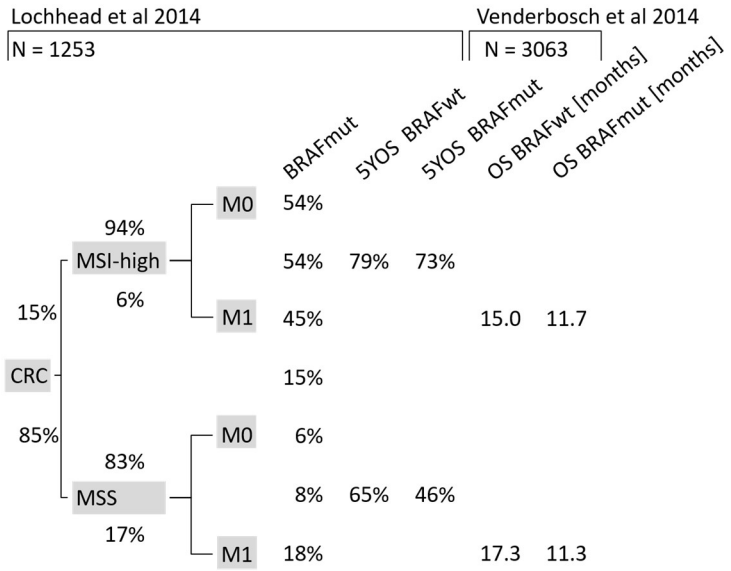

Figure 3: *Prognosis of BRAFV600mut CRC.*
Abbreviations: 5-year overall survival (5YOS), colorectal cancer (CRC), metastatic stage (M), microsatellite instability-high (MSI-high), microsatellite stability (MSS), patients number (N), mutated (mut), overall survival (OS), wild type (wt)

1.7 Targeting BRAFV600mut CRC

1.7.1 BRAF inhibitors

BRAF inhibitors (BRAFi) are small molecules, which usually block the ATP-binding site of BRAF in a competitive manner (Holderfield et al. 2014). Because the BRAFV600 mutation was initially found in more than 50% of malignant melanomas, BRAFis have been developed primarily for malignant melanoma treatment (Holderfield et al. 2014). Between the first description of mutant BRAF in 2002 (Davies et al. 2002) and clinical approval of the first BRAFi, less than 10 years passed. This highlights, how urgently better treatments for poor prognosis-related advanced BRAFV600mut malignant melanoma were needed. In particular, the second generation BRAFi vemurafenib (V) has been FDA-approved for treatment in advanced BRAFV600mut malignant melanoma as monotherapy in 2011 (Mullard 2012), and dabrafenib (D) in combination with the MEK inhibitor trametinib in 2014 (U. S. Food and Drug Administration, Center for Drug Evaluation and Research 2014). Encorafenib in combination with the MEK inhibitor binimetinib obtained approval in 2018 (U. S. Food and Drug Administration, Center for Drug Evaluation and Research 2018). In contrast to first generation BRAFis like sorafenib, second generation BRAFis like V, D and encorafenib selectively block kinase activity of class 1 BRAFV600mut monomers (Yao et al. 2017). V suppresses BRAFV600mut malignant melanoma cells with a 50-fold higher potency compared to BRAFwt cells (Holderfield et al. 2014).

1.7.2 Adverse effects and paradoxical ERK activation of BRAFis

In general, V, D and encorafenib are well tolerated. Typical side effects are symptoms like alopecia, arthralgia, fatigue, headache and most importantly, skin toxicities (Blank et al. 2017; U. S. Food and Drug Administration, Center for Drug Evaluation and Research 2014). Patients often suffer from hyperkeratosis, photosensitivity reactions, benign skin lesions and, surprisingly, also malign skin lesions. Up to 22% of patients treated with V develop cutaneous squamous cell carcinoma, which represents the most prominent grade 3 and 4 adverse effect (Adelmann et al. 2016). Secondary neoplasms and relapse of primary neoplasms (Andrews et al. 2013) are the major problem in terms of BRAFis induced side effects and typically occur within the first 8 weeks of BRAFi treatment (Menzies et al. 2013). At this point, two different key mechanisms for these adverse reactions observed are known: paradoxical MAPK/ERK activation in BRAFwt cells (Adelmann et al. 2016) and suppression of apoptosis (Vin et al. 2013).

In spite of their great specificity for monomeric acting BRAFV600 mutants, second generation BRAFis are not exclusively targeting BRAFV600. They also bind to dimeric BRAFwt and CRAF, albeit much less effectively (Menzies et al. 2013). Although this inhibition is much weaker, compared to that elicited upon BRAFV600, the inhibition of BRAFwt and CRAF is sufficient to disturb negative feedback mechanisms between ERK1/2 and upstream kinases, leading to rebound effects and paradoxically elevated MAPK/ERK signalling (Menzies et al. 2013). Moreover, BRAFi bound BRAFwt seems to induce BRAF/CRAF heterodimerisation and transactivates the BRAFi-free protomer in a manner similar to class 3 BRAF mutations. This leads to elevated MAPK/ERK signalling in BRAFwt cells (Cope et al. 2018; Heidorn et al. 2010). Another proposed mechanism is the BRAFi-dependent prevention of inhibitory BRAF autophosphorylation (Holderfield et al. 2013). Nevertheless, these mechanisms still remain incompletely understood. However, in the presence of RAS mutations and BRAFwt, BRAFi-induced paradoxical MAPK/ERK activation seems to induce secondary malign lesions, as well as relapse of primary malign lesions. Indeed, BRAFi-induced cutaneous squamous cell carcinomas are associated with HRAS (Harvey rat sarcoma viral oncogene homolog) mutations (Adelmann et al. 2016).

On the other hand, upstream kinases of JNK (c-Jun N-terminal kinase), which is a non-classical MAPK involved in stress-induced response signalling and apoptosis, represent off-targets of BRAFis. Their inhibition leads to apoptosis suppression, which is also important for driving cancerogenesis (Vin et al. 2013).

To reduce paradoxical activation, newer BRAFis are more selective for BRAFV600. Patients treated with D or encorafenib develop cutaneous squamous cell carcinoma in only 6% or 3.7% of cases, respectively, compared to 22% in V-treated patients (Adelmann et al. 2016). To even further avoid paradoxical activation, so called 'paradox breaker', third generation BRAFis are under development (Tutuka et al. 2017).

1.7.3 Resistance to BRAFi therapy

In malignant melanoma, BRAFi monotherapy showed striking initial efficacy with complete or partial remission for the majority of treated patients (Flaherty et al. 2010). In stark contrast, in CRC, no convincing efficacy could be shown at all (Kopetz et al. 2015). However, remissions in malignant melanoma patients commonly lasted a few months only until relapse (Wagle et al. 2011). So why do BRAFV600mut CRCs show such a pronounced primary resistance against BRAFis and why do BRAFV600mut neoplasms escape from BRAFi therapy that rapidly? These questions were investigated intensely, revealing several mechanisms of resistance. Molecular alterations as well as alterations due to disturbed regulatory feedback, leading to BRAFi resistance, are mainly related to the MAPK/ERK pathway itself, or to cross-talking pathways, respectively (***Appendix, Table 4***).

Similar to paradoxical ERK activation in BRAFwt cells, sudden loss or reduction of markedly elevated ERK activity due to inhibition of BRAFV600 leads to a loss of negative feedback inhibition of upstream targets in BRAFV600mut cells (***Figure 2***). Since EGFR signalling and consequently MAPK/ERK signalling is much more important in CRC than in malignant melanoma, those 'rebound effects' are much more pronounced in CRC, which might explain the poor BRAFi response compared to malignant melanoma (Lito et al. 2012). For instance, EGFR reactivation (Corcoran et al. 2012) or RASwt amplification (Yaeger et al. 2017) were reported in BRAFV600mut CRC, but not in malignant melanoma. A central factor in BRAFi resistance is the promotion of BRAF dimerisation (Yaeger et al. 2017). Since BRAFis were designed to bind monomeric BRAFV600, the inhibition of dimerised BRAF is not particularly potent. Unfortunately, BRAFis even induce dimerisation and thus enable escape from therapy (Cope et al. 2018). In addition, RAS mutations, over-expression of RAS and alternatively spliced BRAFV600 can induce RAF dimerisation as well (Yaeger et al. 2017).

As mentioned above, the MAPK/ERK pathway is linked to many other crucial signalling pathways. The multi-site docking protein GAB1, up-regulated by BRAF inhibition (Herr et al. 2018), is a key player in signalling pathway cross-talk. For instance, it connects the PI3K/AKT(protein kinase B)/mTOR (mechanistic target of rapamycin kinase) pro-survival pathway to MAPK/ERK (Fritsche-Guenther et al. 2016; Wang et al. 2015).

While the mechanistic details remain unclear, PI3K is considered to force CRAF activation independently from RAS (Ebi et al. 2013). Up-regulation or activating mutations of PI3K and loss of PTEN (phosphatase and tensin homolog), a suppressor of PI3K/AKT/mTOR pathway, are frequently present in BRAFi-treated BRAFV600mut CRCs, driving primary or acquired BRAFi resistance (Mao et al. 2013). Recently, up-regulated SHP2 (SH2 domain-containing protein tyrosine phosphatase 2), which also docks onto GAB1, has been revealed to be a major driver of resistance in CRC, but not in malignant melanoma. SHP2 is a phosphatase, which removes inhibitory phosphorylations from RAS, and is thus important for RAS recycling and re-activation (Herr et al. 2018; Prahallad et al. 2015). In association with MAPK/ERK rebound, elevated PI3K/AKT/mTOR signalling and apoptosis suppression, BRAFi resistant cells frequently show elevated levels of EIF4F (eukaryotic translation initiation factor 4F), which is important for initiation of translation (Boussemart et al. 2014).

All in all, targeting BRAFV600 by monotherapy is clearly not sufficient for the effective targeting of BRAFV600mut CRC. Consequently, a number of different approaches of combining drugs vertically (within MAPK/ERK signalling) or horizontally (across different pathways) have been developed with the intention to overcome resistance (Cohen et al. 2017).

1.7.4 Combination treatment approaches in CRC

The main aims of combining drugs in BRAFV600mut cancer are (i) overcoming resistance, (ii) avoiding resistance development and (iii) the reduction of side effects through blocking paradoxical ERK activation. In advanced BRAFV600mut malignant melanoma, the combination of BRAFi with a MEK inhibitor (MEKi) evolved into a standard therapy regimen, raising OS from less than 9 months under standard chemotherapy (Flaherty et al. 2010) to 33.6 months in patients receiving encorafenib combined with binimetinib (Liszkay et al. 2019). In comparison, patients treated with encorafenib or V alone reached OS of at least 23.5 months or 16.9 months, respectively (Liszkay et al. 2019). Recently, data of five year treatment with D-trametinib-combination in metastasized BRAFV600mut malignant melanoma patients became available, which show an incredible 5YOS rate of 34% (Robert et al. 2019).

Unfortunately, in CRC a therapeutic break through, such as in malignant melanoma, is still lacking (***Appendix, Table 3***). Although the triple combination of BRAFi, MEKi and EGFR inhibitor (EGFRi), namely encorafenib, binimetinib and cetuximab, shows emerging efficacy in a recent randomised phase III study, the absolute improvement of OS depicts only a few months (Kopetz et al. 2019). Therefore, other approaches are required to advance patient's survival markedly. Obviously, the combination of inhibitors of different members along or across the MAPK/ERK pathway does not keep BRAFV600mut CRC cells from circumventing inhibitory therapy through collateral signalling (Ducreux et al. 2019; Yaeger et al. 2017).

1.8 HSP90 – a promising target?

The chaperones HSP70 (heat shock protein 70) and especially HSP90 are the most important members of the human chaperome, a network of various chaperones, co-chaperones, scaffolding proteins, adaptor proteins and folding proteins (Rodina et al. 2016). Chaperones are often described as helper proteins, which interact with so-called 'client' proteins to ensure their correct folding. They stabilize the different functional conformations and enable an active structure of their clients (Schopf et al. 2017). Heat shock proteins were found initially to be elevated in circumstances of cellular stress. Eponymously, in case of heating they protect protein function against misfolding termed denaturation (Schopf et al. 2017). In contrast to most other chaperones, HSP90 is also expressed at basal levels in non-stress situations, suggesting a critical role in cellular processes even under physiological conditions (Schopf et al. 2017). Indeed, HSP90 has hundreds of client proteins. For example, more than 60% of all human kinases require HSP90 for proper function (Picard 2019; Schopf et al. 2017). In particular, HSP90 supports complex formation (e.g. BRAF-dimerisation (Diedrich et al. 2017), β-catenin-destruction-complex (Cooper et al. 2011)), enables ligand binding by stabilization of an open conformation and modulation of the binding cleft (e.g. ATP binding to kinases (Polier et al. 2013; Pratt et al. 2008)) and supports stabilization of distinct functional conformations (e.g. active and inactive BRAF, ***see 1.4.2***). Interestingly, many proteins involved in resistance mechanisms to BRAFi therapy are dependent on HSP90. Indeed, in BRAFV600mut malignant melanoma cells HSP90 inhibition was reported to overcome acquired BRAFi resistance by increased apoptosis and degradation of multiple proteins considered to contribute to BRAFi resistance (Paraiso et al. 2012). Besides direct BRAF regulation, HSP90 stabilizes AKT and mTOR as part of PI3K pathway, HER2 (human epidermal growth factor receptor 2) becomes rapidly degraded in absence of HSP90 (Pratt et al. 2008) and ARAF, CRAF, MEK1/2 and ERK1/2 are HSP90 dependent as well (Grbovic et al. 2006; Kryeziu et al. 2019). Since mutations disturb protein structure, mutated proteins often become more dependent on stabilization by HSP90 than their wild type counterparts (Schopf et al. 2017).

In line with this, mutated EGFR requires HSP90 for stabilization, while EGFRwt is less dependent on HSP90 (Ahsan et al. 2013). Unless V600mut BRAF is not bound by HSP90, it becomes rapidly degraded compared to BRAFwt (Grbovic et al. 2006). RASmut cells become highly HSP90 dependent, whereas RASwt is not considered to be a HSP90 client (Azoitei et al. 2012). That means, HSP90 'buffers' mutations, which might lead to disturbed protein structure and loss of function (Schopf et al. 2017). Taken together, tumour cell functions are apparently more dependent on HSP90 than normal cell functions, as indicated by an elevated HSP90 and HSP70 machinery activity in more than 50% of cancers (Rodina et al. 2016).

Interestingly, especially CMS1 and CMS4 CRCs were reported to be dependent on HSP90 (Sveen et al. 2018). As mentioned above, CMS1 CRCs are associated with V600mut BRAF and MSI with a hypermutation phenotype, which might explain the high requirement for HSP90 mediated stabilization of proteins. However, MSS CMS1 and CMS4 CRCs without hypermutation phenotype also seem to be more HSP90 dependent than CRCs of the other two CMS groups (Sveen et al. 2018). Targeting HSP90 might hence open a new therapeutic window in CRC therapy. Several clinical trials are currently running or were already performed investigating therapeutic potential of HSP90 inhibition in various cancer patients. However, while HSP90 inhibitor (HSP90i) monotherapy seemingly lacks sufficient efficacy (Cercek et al. 2014), inhibition of HSP90 seems to sensitize solid cancers against conventional chemotherapy. Patients with advanced NSCLC treated more than 6 months after diagnosis with an HSP90i and docetaxel have a slightly better OS than patients treated with docetaxel only (Ramalingam et al. 2015). Even CRC patients seem to profit from combining HSP90is with capecitabine (Bendell et al. 2015). Combined with targeted therapy, HSP90is show initial efficacy in HER2 positive breast cancer patients treated with paclitaxel and trastuzumab (Jhaveri et al. 2017) as well as in CRC patients treated with cetuximab (Subramaniam et al. 2015). Again, in BRAFV600mut malignant melanoma, the combination of BRAFi and HSP90i shows striking efficacy with an increased OS from 9.2 months up to 34.6 months when treated with V mono-therapy vs. combination-therapy with the novel HSP90i XL888, respectively (Eroglu et al. 2018).

However, in CRC the combination of HSP90i with BRAFi has not been clinically tested yet. Initial preclinical results report beneficial effects of combining both compounds (Wang et al. 2016), but more evidence is urgently needed to expand the options of CRC treatment by novel potential treatment approaches.

2 Aim of the thesis

Over the past decades, modern diagnostics revealed BRAFV600 mutation in MSS and metastasized CRC as an independent negative prognostic marker, which is furthermore associated with resistance against conventional chemotherapy. In contrast to BRAFV600mut malignant melanoma, targeting BRAFV600mut CRC was revealed to be entirely inefficient, because of a striking repertoire of resistance mechanisms against inhibition of BRAFV600. Several efforts have been taken to overcome BRAFi resistance by combining BRAFis with different kinase inhibitors, monoclonal antibodies or chemotherapy. Unfortunately, despite promising preclinical results, clinical trials only show modest improvements of BRAFV600mut CRC patient's outcome. Therefore, new approaches are urgently needed. Combining BRAFis with one or two additional and very selective compounds might not stop aberrant signalling in BRAFV600mut CRC sufficiently. Since most of the proteins involved in BRAFi resistance are HSP90 dependent, HSP90 might be a sensible target for combination treatment with BRAFis, in order to overcome BRAFi resistance, by targeting multiple resistance mechanisms simultaneously. Recently, promising clinical efficacy could be shown in BRAFV600mut malignant melanoma patients and initial preclinical investigations could show interesting results in BRAFV600mut CRC cells, suggesting treatment benefits of combining HSP90is with BRAFis. However, while HSP90 seems to be a key player in the resistance against BRAFi therapy in BRAFV600mut CRC, convincing evidence of efficacy of combining BRAFis with HSP90is is still lacking and urgently needed.

Against this background, the major objective of this study is to investigate whether HSP90is are sufficiently potent combination therapy partners for BRAFis. Moreover, this study investigates how the combination of HSP90is and BRAFis behaves in different setups, to get information about robustness of combinatory approach. Therefore, this study investigates how the combination of BRAFis and HSP90is affects the cell viability in two-dimensional (2D) monolayer culture conditions as well as the colony forming activity in three-dimensional (3D) anchorage-independent culture conditions. Furthermore, this study investigates, whether combination treatment effects are consistent in different BRAFV600mut CRC cell lines using different BRAFis and HSP90is. Finally, this study investigates how the combination of BRAFis and HSP90is affects tumour growth and metastasis in mice injected with BRAFV600mut CRC cells and whether mice tolerate the combination treatment. The *in vivo* studies were done in a collaboration.

3 Methods and materials

3.1 Cell lines and growth conditions

Cells were essentially cultured according to previously described conditions (Emaduddin et al. 2008; Frejno et al. 2017). HT-29, COLO 201, RKO and Caco-2 cells were previously purchased from American type culture collection, OX-CO-1 cells were a kind gift from Khoon Lin Ling (Mount Elizabeth Medical Centre, Singapore; before at Weatherall Institute of Molecular Medicine, University of Oxford) and Vincenzo Cerundolo (Weatherall Institute of Molecular Medicine, University of Oxford) (***Appendix, Figure 12***). Cells were cultured in Dulbecco's modified eagle medium (DMEM) (41966052, Fisher Scientific) supplemented with 10% fetal bovine serum (FBS) (10270106, lot 41F5644K, Fisher Scientific) and 100 U/mL penicillin-streptomycin (Pen-Strep) (15140-122, Fisher Scientific) at 37 °C in 10% carbon dioxide (CO_2) humidified atmosphere. Cells were split when they reached approximately 80% confluency, using 5x concentrated trypsin, made from 10x concentrated trypsin-ethylene diamine tetraacetic acid (EDTA) solution (15400-054, Fisher Scientific) diluted with phosphate buffered saline (PBS) (10010056, Fisher Scientific)) for two to five minutes, depending on the adherence properties of the individual cell line, to detach the cells. Trypsin digestion was terminated by adding 10% FBS in PBS and cells were gently resuspended to separate cell clumps into single cells. Cells were counted, using an improved Neubauer haemocytometer (AS1000, Hawksley) and an inverted phase contrast microscope (NIKON eclipse TS100) at 100x magnification. Trypan blue (CN76.1, Carl Roth) staining was employed to recognize nonviable cells. After that, the appropriate cell number was transferred into new polystyrene culture flasks with 25, 75 or 175 cm^2 area, respectively (430639, 430641U, 431080, Corning), containing cell culture medium. Every two to three days, the cell culture medium was replaced by fresh cell culture medium.

3.2 2D monolayer culture resazurin assay

The protocol of the 2D monolayer culture resazurin assay, which was previously described (Riss et al. 2004), was slightly modified for our studies. RKO, Caco-2 and OX-CO-1 cells were harvested at approximately 80% confluency. HT-29 cells were harvested at approximately 60% confluency, because otherwise cells would remain in clumps of more than five cells after resuspending, which makes correct cell-counting impossible. For the 2D monolayer culture resazurin assay, DMEM without glucose or pyruvate (11966-025, Fisher Scientific) was supplemented with FBS, Pen-Strep and glucose (15384895, Fisher Scientific) to get a final solution containing 6 mM glucose, 5% FBS and 100 U/mL Pen-Strep. Cells were seeded to 96 well plates (3596, Corning) to a density of 2000 cells/well in case of HT-29 and OX-CO-1 cells and 3000 cells/well in case of RKO and Caco-2 cells, respectively. After cells were allowed to attach overnight in 37°C, 10% CO_2

humidified atmosphere condition, the old medium was discarded and cells were treated with medium alone (untreated control (Ctrl)), medium-containing drug solvent (vehicle) (vehicle-treated Ctrl), single compounds and combined compounds. The outer wells of the 96-well plate were kept cell-free but were filled with water to avoid increased evaporation of outer border wells, which contain cells. For treatment, the BRAFis D (dabrafenib, S2807, lot 4, Selleckchem) and V (vemurafenib, S1267, lot 9, Selleckchem) and the HSP90is HSP990 (H) (S7097, lot 1, Selleckchem) and 17-(Allylamino)-17-demethoxygeldanamycin (A) (S1141, lot 2, Selleckchem) were used. The vehicle (drug solvent) for all compounds was dimethyl sulfoxide (D2650, Sigma-Aldrich), which was used at a final concentration of 0.1% for all 2D monolayer culture resazurin assay experiments. After a 72 h incubation in 37°C, 10% CO_2 humidified atmosphere, cells of row 11 (***Appendix, Figure 9***) were killed for background Ctrl by replacing medium with 70% ethanol (64-17-5, Carl Roth) for two minutes. Then, medium or ethanol was replaced by the staining solution, which is a 1:500 dilution of saturated, filter-sterilized 50 mg/mL resazurin in PBS (199303-5G, Sigma-Aldrich) diluted in phenol red-free DMEM (21063-029, Fisher Scientific). Subsequently, cells were incubated at 37°C, 10% CO_2 humidified atmosphere for 1 h in the case of HT-29 cells and 2 h for OX-CO-1, RKO and Caco-2 cells. Finally, resorufin fluorescence at 560 nm excitation and 590 nm emission was measured with a photometric microplate reader (Tecan Infinite M200 PRO) and data were transferred into Microsoft Excel. At least three independent experiments for each combination and each cell line were performed. COLO 201 cells grow in suspension with only few low adherent cells. Therefore, they are not suited for 2D monolayer culture resazurin assays, because of the loss of the majority of cells during the multiple medium changing steps.

3.3 3D soft agar anchorage-independent growth assay

The 3D soft agar anchorage-independent growth assay is known for decades and widely used (Hamburger and Salmon 1977). For this thesis it was newly established in our laboratory.

For experiments, an autoclaved agar stock solution was used at a concentration of 1.2% agar noble (214220, Becton, Dickinson) in sterile water. To prepare agar layers, agar stock solution was melted in a conventional microwave at 700 W for one to two minutes. This agar was mixed with prewarmed double concentrated medium, prepared from powdered DMEM (31600-083, Fisher Scientific) to obtain the soft agar medium, consisting of 1x DMEM with 5.5 mM glucose and 10% FBS. To avoid preliminary solidifying of agar dilutions, solutions were kept in a 42°C water bath and the cell culture plates were placed on a heating plate (P853.1, Carl Roth), equipped with a laboratory glass ceramic protective plate (A386.1, Carl Roth) at lowest heat

level, during preparation of the bottom layer. 42°C exposure to cells was kept as short as possible and did not exceed two minutes.

Before transferring cells and soft agar, 24 well culture plates were pre-prepared with a bottom layer containing 0.6% agar noble in soft agar medium, containing double concentrated vehicle, single compounds or combined compounds at a volume of 1 mL. The bottom layer was allowed to solidify for at least 30 minutes at room temperature.

In the meantime, cells were harvested as described above (***see 3.2***). Since single cells were required for seeding, cells were gently resuspended very carefully. Then, cells were counted and mixed with agar noble/soft agar medium solution, without any vehicle or compounds to a final concentration of 0.3% agar noble. 1 mL suspension containing cells was added on top of the bottom layer to a final cell count of 2000, 4000 and 16,000 cells/well for HT-29, COLO 201 and Caco-2 cells, respectively. After 30 minutes at room temperature, the agar layer containing cells has been solidified. Then, a superficial liquid layer containing soft agar medium with one-fold concentrated vehicle, single compounds or combined compounds, was added (***Appendix, Figure 10***). Empty spaces between wells were filled with medium to prevent wells of interest to suffer from increased evaporation. Plates were placed at 37°C 10% CO_2 humidified atmosphere for 14 days. Every three to four days, 100 µL fresh soft agar medium containing one-fold concentrated vehicle, single compounds or combined compounds was added.

On day 14, staining solution containing 0.5 mg/mL nitrotetrazolium blue chloride (4421.1, Fisher Scientific) in PBS was added to each well. Plates were then incubated overnight at 37°C 10% CO_2 humidified atmosphere for image acquisition on the next day.

3.4 Image acquisition and processing

For evaluation of 3D soft agar anchorage-independent growth assay, 24 well plates were placed on top of an illumination box and pictures of each well were taken with fixed distance between the macro-objective (SEL30M35, Sony) and plate, using a self-constructed camera stand with adapted camera (ILCE-5100L, Sony) and fixed camera settings for all experiments (***Appendix, Figure 11***). Each well was centred manually under the camera objective. Images were taken of each well, using Sony Remote Camera Control v3.6 on a personal computer, equipped with Microsoft Windows 7 Professional to avoid shake artefacts. A nearly closed aperture, optimized for image sharpness and depth of field, was used. Additionally, a scale was imaged with same settings to recalculate colony size during data processing. Then, images were imported to RawTherapee v4.2.1148 and processed, using a standardized processing profile with same settings across all images to obtain uniformly cropped and uniformly processed

images for further analysis. Finally, images were imported into (Fiji Is Just) ImageJ v1.51n for automated colony count, using a macro (***Appendix, Figure 13***), which runs the function 'analyse particles' and which exports data of colony size in mm^2 and colony count to .xls files. The files were imported to a prepared and standardized Microsoft Office 2016 Excel sheet, using a macro (***Appendix, Figure 14***) for further data evaluation.

3.5 Mouse xenografts

In vivo experiments were performed by Thomas Müller (Arbeitsgruppe Experimentelle Onkologie, Klinik für Innere Medizin IV, Universitätsklinikum Halle). The experiments were done according to regional standards and regulations and were approved by the state administration of Saxony-Anhalt (official file number 42502-2-1413 MLU). Five million luciferase-expressing HT-29 cells were injected into the right flank of male athymic nude mice subcutaneously (Athymic Nude-Foxn1nu/nu, local breeding, ZMG of Medical Faculty of MLU Halle). The luciferase-expressing HT-29 cells, named HT29-Luc, were previously generated, established and successfully used by the Arbeitsgruppe Experimentelle Onkologie, Klinik für Innere Medizin IV, Universitätsklinikum Halle. Tumours were established after ca. 14 days, reaching a volume between 50 and 300 mm^3. Mice were divided into four groups, containing eight mice each, with an equal mean tumour volume and equal volume distribution across the groups. The groups were treated by intraperitoneal injection with vehicle (10% Tween80, 10% Ethanol, 80% saline), D, H or with the combination of D and H for 30 days. 30 mg/kg D were applied daily, except on weekends, and 5 mg/kg H were applicated once a week. Dosing was adopted from previously described xenograft experiments, using D and H (King et al. 2013; Menezes et al. 2012). Mice were weighed daily and checked for abnormal behaviour, except on weekends. Tumour size was measured using a calliper and volume was calculated using the formula:

$$V = a^2 \cdot b \cdot \frac{\pi}{6}$$

Where **V** represents volume, **a** the short and **b** the long dimension. On day 34 since treatment start, mice were sacrificed and tumours and lungs were excised. Tumours were weighed and the lung metastasis was analysed, using bioluminescence imaging on an IVIS Spectrum (Perkin Elmer) and quantified using Living Image® software (Perkin Elmer).

3.6 Synergy evaluation and hypothesis testing

Prior to synergy evaluation, data were collected in Microsoft Office 2016 Excel, normalized between vehicle-treated Ctrl and background Ctrl for the 2D monolayer culture resazurin growth assay or normalized to vehicle-treated Ctrl for the 3D anchorage-independent growth assay and *in vivo* experiments, respectively. For the 3D anchorage-independent growth assay, only colonies with an area of at least 0.001 mm^2 were included to exclude single cells or dust.

For the evaluation of combinational treatment effects, the well-established methods of Bliss-independence and highest single agent (HSA) were performed (Foucquier and Guedj 2015). Bliss-combination indices (Bliss-CI) were calculated in Microsoft Office 2016 Excel using the following formula:

$$Bliss - CI = \frac{E_A + E_B - E_A \cdot E_B}{E_{A+B}}$$

E_A and E_B are the treatment effects of the two different compounds in single treatment and E_{A+B} is the combination treatment effect of both compounds combined. E ranges between 0 (no effect) and 1 (e.g. 100% of cells are dead). Because in this thesis effects of different treatments were visualized as plots, showing the measured size instead of treatment effect E (e.g. colony count in % of Ctrl, metabolic active cells in % of Ctrl, etc.), data were transformed to calculate E, using the following formula:

$$E = \frac{Ctrl - X}{Ctrl}$$

X is the respective measured size and Ctrl the corresponding vehicle-treated Ctrl. To check, if Bliss-CI is different from 1, a one sample T test was performed using GraphPad Prism 6.

Since Bliss-CIs are valid only for E between 0 and 1, HSA was used in cases, where these requirements were not fulfilled. Therefore, the respective groups treated with the most effective single compound were compared to the combination treatment groups and to vehicle-treated Ctrls with a one-way ANOVA, corrected for multiple comparison, using the Dunett-test in GraphPad Prism 6. The same ANOVA test has been used for comparison of different treatment conditions in 2D monolayer culture resazurin assay, 3D soft agar anchorage-independent growth assay and mouse xenografts. According to the recommendations of the American Statistical Association on statistical significance, a significance threshold like '$p \leq 0.05$' has not been set (Wasserstein and Lazar 2016). Nevertheless, *p* values were consistently reported.

4 Results

4.1 Different cell lines respond differently to D, V, H and A in 2D

For assessing potential combination treatment effects of BRAFis and HSP90is in 2D monolayer cell culture, well-adherent CRC cell lines with suitable growth properties on plastic surfaces were selected, namely the three BRAFV600mut CRC cell lines HT-29, OX-CO-1 and RKO and the BRAFwt CRC cell line Caco-2. The resazurin assay is well-suited for high throughput drug screening and was firmly established in our laboratory before the start of this project. Metabolically active cells reduce the deeply blue coloured and nonfluorescent resazurin to pink coloured and fluorescent resorufin (Riss et al. 2004), which can be quantified, using a fluorescence detector. The assay does not measure cell viability directly, but monitors the cells' capability to reduce resazurin, which is considered to represent cells' metabolic activity and which in turn is a surrogate marker for cell viability (Riss et al. 2004).

Before starting combinational treatment studies, each cell line was treated with single compounds for 72 h to evaluate appropriate drug concentration ranges (***Figure 4***). Treatment effects were normalized between cells treated with vehicle only (= 100%) and vehicle-treated cells killed with ethanol before readout (= 0%). As expected, BRAFV600mut cells are more sensitive to BRAFis than BRAFwt Caco-2 cells. RKO cells show the highest BRAFi resistance of tested BRAFV600mut cells. The BRAFV600mut cell lines analysed in this study are also more sensitive to HSP90is than BRAFwt Caco-2 cells. Especially against A, Caco-2 cells show resistance with an approximately 100 times higher half effective inhibitory concentration (IC_{50}), compared to HT-29 cells. Moreover, low concentrations of A seem to stimulate Caco-2 cells metabolic activity. In H treatment, sensitivity varies not very much across the different cell lines. Instead, the IC_{50} in Caco-2 cells seems to be slightly lower than in RKO cells, but an inhibition of metabolic activity of nearly 50% in RKO- cells and 20% in Caco-2 cells, compared to the respective vehicle-treated Ctrl reveals RKO cells as being more sensitive to H than Caco-2 cells. HT-29 is the most sensitive cell line for all tested compounds. D is generally more potent than V and H is more potent than A. All in all, effective compound concentrations in BRAFV600mut cell lines were much below plasma concentrations reached in patients (***Table 1***).

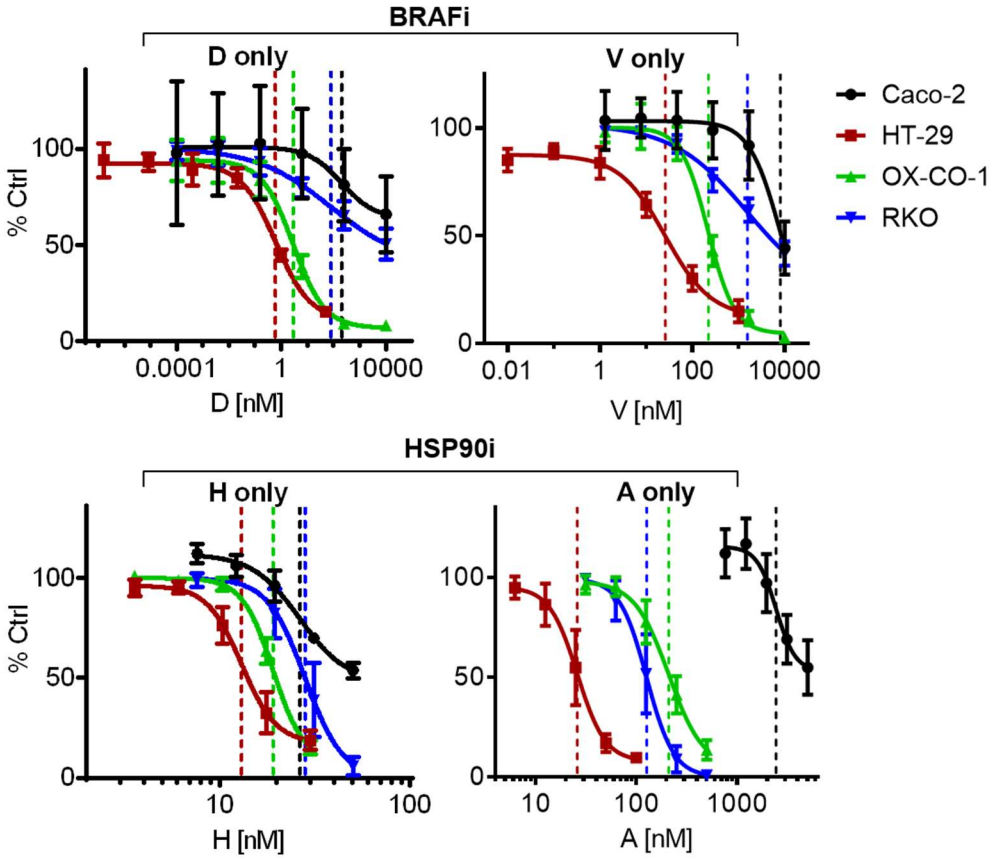

Figure 4: *Dabrafenib (D), vemurafenib (V), HSP990(H) and 17-AAG (A) single agent effects in CRC cell lines treated for 72 h and analysed by resazurin assay. Normalized data between background (0%) and vehicle control (Ctrl) (100%). Broken lines indicate respective relative IC_{50}. In each case, at least three independent experiments were conducted.*

Table 1: *Average relative IC_{50} values with corresponding cell metabolic activity.*

	IC_{50} [nM] (%Ctrl)					
	HT-29	OX-CO-1	RKO	Caco-2	c_{blood} [nM]	ref
D	0.60 (52)	2.8 (50)	80 (70)	210 (82)	72	(Puszkiel et al. 2019)
V	26 (50)	220 (52)	1600 (61)	8000 (52)	5900	(Zhang et al. 2017)
H	13 (57)	19 (54)	28 (50)	26 (80)	700	(Spreafico et al. 2015)
A	26 (52)	210 (52)	130 (59)	2400 (84)	1000	(Goetz et al. 2005)

Abbreviations: 17-AAG (A), blood concentration reached at steady state (c_{blood}), vehicle-treated control (Ctrl), dabrafenib (D), HSP990 (H), half maximal inhibitory concentration (IC_{50}), reference (ref), vemurafenib (V)

4.2 Combination of BRAFis with HSP90is shows additive combination effects at nanomolar concentrations in BRAFV600mut CRC cells in 2D

Once appropriate concentration ranges were defined around IC_{50} values, single treatments were escalated to combination treatments. Cells were treated with increasing concentrations of BRAFis and HSP90is alone or in combination in a matrix-type manner (***Appendix, Figure 9***). In all tested BRAFmut cell lines, the combination of BRAFis with HSP90is shows typically more efficacy than single treatments (***Figure 5***). When different compounds and their combinations are compared, the observed combination effects remain consistent within each cell line.

Interestingly, in RKO, the most resistant BRAFmut cell line tested, combining BRAFis and HSP90is shows the strongest combination treatment effect of all cell lines. As expected, in BRAFwt Caco-2 cells, combination treatment effects were not as strong as in BRAFmut cell lines. As described for single A treatment above, also in combination treatment, Caco-2 cells seem to be slightly stimulated in their metabolic activity when treated with low concentrations of HSP90is. In HT-29 cells treated with highest V concentration, combined with low concentrations of HSP90is, the cells seem to be less affected in combination compared to V only. Therefore, data points of the combination effects of 1000 nM V, combined with the respective concentrations of H or A (***Figure 5***), were compared to V single treatment Ctrl in HT-29 cells. A null hypothesis claiming there is no difference and a working hypothesis that there is a difference between 1000 nM V single treatment Ctrl and combinations were investigated using a one-way ANOVA. The *p* values were not lower than 0.28 or 0.058 for 1000 nM V combined with 10 nM H or 13 nM A, respectively.

According to Bliss (1939), three different types of interactions can be distinguished when drugs are added in combination: similar joint action, independent joint action and synergistic/antagonistic action (Bliss 1939). In case of similar joint action, the combined compounds act independently in the same mechanistic system, for example on one signalling pathway. Their dose-response curves are assumed to run in parallel and they are considered to be exchangeable in a fixed dose ratio to produce the same effect. In contrast, independent joint action means that the compounds act on different targets of different systems. In more recent literature the term Bliss-independence became established as a model of drug-drug interactions and is also used when compounds act in the same system, but affect different binding sites, for example (Foucquier and Guedj 2015).

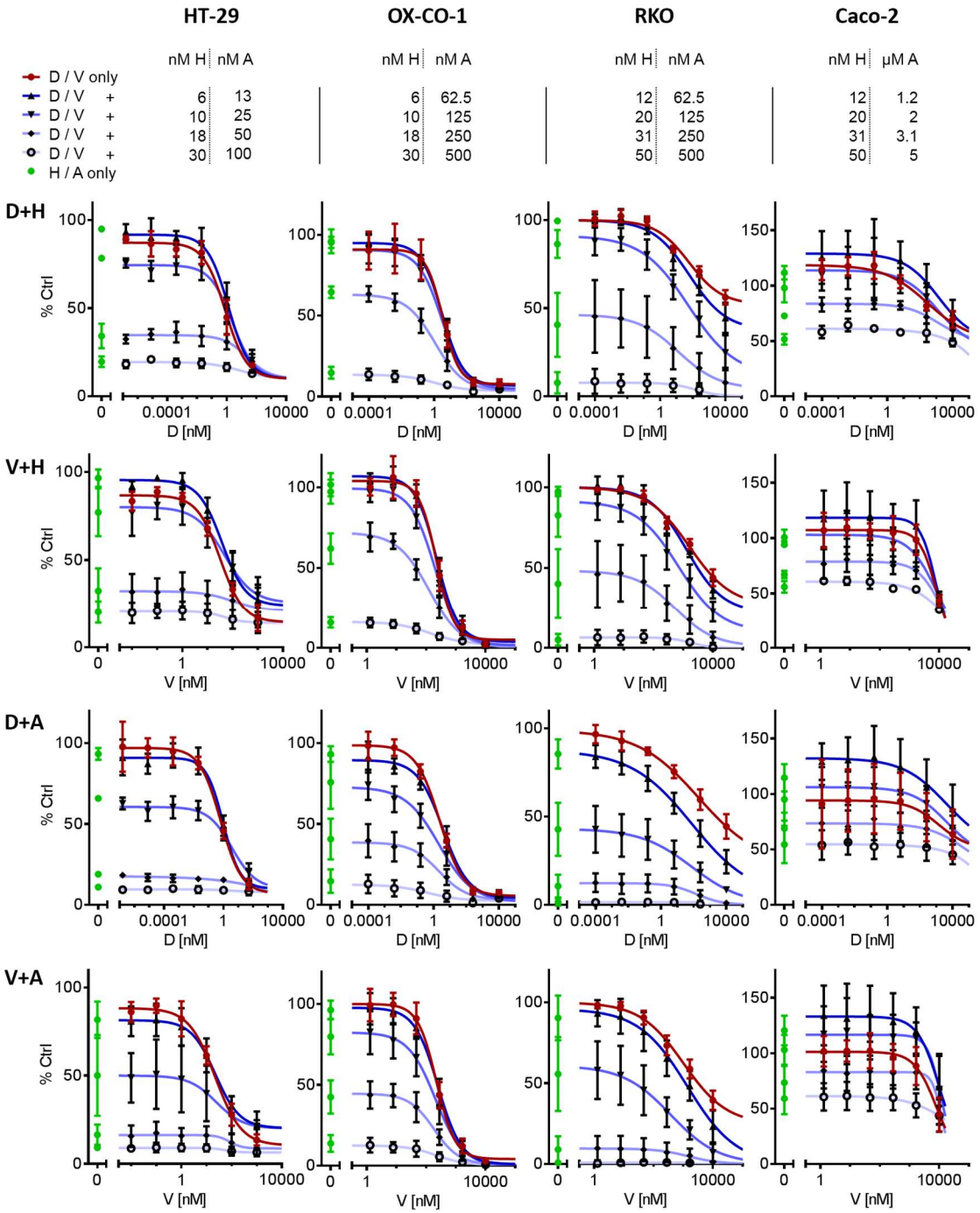

Figure 5: *Effects of dabrafenib (D) and vemurafenib (V) combined with HSP990 (H) and 17-AAG (A) in CRC cell lines for 72 h monitored by resazurin assay. Normalized data between background (0%) and vehicle-treated control (Ctrl) (100%) are shown. In each case, at least three independent experiments were conducted.*

To distinguish between Bliss-independence, which is synonymously termed additivity and synergism/antagonism, the Bliss-CI was introduced. Again, one can only speak of Bliss-CI, if E ranges between 0% and 100%. If Bliss-CI is less than one, the combination is considered to be synergistic, if Bliss-CI is greater than one, as antagonistic. If Bliss-CI equals one, the compounds are considered to act additively (Foucquier and Guedj 2015).

Therefore, Bliss-CIs were calculated for combinations from the slope region of the dose-response curves to fulfil this requirement representatively shown for combination D+H in HT-29, OX-CO-1 and RKO (***Figure 6***). A one sample t-test checks, if the Bliss-CIs are different from one. For most combinations, the Bliss-CI is almost equal to one, especially in OX-CO-1 cells. As already seen in ***Figure 5***, combining BRAFi with HSP90i in RKO is most effective with Bliss-CIs less than one (for 250 nM D + 20 nM H, Bliss-CI = 0.69 (95% confidence interval (CI): 0.66-0.72)). Surprisingly, in HT-29 Bliss-CIs are often greater than one (for 1 nM D + 10 nM H, Bliss-CI = 1.27 (95% CI: 1.15-1.38)). For the combinations D with A and V with H or A, the Bliss-CIs are distributed consistently.

That means that the combination treatment with BRAFis and HSP90is predominantly acts in an additive manner in 2D monolayer culture growth assays among the used BRAFV600mut CRC cell lines, ranging from slight antagonistic effects in HT-29 cells to slight synergistic effects in RKO cells.

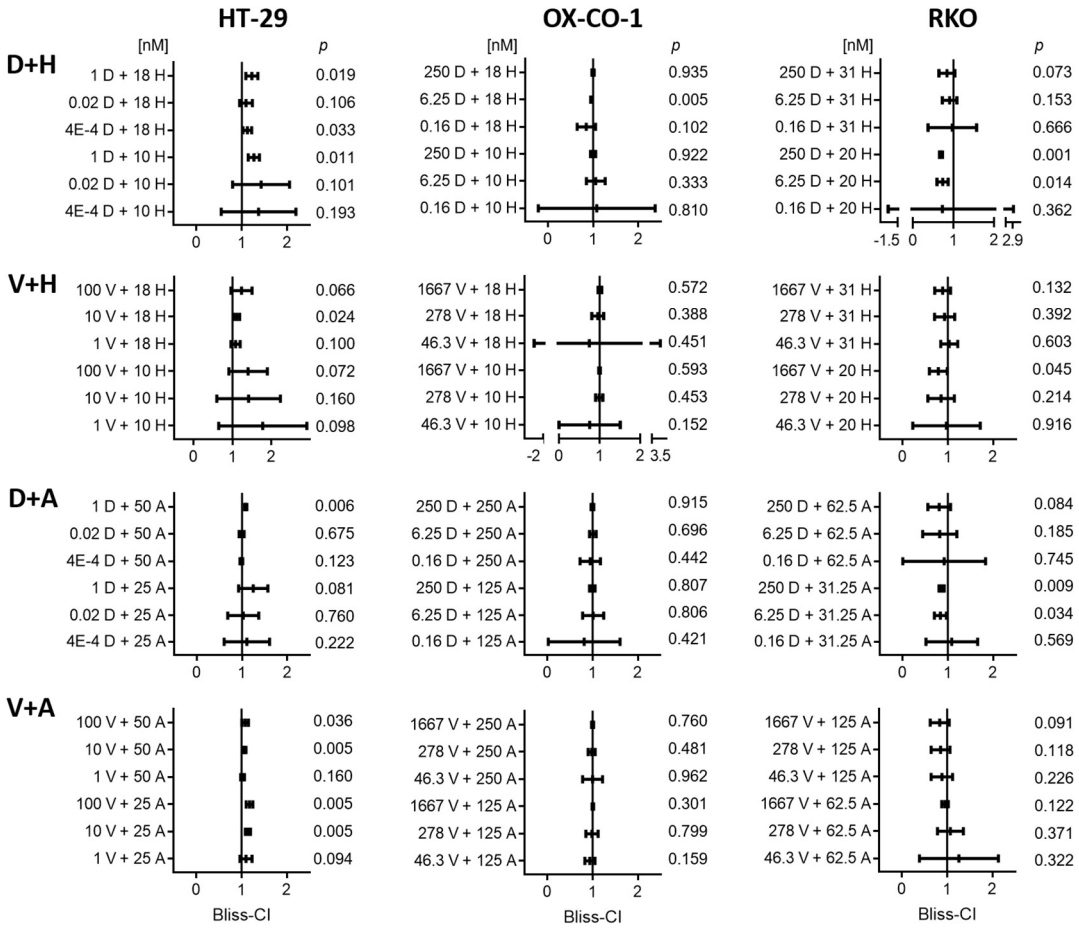

Figure 6: *Bliss combination indices (Bliss-CI) (means with 95% CI) of the combination treatments vemurafenib (V) or dabrafenib (D) and 17-AAG (A) or HSP990 (H) in different BRAFV600mut CRC cell lines. p values of one sample t-test (Bliss-CI ≠ 1).*

4.3 Combination of BRAFi with HSP90i shows synergistic combination treatment effects in BRAFV600mut CRC cells in 3D culture

2D monolayer cell culture is quite an artificial setting when compared with the situation *in vivo*. Cells grow on a plastic surface, are surrounded by nutrition solution and come into contact with only a few cells, far from the natural environment *in vivo*. Under such conditions, even non-malignant cells can manage to divide rapidly, until they reach senescence (Schmitz 2011). In organisms, cells grow three-dimensionally with close contact to, as well as interaction with neighbouring cells and extracellular matrix. The nutrition and oxygen supply are inhomogeneous, depending on the cells' location in the tissue. Therefore, it is not surprising that effects seen in 2D monolayer cell culture often differ from *in vivo* studies and from clinical trial results (Edmondson et al. 2014). For a somewhat better prediction of *in vivo* properties, different 3D cell growth assay systems mimicking microenvironments have been established. Moreover, 3D cell viability assays enable us to study longer term treatment effects, which is

important especially in cells developing resistance against the used compounds, such as seen in the treatment of BRAFV600mut CRC cells with BRAFis.

Therefore, for this thesis, a soft agar anchorage-independent growth assay has been established in our laboratory, to study combination treatment effects of BRAFis with HSP90is over two weeks, before escalation to an *in vivo* mouse model.

Anchorage-independent growth assays were established in anticancer drug discovery, because the capability of colony formation without contact to extracellular matrix or other cell types is a hallmark of cancerogenesis and correlates with the cancerogenicity of cells in mice (Hamburger and Salmon 1977; Maeno et al. 2006). Indeed, treatment with BRAFis and HSP90is in 3D soft agar assay over two weeks shows some differences compared to 2D monolayer culture.

HT-29, RKO and Caco-2 cells grew very well in soft agar, forming well-defined and dense colonies. OX-CO-1 cells grew very well, too, but colonies were blurred by spread single cells, disturbing the final read out. The BRAFV600mut COLO 201 cell line, which grows low-adherent in 2D monolayer culture, making it not suitable for resazurin assay, grows well in soft agar and forms well-defined small colonies optimal for read out. So, OX-CO-1 cells were excluded from 3D soft agar anchorage-independent growth assay, but COLO 201 cells were included.

BRAFis in single treatment show similar effects compared to 2D monolayer culture in HT-29 and Caco-2 cells. Surprisingly, HSP90i single treatment shows effects in 3D at a much lower concentration than expected in 2D. Therefore, the effect of H when cells were treated with 5.5 nM in 3D was equal to the effect reached at a concentration of 14 nM in HT-29 and 17 nM in Caco-2 in 2D, respectively. Similar to that, when cells were treated with 6 nM in 3D the effect of A was equal to the treatment effect reached at a concentration of 32 nM in 2D in HT-29 and more than 2000 nM in Caco-2 in 2D (***Figure 4, Figure 7***).

By combining BRAFis with HSP90is, BRAFV600mut cells were affected strikingly (***Figure 7***). In contrast to 2D monolayer culture, the combination in HT-29 shows slight synergistic or at least additive effects (***Table 2***) rather than slight antagonistic effects. Unfortunately, results in COLO 201 do not fulfil requirements for Bliss-CI calculation. But the combination of BRAFi with HSP90i shows clear beneficial effects in COLO 201 cells, consistent for all used compounds, suggesting synergism. In contrast to COLO 201, in HT-29 cells non-effective concentrations in single treatment remained non-effective when combined (***Appendix, Figure 16***).

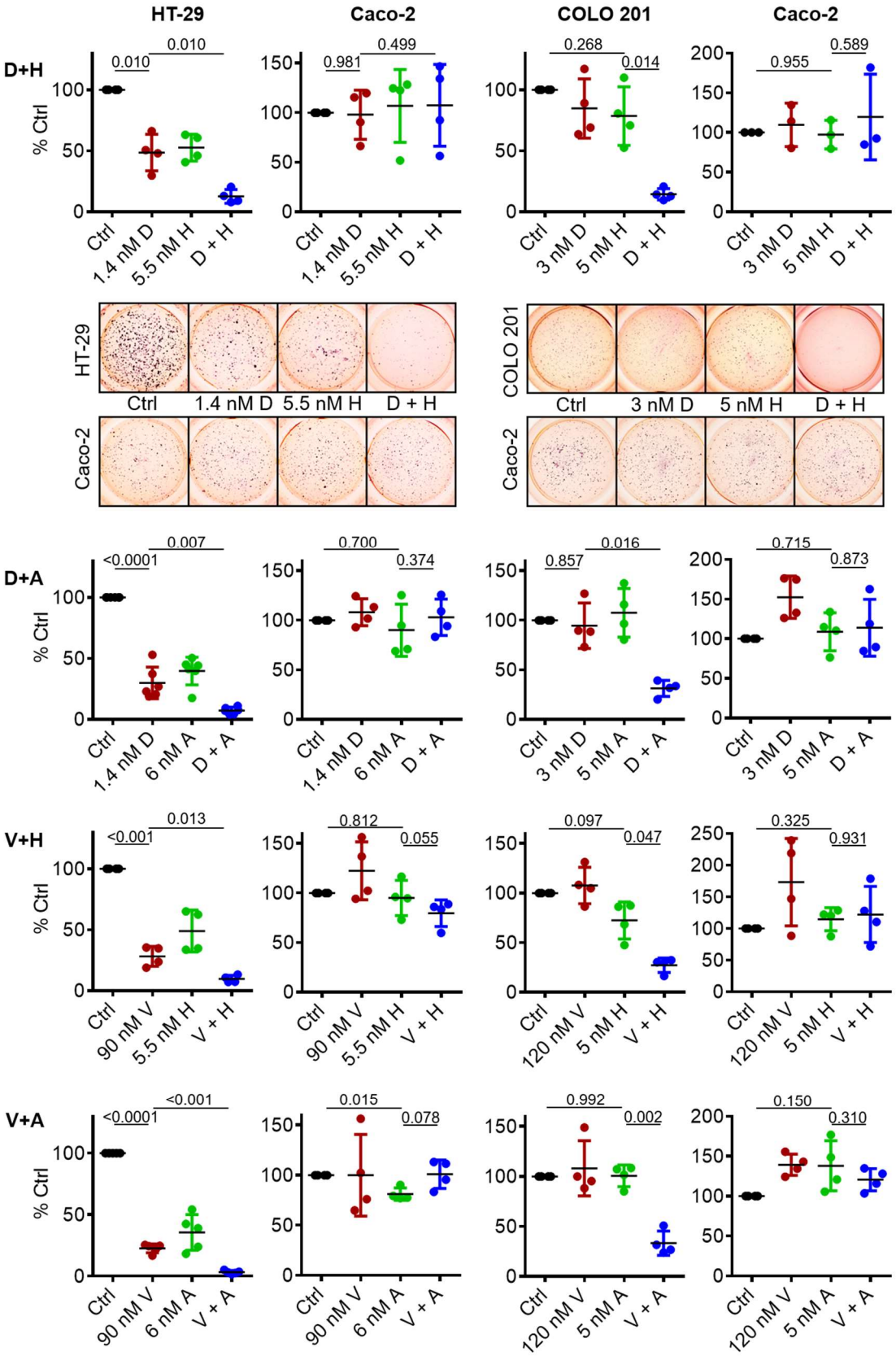

Figure 7: *HT-29, COLO 201 and Caco-2 were treated with dabrafenib (D), vemurafenib (V), HSP990 (H) and 17-AAG (A) in combination or alone for 14 d in soft agar (means with standard deviation). Colony count was normalized to vehicle treated control (Ctrl). p values of one-way ANOVA (most effective single treatment vs. Ctrl or combination).*

Caco-2 cells were treated with the same concentrations as HT-29 and COLO 201 to enable direct comparison. In contrast to the tested BRAFV600mut cell lines, BRAFwt Caco-2 cells were not affected to a similar extent. Caco-2 cells even seem to be slightly stimulated by BRAFi and HSP90i single treatments. However, these effects are not entirely reproducible.

Table 2: *Bliss-CI of BRAFi+HSP90i in HT-29 cells treated in soft agar assay.*

	Bliss-CI mean (95% CI)	*p* (Bliss-CI ≠ 1)
D + H	0.84 (0.71 - 0.97)	0.035
D + A	0.94 (0.89 - 1.00)	0.062
V + H	0.94 (0.84 - 1.05)	0.190
V + A	0.95 (0.92 - 0.98)	0.018

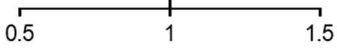

Abbreviations: 17-AAG (A), Bliss-Combination index (Bliss-CI), Confidence interval (CI), dabrafenib (D), HSP990 (H), vemurafenib (V)

4.4 Combining BRAFi with HSP90i inhibits tumour growth in mice

Although 3D anchorage-independent growth conditions are somewhat closer to the natural *in vivo* situation than 2D monolayer cultures, they still remain an artificial system. Therefore, the efficacy of the combination treatment was further investigated *in vivo* in mice. The mouse experiments were kindly performed by our collaborator Thomas Müller (Arbeitsgruppe Experimentelle Onkologie, Klinik für Innere Medizin IV, Universitätsklinikum Halle). As part of this thesis, the analysis of *in vivo* data was performed.

In contrast to COLO 201, HT-29 cells are widely used for xenograft models and their use is also well established in Thomas Müller's laboratory. Since HT-29 cells show synergistic or at least additive combination treatment effects for D combined with H in 3D, the *in vivo* study of combination effects was conducted with these HT-29 cells.

Mice were injected with luciferase-expressing HT-29 cells, which were then treated with vehicle, D, H or with the combination of D with H. For each treatment group, eight mice were used. In H single treatment group, one mouse had to be excluded from analysis of tumour growth and metastasis, because of insufficient tumour establishment. In general, mice tolerated the treatment well, without recognisable behavioural changes. Mice treated with a combination of D and H lost weight up to 13.9% one day after injection, but they recovered after two to three days. Additionally, mice treated with D and H in combination showed diarrhoea more often compared to H only, but not longer than two days after injection. No diarrhoea occurred in mice treated with vehicle or D alone (***Appendix, Figure 17***).

Tumours in mice treated only with D or H seemed to be smaller and to grow slower compared to tumours in vehicle-treated mice (***Figure 8***). However, when tumour volumes were compared to vehicle-treated Ctrl, data were too similar to claim a substantial treatment effect for single treatments (p=0.211 or 0.120 for D or H vs. Ctrl at day 30, respectively). When D and H were combined, tumour growth in mice was remarkably suppressed and tumours were on average more than three times smaller than in mice treated with vehicle only (D+H *vs.* Ctrl: p=0.005). Compared to the most effective single agent, which was H, tumours in combination-treated mice were on average half in size at day 30 (D+H *vs.* H only: p=0.345).

To ensure that the bioluminescence data about tumour volume were representative for the actual tumour burden, tumours were excised and weighed after killing mice at day 34 (***Figure 8 D***). Again, tumours of mice treated with combination of D and H were considerably lighter than those of mice treated with vehicle only (D+H *vs.* Ctrl: p=0.009). Compared to the most effective single agent H, the weight of tumours in combination-treated mice was on average half as high (D+H *vs.* H only: p=0.308).

To investigate the treatment effects in terms of metastasis, lungs were taken out after killing mice at day 34 and bioluminescence of luciferase-expressing HT-29 cells metastasized into the lungs was measured (***Figure 8 C***). All in all, data points were substantially overlapping. Nevertheless, metastases developed somewhat less frequently in mice treated with H only, compared to vehicle-treated mice (H only *vs.* Ctrl: p=0.305). In D-only-treated mice, there was no reduction of metastasis development compared to vehicle-treated mice. Mice treated with D in combination with H developed metastasis more inconsistently, but on average less metastases were developed compared to vehicle-treated Ctrl (D+H *vs.* Ctrl: p=0.340). Combination-treated mice compared to most effective single agent H-treated mice developed only slightly less metastases (D+H *vs.* H only: p=0.971). However, some combination-treated mice showed remarkably higher, some remarkably less metastatic burden than H-only-treated mice.

After normalization, single data points of D only treated mice are higher than vehicle-treated Ctrl, which prohibits Bliss-CI calculation including all data. Therefore, Bliss-CIs were calculated as an orientation only, using the means of each treatment group without considering any CIs or distributions. For all three outcomes, namely tumour volume *in situ* at day 30, tumour weight *ex situ* and lung metastasis, the Bliss-CIs are less than one: 0.91, 0.84 and 0.76, respectively.

All in all, in this mice experiment data were too overlapping to allow clear conclusions, but treatment effects show a promising tendency towards synergism for the combination of H with D in mice.

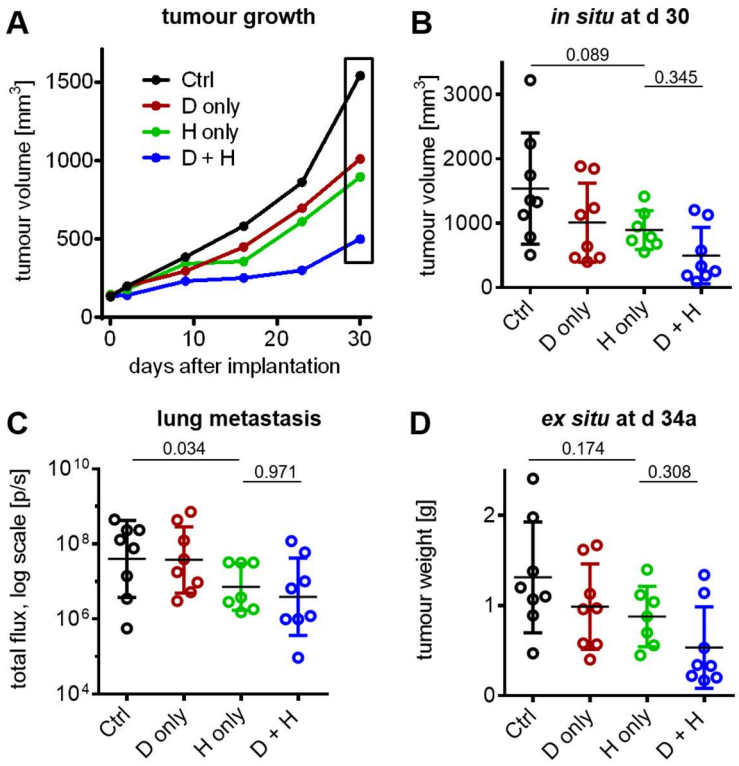

Figure 8: *HT-29 xenografts treated with dabrafenib (D), HSP990 (H) or vehicle-treated control (Ctrl)* ***A*** *Tumour volume in situ, measured by bioluminescence over 30 days, means only.* ***B*** *Tumour volume in situ at day 30 (means with standard deviation (SD), out of the black frame in A).* ***C*** *Lung metastasis measured by bioluminescence (means with SD), Y-axis in log-scale.* ***D*** *Weight of explanted tumour (means with SD). p values of one-way ANOVA (most effective single treatment vs. Ctrl and combination).*

5 Discussion

A significant number of CRC harbours a BRAFV600 mutation, which is associated with poor prognosis and escape from chemotherapy responses (Gonsalves et al. 2014; Ursem et al. 2018). Unfortunately, in contrast to BRAFV600mut malignant melanoma, promising preclinical studies in CRC led to very limited clinical successes, although much effort has been taken to improve progression-free survival and OS (***Appendix, Table 3***). Since CRC is a highly complex disease, with high signalling plasticity and high intra- and intertumour heterogeneity, targeted therapy becomes very challenged and complicated, because of the development of many resistance mechanisms, as seen in BRAFi treatment (***Appendix, Table 4***). Targeting only a few key players in a signalling network might therefore not be enough to prevent or overcome resistance development. Therefore, combining a selective BRAFi with a HSP90i, which affects multiple known members of resistance simultaneously, might be a more viable approach to combination treatment of BRAFV600mut CRC.

This thesis shows that the viability of different BRAFV600mut CRC cell lines was effectively reduced, combining BRAFis with HSP90is, compared to single treatment in 2D monolayer culture. Subsequently, striking combination treatment effects in 3D anchorage-independent culture were observed. Finally, combining BRAFi with HSP90i shrinks BRAFV600mut mice xenografts somewhat more effectively than single treatments.

Taken together, these results indicate that synergistic treatment effects of BRAFis combined with HSP90is in BRAFV600mut CRC cells can occur and further studies are warranted to clarify more details.

5.1 Discussion of results

Since the analysed CRC cell lines were derived from different patients, they have a heterogeneous mutational background (Medico et al. 2015), analogue to great heterogeneity of CRC in patients. Therefore, it is not at all surprising that the cell lines studied in this thesis slightly differ in their treatment responses, even if they share a joint mutation like BRAFV600E. Recently, Sveen et al. analysed many CRC cell lines regarding MSI status and CMS classification and they checked for HSP90i response among others (Sveen et al. 2018). OX-CO-1 cells were classified as MSS CMS4 and HT-29 cells as MSS CMS3. RKO cells were revealed MSI, but they could not be clearly assigned to one single CMS group. However, they showed more similarities with CMS1 and 4 rather than CMS2 and 3. Interestingly, CMS1 and 4 CRC cell lines were shown to be substantially impacted by HSP90i treatment, whereas CMS2 and 3 CRC cell lines were shown to be more HSP90i resistant. In 2D monolayer cell culture, viability of BRAFV600mut cells was

reduced more effectively when treated with the combination regimen rather than single treatment (***Figure 5***). However, HT-29 cells showed slight antagonistic effects, whereas OX-CO-1 cells strictly undulated around additivity. RKO cells showed slight synergism when moderate concentrations of compounds were applied (***Figure 6***). These differences are in line with the findings of Sveen et al.. Especially MSI in RKO and the resulting hypermutation phenotype, which makes physiological function of proteins more dependent on sufficient support by chaperones (Schopf et al. 2017), might contribute to stronger combinational treatment effects in RKO cells than in MSS OX-CO-1 and HT-29 cells. However, in single treatment, the three cell lines behaved completely contrary (***Figure 4***). Here, HT-29 cells were the most sensitive and RKO cells the most resistant BRAFV600mut cells against HSP90i treatment. MSS CMS4 Caco-2 cells, which should be very HSP90i sensitive according to Sveen et al., turned out the most HSP90i resistant cells in this thesis, especially against A. However, direct comparisons of cells' response between this thesis and the findings of Sveen et al. should be taken with caution, because of different HSP90is utilised in both studies: ganetespib, luminespib and radicicol vs. A and H. In a different paper where A was tested in Caco-2 and HT-29 cells, results were highly consistent with A and H single treatment results of this thesis (Mayor-López et al. 2014). Because of a lack of NQO1, which is a dehydrogenase required for sufficient A function, Caco-2 cells bear an intrinsic resistance against A (Mayor-López et al. 2014), which might explain the low response to A single treatment. The high BRAFi resistance of RKO cells (***Figure 4***) and the synergistic combination treatment effect, combining HSP90i with BRAFi in this cell line might be in part explained by a PI3K gain of function mutation (Medico et al. 2015). As mentioned above (***see 1.7.3***), PI3K and the downstream AKT and mTor are key players in BRAFi resistance (Mao et al. 2013) and the PI3K pathway is highly dependent on HSP90 (Kryeziu et al. 2019; Pratt et al. 2008). It was shown that A treatment in RKO cells remarkably reduces phospho-AKT levels (Saturno et al. 2013). However, when treated with a different HSP90i, AKT was shown to drive HSP90i resistance in RKO cells, even in combination with a BRAFi (Wang et al. 2016). Therefore, the mechanisms of interactions of HSP90is and BRAFis might be a promising research topic for future studies to clarify their action at the proteomic level. The slight stimulation of Caco-2 cells when treated with low doses of BRAFi might be explainable; it may occur because of the often mentioned paradoxical MAPK-cascade activation effect in BRAFwt cells (Adelmann et al. 2016; Menzies et al. 2013).

Initially observed slight antagonistic effects in HT-29 cells grown in 2D turned into slight synergistic effects or at least additive effects in 3D anchorage-independent cell culture. Moreover, COLO 201 cells showed striking synergistic effects, when treated with the

combination of HSP90i and BRAFi (***Figure 7***). In contrast, BRAFwt Caco-2 cells did not seem to be much affected by the same compound concentrations, whether applied as single or as combination treatment. COLO 201 cells are MSS (Medico et al. 2015). Unfortunately, Sveen et al. did not analyse COLO 201 cells for CMS status, but only COLO 205 cells. Both cell lines are derived from the same patient: COLO 201 from the primary tumour and COLO 205 from a metastatic site (Ilyas et al. 1997). Both show the same profile, when they were analysed for different mutations, MSI status and short tandem repeat loci (Medico et al. 2015). So, they also might behave similarly regarding CMS classification. COLO 205 cells were classified as MSS, too, but, like RKO cells, they could not exactly be assigned to one CMS group. However, they showed more similarities with CMS1 rather than with other groups (Sveen et al. 2018). As mentioned above, BRAFmut MSS CMS1 CRCs are associated with a very poor prognosis, because of frequent metastasis, among other causes (Smeby et al. 2018). Since cancer cells, which are easily able to form colonies in anchorage-independent environment, are considered to have high metastatic and carcinogenic potential (Mani et al. 2008; Morata-Tarifa et al. 2016; Nomura et al. 1989), the striking reduction of colonies when treated with HSP90i and BRAFi in combination in COLO 201 cells is highly promising. Interestingly, HSP90i treatment effects in 3D cell culture were reached at much lower concentrations than in 2D. HSP90 has been shown to be involved in EMT in CRC cells (Nagaraju et al. 2015). EMT is a hallmark of metastasis and cancer progression (Pastushenko and Blanpain 2019). Cells, which undergo EMT, have been shown to increase their ability to form colonies, especially in anchorage-independent environment (Mani et al. 2008). This might be an explanation, why cells were more sensitive to HSP90i in soft agar compared to 2D monolayer culture, where cells were allowed to grow on a plastic surface. In line with this proposition, treatment with H, but not with D has led to reduction of metastasis development in mice (***Figure 8***).

In mice, combination treatment of H and D led to a remarkable reduction of tumour size and tumour weight compared to vehicle-treated Ctrl, which was on average greater than the reduction of tumour size and weight in the single treatment groups. Additionally, roughly calculated Bliss-CI values for tumour shrinkage and metastasis development were below one, which does not contradict prior *in vitro* data. However, as mentioned above in section 4.4, Bliss-CI values calculated from *in vivo* data here were not robust enough to perform proper hypothesis testing or to use for further calculations, but they might serve as an orientation for future studies.

All in all, *in vivo* data seem to confirm the prior *in vitro* data, even if not as convincing as expected, keeping in mind, that conclusions from small datasets are inherently very limited.

In the last two decades, several HSP90i entered clinical trials. However, none of them was finally approved for clinical use, yet. Ineffective in single treatment and with severe adverse effects, HSP90i often entered only phase I trials (Kryeziu et al. 2019; Sanchez et al. 2020). For example H, which was considered a highly promising oral available candidate when experiments in this thesis began, with tolerable side effects in rodents, turned out to be neurotoxic in humans, which was not seen in mice before (Spreafico et al. 2015). Diarrhoea was the most frequent adverse effect seen in the majority of patients (Spreafico et al. 2015). Although compounds used in this thesis were tolerated relatively well by mice, mice treated with H also developed diarrhoea more often than mice treated with vehicle or D only.

However, new HSP90i currently are under development, which might be more effective and less toxic (Sanchez et al. 2020). AUY992, a relative to H is the best studied HSP90i right now, which was tested in several phase II trials, displaying a moderate toxicity (Bendell et al. 2016; Felip et al. 2018; Renouf et al. 2016). AUY992 shows promising activity in patients with EGFR-mutated non-small cell lung cancer with tolerable adverse effects as single treatment (Felip et al. 2018; Piotrowska et al. 2018). Unfortunately, in combination with erlotinib, which is an EGFRi, severe neurological toxicities led to trial termination before the endpoint was reached (Johnson et al. 2015). In patients with trastuzumab-resistant breast cancer and in patients with gastrointestinal stroma tumours, AUY992 showed activity, too (Bendell et al. 2016; Kong et al. 2016). However, CRC seems to be highly resistant against AUY992 *in vitro* (Lee et al. 2017). When different compounds were tested in this thesis, AUY992 was also tested with almost no effectivity in HT-29 cells at nanomolar concentrations, while A and H showed striking reduction in cell viability (***Appendix, Figure 15***). One explanation was that AUY992 might have a weaker affinity to its binding site and consequently a weaker ability to maintain protein degradation compared to H (Lee et al. 2017). Another potential explanation was given by Wang et al., namely ERK and AKT reactivation after AUY992-treatment in BRAFmut RKO cells, due to the replacement of HSP90 chaperoning effect by the HSP90 co-chaperone CDC37. CDC37 obviously becomes able to stabilise BRAFV600 and AKT in BRAFmut RKO cells, when HSP90 itself becomes inhibited. In contrast, chaperoning seems to be CDC37-independent in BRAFwt Caco-2 cells. Additionally, V was shown to sensitize RKO cells to AUY992 by suppressing AKT activity by BRAF inhibition, resulting in more efficient combination effects compared to single treatment in 3D culture (Wang et al. 2016). This is highly promising and in line with findings of this thesis: it suggests an overcoming of resistance against BRAFi, because of HSP90i and vice versa. However, Wang et al. did not use other cell lines or other HSP90is for comparison in their mechanistic studies, so it remains unclear, why RKO cells remain more resistant against AUY992, but not as much against

A or H, as seen in this thesis. Moreover, Wang et al. concluded, that BRAFmut CRCs cells were generally more resistant against HSP90is, compared to BRAFwt CRC cells, which was clearly not seen in this thesis (***Figure 4***) or in other publications (Mayor-López et al. 2014). This shows the great importance of choosing the compounds to use in a special system very carefully, even if they show promising effects in different, albeit similar system. It also shows the importance of testing different compounds with comparable mechanisms, to reduce the risk of missing important effects of a compound class. For example, if only AUY992 would have been used in this thesis as representative member of HSP90i-family, beneficial effects of other HSP90is like A and H would not have been recognised. Furthermore, testing different compounds with comparable mechanisms in parallel reduces the risk to misinterpret off-target effects as real, hypothesis-supporting on-target effects. In addition, it is very important to evaluate a specific question in different model systems, to ensure that measured effects are neither outliers nor artificial. Therefore, different cell lines, different compounds and different cell culture systems were used in this thesis.

5.2 Discussion of methods and limitations

Comparisons of the results generated as part of this thesis research by 3D- and 2D culture experiments had to be done cautiously, because, on one hand, the assays measure different cell properties: proliferation – and in line with this metabolic activity – versus anchorage-independent colony forming ability. On the other hand, different cell culture conditions had to be employed in this thesis. Firstly, for technical reasons, to obtain a one-fold concentrated agar/DMEM solution, the basal medium was changed from the ready-to-use liquid DMEM to a powdered DMEM, which was dissolved according to manufacturer's instructions. Secondly, different FBS concentrations were applied. In 2D assays, which were performed prior to 3D soft agar anchorage-independent growth assays, cells were kept at low glucose and low FBS conditions to avoid flushing cells with an excess of growth factors and nutrients, which might reduce the observable drug effects. Glucose at concentrations of ca. 6 mM instead of 25 mM and 5% FBS instead of 10% FBS were used. These were the lowest concentrations well-tolerated by the cell lines investigated. However, in 3D soft agar anchorage-independent growth assays, the cells started to die when they were cultured in 5% FBS. Therefore, it was necessary to change FBS concentration from 5% to 10%. Glucose concentrations were kept similar. COLO 201 cells were tested in 2D- monolayer cell culture as well, but showed a very low adherence, with the majority of cells growing in suspension. Therefore, COLO 201 were only used in 3D soft agar anchorage-independent growth assays.

The *in vivo* experiments have been done by Thomas Müller (Arbeitsgruppe Experimentelle Onkologie, Klinik für Innere Medizin IV, Universitätsklinikum Halle) as a collaboration. The results seem to support the hypothesis of synergistic combination treatment effects of HSP90i and BRAFi. However, the data points were too scattered to show clear superiority against the most effective single agent, according to HSA model or to allow proper hypothesis testing for Bliss-CIs. One reason might be the evaluation of a relatively weak synergism with a Bliss-CI close to 1 in a system highly sensitive against external disturbing factors (Bliss-CI of D+H in HT-29 in 3D-Soft agar independent assay: 0.84 (95%CI: 0.71-0.97)). Although recent *in vivo* experiments were well-controlled and had a high degree of standardisation, they are still a very complex system, with living animals in an environment impacted on by many factors, which are barely controllable or not influenceable at all (Abdulai-Saiku et al. 2017; Kafkafi et al. 2018). For example, even different sexes of care takers might affect stress levels in mice and this might affect experimental outcomes (Arranz et al. 2010; Sorge et al. 2014). Doses of compounds were administered as suggested in the previous literature (King et al. 2013; Menezes et al. 2012). However, compound concentrations reached in blood and especially in xenografts were not measured in this thesis, so it remains unknown if the same final concentrations were reached. Another reason could be the reduction of evaluated mice in one group. Initially, 8 mice were used in each group. Unexpectedly, one mouse had to be excluded in the evaluation of tumour shrinkage and metastasis development, because of insufficient tumour formation after injection with HT29 cells. Therefore, only 7 mice were followed up in the H only group while in the other three groups, data were generated from all 8 mice. Since the number affects the test power directly, exclusion of one mouse in the H-group might have led to overlapping data. Nevertheless, even if mice numbers would have been increased or if compound blood concentrations were monitored, it remains possible that the combination effects of H and D in HT-29 xenografts are not as synergistic as expected in mice. Therefore, it would be of great interest to test different BRAFmut CRC cell lines, like COLO 201 or RKO, and to test different compounds in mice as well. If there would be substantial differences in response observed between the different cell lines, mutational or proteomic profile analyses might reveal a favourable phenotype regarding the sensitivity against specific HSP90i and BRAFi combination.

Taken together, it is very important to analyse the generated data in an appropriate manner, fully knowing and considering the limitations of the respective methods. For example, when combination treatment effects are only compared to vehicle-treated Ctrl or single treatment, it is not appropriate to conclude a superiority of combination treatment over single treatment, just based upon a reduction in cell number or viability.

Although scientific discussions on how to evaluate synergism correctly already started more than a century ago (Bliss 1939; Foucquier and Guedj 2015), there is still no universally accepted method to determine this available, depicting the striking complexity of this topic (Foucquier and Guedj 2015).

However, two widely used methods were established: Loewe additivity and Bliss independence. The Loewe additivity model defines additivity as the treatment effect observed when a compound is combined with itself, i.e. without any interaction between compounds (Loewe and Muischnek 1926). Effects above or beneath Loewe additivity were consequently defined as synergism or antagonism, when drug – drug interactions occur. The Loewe additivity model is considered to be the most accurate model depicting drug – drug interactions, but only in a very limited framework (Roell et al. 2017): First, it requires very well characterised dose- or concentration-effect curves, by measuring as many dose or concentration points as possible. This was implemented in the experimental set-up for the 2D monolayer culture resazurin assay in this thesis research. Second, when a nonlinear regression model is fitted to that dataset, the data need to fit to an almost perfectly shaped sigmoidal function between 1 (Ctrl-normalized maximum treatment effect) and 0 (Ctrl-normalized minimum treatment effect), which very often fails in reality, as, for example, in this thesis research. And third, the relation of concentrations or doses of the combined compounds needs to be constant over the whole curve. This criterion was also not feasible for the experiments described in this thesis, because of the distinct pharmacodynamics of BRAFis and HSP90is investigated. Concentration-effect curves of A and H showed a much steeper slope with a much shorter concentration range between maximum effect and non-effectiveness at all, compared to V and D (***Figure 4***). Therefore, quite different dilution factors were required in order to prepare serial dilutions of compounds to get enough meaningful data points. For example, in RKO cells the dilution factor was 1.6 versus 40 for serial dilutions of H and D, respectively. If the concentration ratio had been fixed, the generation of evaluable data between 0 and 100% treatment effect would have been all but impossible. For this reason, the utilization of the more recently developed and widely accepted Chou-Talalay method was also prohibited, because it requires constant concentration ratios as well (Chou 2010). Choosing the correct model of synergy evaluation for the data of interest is often neglected, leading to invalid results, because limitations of the different models are not considered properly (Roell et al. 2017). Therefore, mainly the Bliss-independence model was chosen for analyses in this thesis. It is based on the assumption that two combined compounds act independently from each other, for example in different organs, different cell compartments or different signalling pathways, which do not affect each other. In this case, the

combinational treatment effect of the two compounds is defined as Bliss-independent or, synonymously, additive (Bliss 1939; Foucquier and Guedj 2015). Again, effects above or beneath additivity are consequently defined as synergism or antagonism. Simultaneously, this depicts the major limitation of Bliss-independence model. When two compounds are combined in a living organism, their actions are seldom completely independent from each other (Roell et al. 2017). But, the Bliss-independence model is more tolerant with respect to dose- or concentration-effect curves and does not necessarily require a well-defined sigmoidal function (Foucquier and Guedj 2015). However, it does only work, if the combinational treatment effects range between 0% and 100%, when normalized to Ctrl (Foucquier and Guedj 2015). So, it was feasible just for a subset of the data in this thesis, especially for the 2D resazurin assays. In 3D soft agar anchorage-independent growth assays, the BRAFi single-treated COLO 201 and Caco-2 cells often showed a higher colony forming activity compared to vehicle-treated Ctrl, which made the use of Bliss-independence model impossible for these two cell lines (***Figure 7***). Therefore, a different approach was used to evaluate combination treatment effects, which is called the HSA approach. It queries if the combination of two compounds is more effective than the most effective single compound used at same concentration as in combination (Foucquier and Guedj 2015). It is important to consider that additive and synergistic treatment effects are not distinguished from each other by HSA. So actually, it is not appropriate to speak about synergism when HSA was used exclusively, except for the case when at least one of the compounds is virtually ineffective when used in a single agent treatment. Then, a higher combination treatment effect is assumed to depict synergism (Foucquier and Guedj 2015), as seen in combination treatment of BRAFi and HSP90i in COLO 201 cells in 3D soft agar anchorage-independent growth assay (***Figure 7***).

As mentioned in the method section, one-way ANOVA and one-sample t-test were performed for hypothesis testing. But the term ‘statistically significant’ was consciously avoided in this thesis. A somewhat arbitrary threshold, which divides results into statistical significant and non-significant, often leads to misinterpretation of data. For example, confounding of the probability that the result data include a distinct effect with the effect itself. If an effect was there, but a low repeat number or a broad distribution of data points has led to broad CIs, including the Ctrl value with a consecutive p value > 0.05 of difference, then it would be false to conclude that there was no effect, because of statistical insignificance (Wasserstein et al. 2019). Unfortunately, this kind of misinterpretation is widely distributed and has been found in more than half of a subset of analysed published articles (Amrhein et al. 2019). Additionally, the strong focus on $p \leq 0.05$ has contributed to selective data publication (Wasserstein et al. 2019). Therefore,

presentation of data was done, according to the recommendations in the statement of the American Statistical Association on statistical significance and *p* values (Wasserstein and Lazar 2016). This means, reporting all *p* values and leaving out asterisks, which suggest the particular importance of selected data.

5.3 State-of-the-art therapies and outlook

As mentioned in section 1.6, MSI-high-status and BRAFV600mut in non-advanced CRC have a relative good prognosis. However, this changes dramatically in metastasised disease (***Figure 3***). In Germany, decision making in choosing treatment regiments for CRC, according to the current S3 evidence based guideline for CRC version 2.1 is based on several components (Deutsche Krebsgesellschaft, Deutsche Krebshilfe, AWMF 2019). First and most important, the patient's general condition determines, whether a curative therapy regiment is pursued or not. Second, the tumour stage according to Union for International Cancer Control (UICC) 2017, which is based on histopathological TNM classification, describing depth of infiltration (T), lymph node metastasis (N) and metastasis to different organs or lymph nodes beyond local lymph drainage area (M) is taken into consideration. Third, MSI-testing and molecular diagnostics, especially in advanced disease, are key determinants. In UICC stage I tumours, which are restricted to the colon wall and do not infiltrate the surrounding fatty tissue, primary complete resections without adjuvant chemotherapy is the therapy of choice. In tumours higher than UICC stage I, MSI diagnostic became fundamentally important as a powerful prognostic and predictive marker (***see 1.6***). In UICC stage II tumours, which are no longer restricted to the colon wall, but infiltrate surrounding fatty tissue, peritoneum or other organs, but without lymph node (UICC stage III) or distant metastasis (UICC stage IV), an adjuvant chemotherapy should be considered. However, patients with MSI-high tumours do not benefit from adjuvant chemotherapy, because of their good prognosis compared to MSS tumours in this stage. So MSI-testing is essential, prior to therapy. Patients with UICC stage III CRC receive chemotherapy, regardless of whether they bear MSI-high tumours or not. But, in contrast to UICC stage II tumours, MSI-high UICC stage III tumours show a greater sensitivity to chemotherapy than MSS UICC stage III tumours (Elsaleh and Iacopetta 2001). In contrast to lower stage CRC, in metastatic CRC, which resembles UICC stage IV, targeted therapy regimens are implemented in clinic yet. If the patient is fit enough for a systemic therapy, different options, consisting of chemotherapy double or triple combination, VEGF antibody bevacizumab and the EGFR-antibodies panitumumab or cetuximab are available. The choice is dependent on tumour location and tumour mutational profile, regarding RAS and BRAF. As mentioned above, BRAFV600 mutations are mutually exclusive for RAS mutations (Pietrantonio et al. 2015). Therefore, specimens are tested for (all)RAS mutations first. According

to the current S3 guideline, those patients with RAS mutations should be treated with a chemotherapy double combination plus bevacizumab, since RAS mutations lead to resistance in anti-EGFR therapy. If the tumour is RASwt, then molecular diagnostics are performed with respect to BRAFV600mut. BRAFwt tumours are then treated with a chemotherapy double combination plus an anti-EGFR Antibody, like bevacizumab or panitumumab. However, this is valid for left sided colon carcinoma only. Interestingly, regardless of BRAFwt or BRAFV600mut, right sided RASwt tumours were shown to be more resistant to anti-EGFR-treatment, traced back to different cancerogenesis pathways and their related different mutational profiles, like serrated pathway and MSI-high, as mentioned in section 1.2 (Holch et al. 2017; Tejpar et al. 2017). Therefore, right sided KRASwt/BRAFwt tumours are treated with a chemotherapy double combination plus bevacizumab. Because BRAFV600 mutations are an independent negative prognostic factor, associated with a worse prognosis in metastatic CRC, efforts were taken to strike hard, initially. Therefore, instead of a chemotherapy double combination, a triple combination plus bevacizumab is recommended as first line. For second line, inclusion in clinical trials is recommended. And, interestingly, an experimental off-label use of BRAFi, MEKi or anti-EGFR antibody is proposed. However, the guideline here refers to a phase II pilot trial of V monotherapy in BRAFmut CRC, where a beneficial treatment effect of V was clearly not seen (Kopetz et al. 2015). Instead, a move onward to combinations of different inhibitors with BRAFis was recommended and performed in clinical trials with initial promising results (Kopetz et al. 2015; Kopetz et al. 2019).

In refractory disease, in spite of chemotherapy and antibody therapy, regorafenib is available as approved drug for advanced CRC (Deutsche Krebsgesellschaft, Deutsche Krebshilfe, AWMF 2019). Regorafenib is a multikinase inhibitor, which inhibits VEGFR (VEGF receptor), TIE2 (tunica interna endothelial cell kinase), PDGFR, FGFR (fibroblast growth factor receptor), KIT (proto-oncogene KIT), RET (RET-proto-oncogene), CRAF and BRAF. Two phase III clinical trials (CORRECT, identifier: NCT01103323; CONCUR, identifier: NCT01584830) could show superior OS in regorafenib-treated patients compared to placebo Ctrl with a 1.4 and 2.5 months longer median OS (Grothey et al. 2013; Li et al. 2015). However, this treatment option is being controversially discussed, because, on the one hand, study results are based on comparison to placebo and not to another therapy regimen currently accepted, and on the other hand, because of high therapy associated toxicity (Deutsche Krebsgesellschaft, Deutsche Krebshilfe, AWMF 2019; Grothey et al. 2013). After a re-evaluation of additional benefits, the ‘Gemeinsamer Bundesausschuss’ came to the result that an additional benefit using regorafenib, in comparison to best supportive care, was not evident, because of lower quality of life, serious disease-related

symptoms and more adverse treatment effects in regorafenib-treated metastatic CRC patients, compared to best supportive care. Additionally, the two phase III trials mentioned above were revealed not to be representative for patients receiving regorafenib in clinical practice, regarding their age and general condition (Gemeinsamer Bundesausschuss 2016). The 'Gemeinsamer Bundesausschuss' is a central institution in Germany for therapeutic benefit assessment, among other duties. Consequently, regorafenib was removed from German market in 2016 (Hillienhof 2016).

Other molecular analysis in UICC stage IV CRC include MSI-status as well, because of promising initial results of checkpoint inhibitor treatment in MSI-high CRC and HER2 status, regarding an off-label use of the anti-HER2/neu antibody trastuzumab as second line. The treatment of rectal cancer differs from colonic cancer, with respect to possible neoadjuvant radiation combined with chemotherapy, depending on UICC stage and location (Deutsche Krebsgesellschaft, Deutsche Krebshilfe, AWMF 2019).

It is quite exciting to see the development of clinical research in treatment of BRAFmut CRC, which accelerates increasingly from BRAFi monotherapy a few years ago, to triple therapy regiments with chemotherapy, BRAFi and a third targeted approach (***Appendix, Table 3***). Very recently, Kopetz et al demonstrated beneficial treatment effects, combining V with irinotecan and with the EGRFi cetuximab (Kopetz et al. 2021). Currently, approximately 40 clinical trials are active, which evaluate a combination therapy of a BRAFi, including regorafenib with at least one other combination partner (search request in https://clinicaltrials.gov: Condition or disease: 'Colorectal Neoplasms'; other terms: 'dabrafenib OR vemurafenib OR encorafenib OR regorafenib'; status: 'Recruiting', 'Not yet recruiting', 'Active, not recruiting', 'Enrolling by invitation'; accessed on 22nd Nov. 2021). Two major types of combinations become apparent: BRAFi with a checkpoint inhibitor or with chemotherapy optionally also combined with an EGFRi or MEKi. In contrast, only one clinical trial evaluates a HSP90i, not combined with a BRAFi, but with a checkpoint inhibitor, which is currently running (identifier: NCT03095781). This indicates that more evidence from preclinical studies is urgently needed, because as mentioned in section 1.8, HSP90 depicts a promising target, because of its role as a central key player in a biochemical network, where many different signalling pathways and especially those, which are involved in resistance mechanisms against BRAFi, were connected (Lopez and Banerji 2017).

Together with the work of Wang et al., the results of this thesis contribute to scientific evidence of a synergistic interaction of BRAFi and HSP90i, which might be a promising therapy approach in BRAFV600mut CRC (Wang et al. 2016). As mentioned above, although HSP90is did not show

substantial efficacy in colorectal cancer in clinical trials, yet, in malignant melanoma patients, promising results were reported recently. The combination of the new developed HSP90i XL888 with V shows synergistic treatment effects in BRAFmut malignant melanoma *in vitro*, *in vivo*, and even beneficial effects in a clinical phase I trial (Eroglu et al. 2018; Paraiso et al. 2012). In contrast to the previously reported toxic side effects of different HSP90is, XL888 seems to be relatively well tolerated, although, diarrhoea was reported as most common grade 3 and grade 4 adverse effect and as most common dose-limiting effect in the prior single treatment trial (Eroglu et al. 2018). Interestingly, the combination with XL888 seems to reduce V-typical skin toxicities, like development of squamous cell carcinomas or acanthomas by blocking paradoxical MAPK activation (Eroglu et al. 2018). In a context where the combination of different targeted therapy approaches often lead to severe adverse effects, which often terminates clinical trials or therapy regiments prematurely, a potentiation of treatment effects on the one hand and a reduction of adverse treatment effects on the other hand is remarkable (Lopez and Banerji 2017). Further clinical trials with XL888 are currently ongoing in malignant melanoma patients (identifier: NCT02097225, NCT02721459) and in CRC patients, as well as in combination with pembrolizumab (identifier: NCT03095781). The results are eagerly expected. At least initial data suggest a tolerable side effect profile (Mehmet et al. 2020). Moreover, several new HSP90is are currently under development, to reduce adverse effects, like in case of XL888, or to improve treatment efficacy and resistance development. As mentioned above, Wang et al. revealed the role of CDC37 in resistance against AUY992 in CRC cells. Consequently, they currently develop a compound, called 18h, which targets the HSP90 - CDC37 complex at a binding site different from HSP90-ATP-binding site, leading to HSP90 - CDC37 complex disruption. Since CDC37 is a very specific co-chaperone of HSP90, targeting the HSP90 - CDC37 complex might be a more HSP90-specific approach than ATP-bindings site-blocking HSP90is, which also affect multiple other co-chaperones. This might lead to less adverse effects (Wang et al. 2019; Wang et al. 2020). Further preclinical experiments and, hopefully, clinical trials need to show how successful this approach will be.

Albeit results of this thesis are promising and in line with current literature, additional research has to be done before entering clinical trials with the combination of BRAFi with HSP90i in BRAFmut CRC. For example, subsequent mechanistic studies are required to validate synergistic effects of HSP90 and BRAFV600 inhibition at the proteomic level. Therefore, western blots for several members of MAPK pathway and their phosphorylated isoforms, like EGFR, RAS, ARAF, BRAF, BRAFV600mut, CRAF, ERK1/2, then HSP90 and HSP70, known proteins involved in resistance mechanisms like PIK3CA, AKT etc. (***Appendix, Table 4***), as well as for apoptosis

markers might be appropriate. If the combination of BRAFi with a HSP90i acts as expected, expression levels of HSP90-dependent proteins should decrease, whilst HSP70 increases as a countereffect of HSP90 inhibition. Then, additional scenarios of time schedules for combination therapies could be tested, followed by western blotting of the mentioned proteins at different times. For example, first, a protein expression profile before treatment could be generated, followed by an interval of long term BRAFi single treatment to generate resistant cells, followed by another expression profile and then followed by a combinatory treatment setup of BRAFi and HSP90i with a third expression profile. Comparing the different expression profiles generated at the different steps during therapy could give rise to a deeper understanding how BRAFis and HSP90i do interact, especially regarding synergistic effects, for example because of overcoming resistance mechanisms. To exclude effects resulting from the sequential therapy, expression profiles, generated as described above, should be compared with protein expression profiles, generated after combination therapy without prior monotherapy. Then, experiments should be repeated with new HSP90is, which are currently under development or in clinical trials, as mentioned above. If there is a HSP90i with comparable concentration-effect-curve to BRAFi, the combination could be tested in fixed concentration ratios to evaluate synergistic effects, according to Loewe-additivity model or Chou-Talalay method, in order to confirm synergistic effects with a different approach, i.e. to consolidate evidence.

6 Summary

CRC is one of the most common and most lethal cancer entities in humans. Approximately 10% of CRCs carry a BRAFV600 mutation, which is associated with a very poor prognosis in advanced stages and an escape from standard chemotherapy. Although several compounds are already available to target mutant BRAFV600, they lack therapeutic efficacy in CRC in monotherapy, because of a broad spectrum of resistance mechanisms to escape BRAF inhibition. Therefore, many treatment attempts with BRAFi combined with another targeted therapy or chemotherapy have been initiated. However, substantial improvements of patients' survival are still lacking. Since many resistance mechanisms are dependent on sufficient HSP90 function, HSP90 might be a target of interest for combinational targeted therapy. In BRAFV600mut malignant melanoma, the combination of BRAFi with HSP90i has led to promising results. By contrast, evidence is weak in CRC.

Therefore, combination treatment effects of HSP90is and BRAFis were investigated in a preclinical setting. Different BRAFis and HSP90is were combined in different BRAFV600mut patient-derived cell lines and one BRAFwt CRC cell line, using 2D monolayer culture resazurin assay and 3D soft agar anchorage-independent growth assay as readouts. In addition, in a collaboration, a xenograft mouse model was employed to evaluate combination treatment effects *in vivo*.

This thesis shows that BRAFis and HSP90is reduce colony forming activity in 3D-soft agar anchorage-independent growth assay synergistically in BRAFV600mut CRC cell lines, with slight synergism to additivity in HT-29 cells and striking synergism in COLO 201 cells. In 2D monolayer culture resazurin assay, the proliferative activity of BRAFV600mut CRC cell lines was affected in a range from slight antagonism in HT-29 cells to slight synergism in RKO cells, but all in all generally close to additivity, with some variability, depending on the cell line investigated. In mice, the tested compounds were tolerated relatively well and showed initially promising combination treatment effects regarding tumour shrinkage and metastasis suppression.

In conclusion, this thesis reveals the combination of BRAFis with HSP90is as a promising approach in the treatment of BRAFV600mut CRC and contributes to the growing evidence for further treatment options. In addition, it calls for further studies to investigate the synergistic interaction at the proteomic level and to escalate the experimental settings to a broader spectrum of compounds and cell lines with the perspective to enter clinical trials.

7 References

Abdulai-Saiku S, Hegde A, Vyas A, Mitra R (2017) Effects of stress or infection on rat behavior show robust reversals due to environmental disturbance. F1000Res 6:2097. https://doi.org/10.12688/f1000research.13171.2

Adelmann CH, Ching G, Du L, Saporito RC, Bansal V, Pence LJ, Liang R, Lee W, Tsai KY (2016) Comparative profiles of BRAF inhibitors: the paradox index as a predictor of clinical toxicity. Oncotarget 7:30453–30460. https://doi.org/10.18632/oncotarget.8351

Ahsan A, Ray D, Ramanand SG, Hegde A, Whitehead C, Rehemtulla A, Morishima Y, Pratt WB, Osawa Y, Lawrence TS, Nyati MK (2013) Destabilization of the epidermal growth factor receptor (EGFR) by a peptide that inhibits EGFR binding to heat shock protein 90 and receptor dimerization. J Biol Chem 288:26879–26886. https://doi.org/10.1074/jbc.M113.492280

Amrhein V, Greenland S, McShane B (2019) Scientists rise up against statistical significance. Nature 567:305–307. https://doi.org/10.1038/d41586-019-00857-9

Andrews MC, Behren A, Chionh F, Mariadason J, Vella LJ, Do H, Dobrovic A, Tebbutt N, Cebon J (2013) BRAF inhibitor-driven tumor proliferation in a KRAS-mutated colon carcinoma is not overcome by MEK1/2 inhibition. J Clin Oncol 31:e448-51. https://doi.org/10.1200/JCO.2013.50.4118

Arranz A, Venihaki M, Mol B, Androulidaki A, Dermitzaki E, Rassouli O, Ripoll J, Stathopoulos EN, Gomariz RP, Margioris AN, Tsatsanis C (2010) The impact of stress on tumor growth: peripheral CRF mediates tumor-promoting effects of stress. Mol Cancer 9:261. https://doi.org/10.1186/1476-4598-9-261

Ashida R, Tominaga K, Sasaki E, Watanabe T, Fujiwara Y, Oshitani N, Higuchi K, Mitsuyama S, Iwao H, Arakawa T (2005) AP-1 and colorectal cancer. Inflammopharmacology 13:113–125. https://doi.org/10.1163/156856005774423935

Atreya CE, van Cutsem E, Bendell JC, Andre T, Schellens JHM, Gordon MS, McRee AJ, O'Dwyer PJ, Muro K, Tabernero J, van Geel R, Sidhu R, Greger JG, Rangwala FA, Motwani M, Wu Y, Orford KW, Corcoran RB (2015) Updated efficacy of the MEK inhibitor trametinib (T), BRAF inhibitor dabrafenib (D), and anti-EGFR antibody panitumumab (P) in patients (pts) with BRAF V600E mutated (BRAFm) metastatic colorectal cancer (mCRC). JCO 33:103. https://doi.org/10.1200/jco.2015.33.15_suppl.103

Azoitei N, Hoffmann CM, Ellegast JM, Ball CR, Obermayer K, Gößele U, Koch B, Faber K, Genze F, Schrader M, Kestler HA, Döhner H, Chiosis G, Glimm H, Fröhling S, Scholl C (2012) Targeting of KRAS mutant tumors by HSP90 inhibitors involves degradation of STK33. J Exp Med 209:697–711. https://doi.org/10.1084/jem.20111910

Battaglin F, Naseem M, Lenz H-J, Salem ME (2018) Microsatellite instability in colorectal cancer: overview of its clinical significance and novel perspectives. Clin Adv Hematol Oncol 16:735–745

Becht E, Reyniès A de, Giraldo NA, Pilati C, Buttard B, Lacroix L, Selves J, Sautès-Fridman C, Laurent-Puig P, Fridman WH (2016) Immune and Stromal Classification of Colorectal Cancer Is Associated with Molecular Subtypes and Relevant for Precision Immunotherapy. Clin Cancer Res 22:4057–4066. https://doi.org/10.1158/1078-0432.CCR-15-2879

Bendell JC, Jones SF, Hart L, Pant S, Moyhuddin A, Lane CM, Earwood C, Murphy P, Patton J, Penley WC, Thompson D, Infante JR (2015) A Phase I Study of the Hsp90 Inhibitor AUY922 plus Capecitabine for the Treatment of Patients with Advanced Solid Tumors. Cancer Invest 33:477–482. https://doi.org/10.3109/07357907.2015.1069834

Bendell JC, Bauer TM, Lamar R, Joseph M, Penley W, Thompson DS, Spigel DR, Owera R, Lane CM, Earwood C, Burris HA (2016) A Phase 2 Study of the Hsp90 Inhibitor AUY922 as Treatment for Patients with Refractory Gastrointestinal Stromal Tumors. Cancer Invest 34:265–270. https://doi.org/10.1080/07357907.2016.1193746

Biechele TL, Kulikauskas RM, Toroni RA, Lucero OM, Swift RD, James RG, Robin NC, Dawson DW, Moon RT, Chien AJ (2012) Wnt/β-catenin signaling and AXIN1 regulate apoptosis triggered by inhibition of the mutant kinase BRAFV600E in human melanoma. Sci Signal 5:ra3. https://doi.org/10.1126/scisignal.2002274

Blank CU, Larkin J, Arance AM, Hauschild A, Queirolo P, Del Vecchio M, Ascierto PA, Krajsova I, Schachter J, Neyns B, Garbe C, Chiarion Sileni V, Mandalà M, Gogas H, Espinosa E, Hospers GAP, Miller WH, Robson S, Makrutzki M, Antic V, Brown MP (2017) Open-label, multicentre safety study of vemurafenib in 3219 patients with BRAFV600 mutation-positive metastatic melanoma: 2-year follow-up data and long-term responders' analysis. Eur J Cancer 79:176–184. https://doi.org/10.1016/j.ejca.2017.04.007

Bliss CI (1939) The toxicity of poisons applied jointly. Annals of Applied Biology 26:585–615. https://doi.org/10.1111/j.1744-7348.1939.tb06990.x

Boussemart L, Malka-Mahieu H, Girault I, Allard D, Hemmingsson O, Tomasic G, Thomas M, Basmadjian C, Ribeiro N, Thuaud F, Mateus C, Routier E, Kamsu-Kom N, Agoussi S, Eggermont AM, Desaubry L, Robert C, Vagner S (2014) eIF4F is a nexus of resistance to anti-BRAF and anti-MEK cancer therapies. Nature 513:105–109. https://doi.org/10.1038/nature13572

Bouvard V, Loomis D, Guyton KZ, Grosse Y, Ghissassi FE, Benbrahim-Tallaa L, Guha N, Mattock H, Straif K (2015) Carcinogenicity of consumption of red and processed meat. The Lancet Oncology 16:1599–1600. https://doi.org/10.1016/S1470-2045(15)00444-1

Bray F, Ferlay J, Soerjomataram I, Siegel RL, Torre LA, Jemal A (2018) Global cancer statistics 2018: GLOBOCAN estimates of incidence and mortality worldwide for 36 cancers in 185 countries. CA Cancer J Clin 68:394–424. https://doi.org/10.3322/caac.21492

Cercek A, Shia J, Gollub M, Chou JF, Capanu M, Raasch P, Reidy-Lagunes D, Proia DA, Vakiani E, Solit DB, Saltz LB (2014) Ganetespib, a novel Hsp90 inhibitor in patients with KRAS mutated and wild type, refractory metastatic colorectal cancer. Clin Colorectal Cancer 13:207–212. https://doi.org/10.1016/j.clcc.2014.09.001

Chen G, Gao C, Gao X, Zhang DH, Kuan S-F, Burns TF, Hu J (2018) Wnt/β-Catenin Pathway Activation Mediates Adaptive Resistance to BRAF Inhibition in Colorectal Cancer. Mol Cancer Ther 17:806–813. https://doi.org/10.1158/1535-7163.MCT-17-0561

Chou T-C (2010) Drug combination studies and their synergy quantification using the Chou-Talalay method. Cancer Res 70:440–446. https://doi.org/10.1158/0008-5472.CAN-09-1947

Clancy C, Burke JP, Kalady MF, Coffey JC (2013) BRAF mutation is associated with distinct clinicopathological characteristics in colorectal cancer: a systematic review and meta-analysis. Colorectal Dis 15:e711-8. https://doi.org/10.1111/codi.12427

Cohen R, Cervera P, Svrcek M, Pellat A, Dreyer C, Gramont A de, André T (2017) BRAF-Mutated Colorectal Cancer: What Is the Optimal Strategy for Treatment? Curr Treat Options Oncol 18:9. https://doi.org/10.1007/s11864-017-0453-5

Cooper LC, Prinsloo E, Edkins AL, Blatch GL (2011) Hsp90α/β associates with the GSK3β/axin1/phospho-β-catenin complex in the human MCF-7 epithelial breast cancer model. Biochem Biophys Res Commun 413:550–554. https://doi.org/10.1016/j.bbrc.2011.08.136

Cope N, Candelora C, Wong K, Kumar S, Nan H, Grasso M, Novak B, Li Y, Marmorstein R, Wang Z (2018) Mechanism of BRAF Activation through Biochemical Characterization of the Recombinant Full-Length Protein. Chembiochem 19:1988–1997. https://doi.org/10.1002/cbic.201800359

Corbit KC, Trakul N, Eves EM, Diaz B, Marshall M, Rosner MR (2003) Activation of Raf-1 signaling by protein kinase C through a mechanism involving Raf kinase inhibitory protein. J Biol Chem 278:13061–13068. https://doi.org/10.1074/jbc.M210015200

Corcoran RB, Dias-Santagata D, Bergethon K, Iafrate AJ, Settleman J, Engelman JA (2010) BRAF gene amplification can promote acquired resistance to MEK inhibitors in cancer cells harboring the BRAF V600E mutation. Sci Signal 3:ra84. https://doi.org/10.1126/scisignal.2001148

Corcoran RB, Ebi H, Turke AB, Coffee EM, Nishino M, Cogdill AP, Brown RD, Della Pelle P, Dias-Santagata D, Hung KE, Flaherty KT, Piris A, Wargo JA, Settleman J, Mino-Kenudson M, Engelman JA (2012) EGFR-mediated re-activation of MAPK signaling contributes to insensitivity of BRAF mutant colorectal cancers to RAF inhibition with vemurafenib. Cancer Discov 2:227–235. https://doi.org/10.1158/2159-8290.CD-11-0341

Corcoran RB, Atreya CE, Falchook GS, Kwak EL, Ryan DP, Bendell JC, Hamid O, Messersmith WA, Daud A, Kurzrock R, Pierobon M, Sun P, Cunningham E, Little S, Orford K, Motwani M, Bai Y, Patel K, Venook AP, Kopetz S (2015) Combined BRAF and MEK Inhibition With Dabrafenib and Trametinib in BRAF V600-Mutant Colorectal Cancer. J Clin Oncol 33:4023–4031. https://doi.org/10.1200/JCO.2015.63.2471

Corcoran RB, Andre T, Atreya CE, Schellens JHM, Yoshino T, Bendell JC, Hollebecque A, McRee AJ, Siena S, Middleton G, Muro K, Gordon MS, Tabernero J, Yaeger R, O'Dwyer PJ, Humblet Y, Vos F de, Jung AS, Brase JC, Jaeger S, Bettinger S, Mookerjee B, Rangwala F, van Cutsem E (2018) Combined BRAF, EGFR, and MEK Inhibition in Patients with BRAF(V600E)-Mutant Colorectal Cancer. Cancer Discov 8:428–443. https://doi.org/10.1158/2159-8290.CD-17-1226

da Rocha Dias S, Friedlos F, Light Y, Springer C, Workman P, Marais R (2005) Activated B-RAF is an Hsp90 client protein that is targeted by the anticancer drug 17-allylamino-17-demethoxygeldanamycin. Cancer Res 65:10686–10691. https://doi.org/10.1158/0008-5472.CAN-05-2632

Dahm CC, Keogh RH, Spencer EA, Greenwood DC, Key TJ, Fentiman IS, Shipley MJ, Brunner EJ, Cade JE, Burley VJ, Mishra G, Stephen AM, Kuh D, White IR, Luben R, Lentjes MAH, Khaw KT, Rodwell Bingham SA (2010) Dietary fiber and colorectal cancer risk: a nested case-control study using food diaries. J Natl Cancer Inst 102:614–626. https://doi.org/10.1093/jnci/djq092

Dankner M, Rose AAN, Rajkumar S, Siegel PM, Watson IR (2018) Classifying BRAF alterations in cancer: new rational therapeutic strategies for actionable mutations. Oncogene 37:3183–3199. https://doi.org/10.1038/s41388-018-0171-x

Davies H, Bignell GR, Cox C, Stephens P, Edkins S, Clegg S, Teague J, Woffendin H, Garnett MJ, Bottomley W, Davis N, Dicks E, Ewing R, Floyd Y, Gray K, Hall S, Hawes R, Hughes J, Kosmidou V, Menzies A, Mould C, Parker A, Stevens C, Watt S, Hooper S, Wilson R, Jayatilake H, Gusterson BA, Cooper C, Shipley J, Hargrave D, Pritchard-Jones K, Maitland N, Chenevix-Trench G, Riggins GJ, Bigner DD, Palmieri G, Cossu A, Flanagan A, Nicholson A, Ho JWC, Leung SY, Yuen ST, Weber BL, Seigler HF, Darrow TL, Paterson H, Marais R, Marshall CJ, Wooster R, Stratton MR, Futreal PA (2002) Mutations of the BRAF gene in human cancer. Nature 417:949–954. https://doi.org/10.1038/nature00766

Dawson JP, Berger MB, Lin C-C, Schlessinger J, Lemmon MA, Ferguson KM (2005) Epidermal growth factor receptor dimerization and activation require ligand-induced conformational changes in the dimer interface. Mol Cell Biol 25:7734–7742. https://doi.org/10.1128/MCB.25.17.7734-7742.2005

Deutsche Krebsgesellschaft, Deutsche Krebshilfe, AWMF (2019) S3-Leitlinie Kolorektales Karzinom. Langversion, AWMF Registrierungsnummer: 021/007OL. http://www.leitlinienprogrammonkologie.de/leitlinien/kolorektales-karzinom/. Accessed 15 August 2019

Diedrich B, Rigbolt KT, Röring M, Herr R, Kaeser-Pebernard S, Gretzmeier C, Murphy RF, Brummer T, Dengjel J (2017) Discrete cytosolic macromolecular BRAF complexes exhibit distinct activities and composition. EMBO J 36:646–663. https://doi.org/10.15252/embj.201694732

Dienstmann R, Vermeulen L, Guinney J, Kopetz S, Tejpar S, Tabernero J (2017) Consensus molecular subtypes and the evolution of precision medicine in colorectal cancer. Nat Rev Cancer 17:79–92. https://doi.org/10.1038/nrc.2016.126

Ducreux M, Chamseddine A, Laurent-Puig P, Smolenschi C, Hollebecque A, Dartigues P, Samallin E, Boige V, Malka D, Gelli M (2019) Molecular targeted therapy of BRAF-mutant colorectal cancer. Ther Adv Med Oncol 11:1758835919856494. https://doi.org/10.1177/1758835919856494

Ebi H, Costa C, Faber AC, Nishtala M, Kotani H, Juric D, Della Pelle P, Song Y, Yano S, Mino-Kenudson M, Benes CH, Engelman JA (2013) PI3K regulates MEK/ERK signaling in breast cancer via the Rac-GEF, P-Rex1. Proc Natl Acad Sci U S A 110:21124–21129. https://doi.org/10.1073/pnas.1314124110

Edmondson R, Broglie JJ, Adcock AF, Yang L (2014) Three-dimensional cell culture systems and their applications in drug discovery and cell-based biosensors. Assay Drug Dev Technol 12:207–218. https://doi.org/10.1089/adt.2014.573

Eischen CM, Packham G, Nip J, Fee BE, Hiebert SW, Zambetti GP, Cleveland JL (2001) Bcl-2 is an apoptotic target suppressed by both c-Myc and E2F-1. Oncogene 20:6983–6993. https://doi.org/10.1038/sj.onc.1204892

Elsaleh H, Iacopetta B (2001) Microsatellite instability is a predictive marker for survival benefit from adjuvant chemotherapy in a population-based series of stage III colorectal carcinoma. Clin Colorectal Cancer 1:104–109. https://doi.org/10.3816/CCC.2001.n.010

Emaduddin M, Bicknell DC, Bodmer WF, Feller SM (2008) Cell growth, global phosphotyrosine elevation, and c-Met phosphorylation through Src family kinases in colorectal cancer cells. Proc Natl Acad Sci U S A 105:2358–2362. https://doi.org/10.1073/pnas.0712176105

Emery CM, Vijayendran KG, Zipser MC, Sawyer AM, Niu L, Kim JJ, Hatton C, Chopra R, Oberholzer PA, Karpova MB, MacConaill LE, Zhang J, Gray NS, Sellers WR, Dummer R, Garraway LA (2009) MEK1 mutations confer resistance to MEK and B-RAF inhibition. Proc Natl Acad Sci U S A 106:20411–20416. https://doi.org/10.1073/pnas.0905833106

Emery CM, Monaco K-A, Wang P, Balak M, Freeman A, Meltzer J, Delach SM, Rakiec D, Ruddy DA, Korn JM, Haling J, Acker MG, Caponigro G (2017) BRAF-inhibitor Associated MEK Mutations Increase RAF-Dependent and -Independent Enzymatic Activity. Mol Cancer Res 15:1431–1444. https://doi.org/10.1158/1541-7786.MCR-17-0211

Eroglu Z, Chen YA, Gibney GT, Weber JS, Kudchadkar RR, Khushalani NI, Markowitz J, Brohl AS, Tetteh LF, Ramadan H, Arnone G, Li J, Zhao X, Sharma R, Darville LNF, Fang B, Smalley I, Messina JL, Koomen JM, Sondak VK, Smalley KSM (2018) Combined BRAF and HSP90 Inhibition in Patients with Unresectable BRAFV600E-Mutant Melanoma. Clin Cancer Res 24:5516–5524. https://doi.org/10.1158/1078-0432.CCR-18-0565

Fang M, Ou J, Hutchinson L, Green MR (2014) The BRAF oncoprotein functions through the transcriptional repressor MAFG to mediate the CpG Island Methylator phenotype. Mol Cell 55:904–915. https://doi.org/10.1016/j.molcel.2014.08.010

Fang JY, Richardson BC (2005) The MAPK signalling pathways and colorectal cancer. The Lancet Oncology 6:322–327. https://doi.org/10.1016/S1470-2045(05)70168-6

Fedirko V, Tramacere I, Bagnardi V, Rota M, Scotti L, Islami F, Negri E, Straif K, Romieu I, La Vecchia C, Boffetta P, Jenab M (2011) Alcohol drinking and colorectal cancer risk: an overall and dose-response meta-analysis of published studies. Ann Oncol 22:1958–1972. https://doi.org/10.1093/annonc/mdq653

Felip E, Barlesi F, Besse B, Chu Q, Gandhi L, Kim S-W, Carcereny E, Sequist LV, Brunsvig P, Chouaid C, Smit EF, Groen HJM, Kim D-W, Park K, Avsar E, Szpakowski S, Akimov M, Garon EB (2018) Phase 2 Study of the HSP-90 Inhibitor AUY922 in Previously Treated and Molecularly Defined Patients with Advanced Non-Small Cell Lung Cancer. J Thorac Oncol 13:576–584. https://doi.org/10.1016/j.jtho.2017.11.131

Fessler E, Drost J, van Hooff SR, Linnekamp JF, Wang X, Jansen M, Sousa E Melo F de, Prasetyanti PR, IJspeert JE, Franitza M, Nürnberg P, van Noesel CJ, Dekker E, Vermeulen L, Clevers H, Medema JP (2016) TGFβ signaling directs serrated adenomas to the mesenchymal colorectal cancer subtype. EMBO Mol Med 8:745–760. https://doi.org/10.15252/emmm.201606184

Flaherty KT, Puzanov I, Kim KB, Ribas A, McArthur GA, Sosman JA, O'Dwyer PJ, Lee RJ, Grippo JF, Nolop K, Chapman PB (2010) Inhibition of mutated, activated BRAF in metastatic melanoma. N Engl J Med 363:809–819. https://doi.org/10.1056/NEJMoa1002011

Foucquier J, Guedj M (2015) Analysis of drug combinations: current methodological landscape. Pharmacol Res Perspect 3:e00149. https://doi.org/10.1002/prp2.149

Frejno M, Zenezini Chiozzi R, Wilhelm M, Koch H, Zheng R, Klaeger S, Ruprecht B, Meng C, Kramer K, Jarzab A, Heinzlmeir S, Johnstone E, Domingo E, Kerr D, Jesinghaus M, Slotta-Huspenina J, Weichert W, Knapp S, Feller SM, Kuster B (2017) Pharmacoproteomic characterisation of

human colon and rectal cancer. Mol Syst Biol 13:951. https://doi.org/10.15252/msb.20177701

Fritsche-Guenther R, Witzel F, Kempa S, Brummer T, Sers C, Blüthgen N (2016) Effects of RAF inhibitors on PI3K/AKT signalling depend on mutational status of the RAS/RAF signalling axis. Oncotarget 7:7960–7969. https://doi.org/10.18632/oncotarget.6959

Goetz MP, Toft D, Reid J, Ames M, Stensgard B, Safgren S, Adjei AA, Sloan J, Atherton P, Vasile V, Salazaar S, Adjei A, Croghan G, Erlichman C (2005) Phase I trial of 17-allylamino-17-demethoxygeldanamycin in patients with advanced cancer. JCO 23:1078–1087. https://doi.org/10.1200/JCO.2005.09.119

Gomez-Roca CA, Delord J, Robert C, Hidalgo M, Moos R von, Arance A, Elez E, Michel D, Seroutou A, Demuth T, Tabernero J (2014) 535PENCORAFENIB (LGX818), AN ORAL BRAF INHIBITOR, IN PATIENTS (PTS) WITH BRAF V600E METASTATIC COLORECTAL CANCER (MCRC): RESULTS OF DOSE EXPANSION IN AN OPEN-LABEL, PHASE 1 STUDY. Annals of Oncology 25:iv182-iv183. https://doi.org/10.1093/annonc/mdu333.38

Gonsalves WI, Mahoney MR, Sargent DJ, Nelson GD, Alberts SR, Sinicrope FA, Goldberg RM, Limburg PJ, Thibodeau SN, Grothey A, Hubbard JM, Chan E, Nair S, Berenberg JL, McWilliams RR (2014) Patient and tumor characteristics and BRAF and KRAS mutations in colon cancer, NCCTG/Alliance N0147. J Natl Cancer Inst 106. https://doi.org/10.1093/jnci/dju106

Grbovic OM, Basso AD, Sawai A, Ye Q, Friedlander P, Solit D, Rosen N (2006) V600E B-Raf requires the Hsp90 chaperone for stability and is degraded in response to Hsp90 inhibitors. Proc Natl Acad Sci U S A 103:57–62. https://doi.org/10.1073/pnas.0609973103

Grothey A, van Cutsem E, Sobrero A, Siena S, Falcone A, Ychou M, Humblet Y, Bouché O, Mineur L, Barone C, Adenis A, Tabernero J, Yoshino T, Lenz H-J, Goldberg RM, Sargent DJ, Cihon F, Cupit L, Wagner A, Laurent D (2013) Regorafenib monotherapy for previously treated metastatic colorectal cancer (CORRECT): an international, multicentre, randomised, placebo-controlled, phase 3 trial. The Lancet 381:303–312. https://doi.org/10.1016/S0140-6736(12)61900-X

Guinney J, Dienstmann R, Wang X, Reyniès A de, Schlicker A, Soneson C, Marisa L, Roepman P, Nyamundanda G, Angelino P, Bot BM, Morris JS, Simon IM, Gerster S, Fessler E, Sousa E Melo F de, Missiaglia E, Ramay H, Barras D, Homicsko K, Maru D, Manyam GC, Broom B, Boige V, Perez-Villamil B, Laderas T, Salazar R, Gray JW, Hanahan D, Tabernero J, Bernards R, Friend SH, Laurent-Puig P, Medema JP, Sadanandam A, Wessels L, Delorenzi M, Kopetz S, Vermeulen L, Tejpar S (2015) The consensus molecular subtypes of colorectal cancer. Nat Med 21:1350–1356. https://doi.org/10.1038/nm.3967

Güldenhaupt J, Rudack T, Bachler P, Mann D, Triola G, Waldmann H, Kötting C, Gerwert K (2012) N-Ras forms dimers at POPC membranes. Biophys J 103:1585–1593. https://doi.org/10.1016/j.bpj.2012.08.043

Haling JR, Sudhamsu J, Yen I, Sideris S, Sandoval W, Phung W, Bravo BJ, Giannetti AM, Peck A, Masselot A, Morales T, Smith D, Brandhuber BJ, Hymowitz SG, Malek S (2014) Structure of the BRAF-MEK complex reveals a kinase activity independent role for BRAF in MAPK signaling. Cancer Cell 26:402–413. https://doi.org/10.1016/j.ccr.2014.07.007

Hamburger AW, Salmon SE (1977) Primary bioassay of human tumor stem cells. Science 197:461–463. https://doi.org/10.1126/science.560061

Heidorn SJ, Milagre C, Whittaker S, Nourry A, Niculescu-Duvas I, Dhomen N, Hussain J, Reis-Filho JS, Springer CJ, Pritchard C, Marais R (2010) Kinase-dead BRAF and oncogenic RAS cooperate to drive tumor progression through CRAF. Cell 140:209–221. https://doi.org/10.1016/j.cell.2009.12.040

Herr R, Halbach S, Heizmann M, Busch H, Boerries M, Brummer T (2018) BRAF inhibition upregulates a variety of receptor tyrosine kinases and their downstream effector Gab2 in colorectal cancer cell lines. Oncogene 37:1576–1593. https://doi.org/10.1038/s41388-017-0063-5

Herrmann C, Martin GA, Wittinghofer A (1995) Quantitative analysis of the complex between p21ras and the Ras-binding domain of the human Raf-1 protein kinase. J Biol Chem 270:2901–2905. https://doi.org/10.1074/jbc.270.7.2901

Hillienhof A (2016) Regorafenib: Onkologen kritisieren Marktrücknahme. Dtsch Arztebl International 113:797

Holch JW, Ricard I, Stintzing S, Modest DP, Heinemann V (2017) The relevance of primary tumour location in patients with metastatic colorectal cancer: A meta-analysis of first-line clinical trials. Eur J Cancer 70:87–98. https://doi.org/10.1016/j.ejca.2016.10.007

Holderfield M, Merritt H, Chan J, Wallroth M, Tandeske L, Zhai H, Tellew J, Hardy S, Hekmat-Nejad M, Stuart DD, McCormick F, Nagel TE (2013) RAF inhibitors activate the MAPK pathway by relieving inhibitory autophosphorylation. Cancer Cell 23:594–602. https://doi.org/10.1016/j.ccr.2013.03.033

Holderfield M, Deuker MM, McCormick F, McMahon M (2014) Targeting RAF kinases for cancer therapy: BRAF-mutated melanoma and beyond. Nat Rev Cancer 14:455–467. https://doi.org/10.1038/nrc3760

Hong DS, van Morris K, El Osta B, Sorokin AV, Janku F, Fu S, Overman MJ, Piha-Paul S, Subbiah V, Kee B, Tsimberidou AM, Fogelman D, Bellido J, Shureiqi I, Huang H, Atkins J, Tarcic G, Sommer N, Lanman R, Meric-Bernstam F, Kopetz S (2016) Phase IB Study of Vemurafenib in Combination with Irinotecan and Cetuximab in Patients with Metastatic Colorectal Cancer with BRAFV600E Mutation. Cancer Discov 6:1352–1365. https://doi.org/10.1158/2159-8290.CD-16-0050

Hyman DM, Puzanov I, Subbiah V, Faris JE, Chau I, Blay J-Y, Wolf J, Raje NS, Diamond EL, Hollebecque A, Gervais R, Elez-Fernandez ME, Italiano A, Hofheinz R-D, Hidalgo M, Chan E, Schuler M, Lasserre SF, Makrutzki M, Sirzen F, Veronese ML, Tabernero J, Baselga J (2015) Vemurafenib in Multiple Nonmelanoma Cancers with BRAF V600 Mutations. N Engl J Med 373:726–736. https://doi.org/10.1056/NEJMoa1502309

IJspeert JEG, Vermeulen L, Meijer GA, Dekker E (2015) Serrated neoplasia-role in colorectal carcinogenesis and clinical implications. Nat Rev Gastroenterol Hepatol 12:401–409. https://doi.org/10.1038/nrgastro.2015.73

Ilyas M, Tomlinson IP, Rowan A, Pignatelli M, Bodmer WF (1997) Beta-catenin mutations in cell lines established from human colorectal cancers. Proc Natl Acad Sci U S A 94:10330–10334. https://doi.org/10.1073/pnas.94.19.10330

International Agency for Research on Cancer (ed) (2019) WHO Classification of Tumours Editional Board: Digestive System Tumours, 5th edn., vol 1, Lyon (France)

Jasperson KW, Tuohy TM, Neklason DW, Burt RW (2010) Hereditary and familial colon cancer. Gastroenterology 138:2044–2058. https://doi.org/10.1053/j.gastro.2010.01.054

Jhaveri K, Wang R, Teplinsky E, Chandarlapaty S, Solit D, Cadoo K, Speyer J, D'Andrea G, Adams S, Patil S, Haque S, O'Neill T, Friedman K, Esteva FJ, Hudis C, Modi S (2017) A phase I trial of ganetespib in combination with paclitaxel and trastuzumab in patients with human epidermal growth factor receptor-2 (HER2)-positive metastatic breast cancer. Breast Cancer Res 19:89. https://doi.org/10.1186/s13058-017-0879-5

Jia M, Gao X, Zhang Y, Hoffmeister M, Brenner H (2016) Different definitions of CpG island methylator phenotype and outcomes of colorectal cancer: a systematic review. Clin Epigenetics 8:25. https://doi.org/10.1186/s13148-016-0191-8

Johannessen CM, Boehm JS, Kim SY, Thomas SR, Wardwell L, Johnson LA, Emery CM, Stransky N, Cogdill AP, Barretina J, Caponigro G, Hieronymus H, Murray RR, Salehi-Ashtiani K, Hill DE, Vidal M, Zhao JJ, Yang X, Alkan O, Kim S, Harris JL, Wilson CJ, Myer VE, Finan PM, Root DE, Roberts TM, Golub T, Flaherty KT, Dummer R, Weber BL, Sellers WR, Schlegel R, Wargo JA, Hahn WC, Garraway LA (2010) COT drives resistance to RAF inhibition through MAP kinase pathway reactivation. Nature 468:968–972. https://doi.org/10.1038/nature09627

Johnson ML, Yu HA, Hart EM, Weitner BB, Rademaker AW, Patel JD, Kris MG, Riely GJ (2015) Phase I/II Study of HSP90 Inhibitor AUY922 and Erlotinib for EGFR-Mutant Lung Cancer With Acquired Resistance to Epidermal Growth Factor Receptor Tyrosine Kinase Inhibitors. JCO 33:1666–1673. https://doi.org/10.1200/JCO.2014.59.7328

Jones JC, Renfro LA, Al-Shamsi HO, Schrock AB, Rankin A, Zhang BY, Kasi PM, Voss JS, Leal AD, Sun J, Ross J, Ali SM, Hubbard JM, Kipp BR, McWilliams RR, Kopetz S, Wolff RA, Grothey A (2017) Non-V600 BRAF Mutations Define a Clinically Distinct Molecular Subtype of Metastatic Colorectal Cancer. JCO 35:2624–2630. https://doi.org/10.1200/JCO.2016.71.4394

Jordan P (2018) Colorectal Cancer Subtypes – The Current Portrait. In: Jordan P (ed) Targeted Therapy of Colorectal Cancer Subtypes. Springer International Publishing, Cham, pp 1–6

Kafkafi N, Agassi J, Chesler EJ, Crabbe JC, Crusio WE, Eilam D, Gerlai R, Golani I, Gomez-Marin A, Heller R, Iraqi F, Jaljuli I, Karp NA, Morgan H, Nicholson G, Pfaff DW, Richter SH, Stark PB, Stiedl O, Stodden V, Tarantino LM, Tucci V, Valdar W, Williams RW, Würbel H, Benjamini Y (2018) Reproducibility and replicability of rodent phenotyping in preclinical studies. Neurosci Biobehav Rev 87:218–232. https://doi.org/10.1016/j.neubiorev.2018.01.003

King AJ, Arnone MR, Bleam MR, Moss KG, Yang J, Fedorowicz KE, Smitheman KN, Erhardt JA, Hughes-Earle A, Kane-Carson LS, Sinnamon RH, Qi H, Rheault TR, Uehling DE, Laquerre SG (2013) Dabrafenib; preclinical characterization, increased efficacy when combined with trametinib, while BRAF/MEK tool combination reduced skin lesions. PLoS ONE 8:e67583. https://doi.org/10.1371/journal.pone.0067583

Kong A, Rea D, Ahmed S, Beck JT, López López R, Biganzoli L, Armstrong AC, Aglietta M, Alba E, Campone M, Hsu Schmitz S-F, Lefebvre C, Akimov M, Lee S-C (2016) Phase 1B/2 study of the HSP90 inhibitor AUY922 plus trastuzumab in metastatic HER2-positive breast cancer patients who have progressed on trastuzumab-based regimen. Oncotarget 7:37680–37692. https://doi.org/10.18632/oncotarget.8974

Kopetz S, Desai J, Chan E, Hecht JR, O'Dwyer PJ, Maru D, van Morris, Janku F, Dasari A, Chung W, Issa J-PJ, Gibbs P, James B, Powis G, Nolop KB, Bhattacharya S, Saltz L (2015) Phase II Pilot

Study of Vemurafenib in Patients With Metastatic BRAF-Mutated Colorectal Cancer. JCO 33:4032–4038. https://doi.org/10.1200/JCO.2015.63.2497

Kopetz S, Grothey A, Yaeger R, van Cutsem E, Desai J, Yoshino T, Wasan H, Ciardiello F, Loupakis F, Hong YS, Steeghs N, Guren TK, Arkenau H-T, Garcia-Alfonso P, Pfeiffer P, Orlov S, Lonardi S, Elez E, Kim T-W, Schellens JHM, Guo C, Krishnan A, Dekervel J, van Morris, Calvo Ferrandiz A, Tarpgaard LS, Braun M, Gollerkeri A, Keir C, Maharry K, Pickard M, Christy-Bittel J, Anderson L, Sandor V, Tabernero J (2019) Encorafenib, Binimetinib, and Cetuximab in BRAF V600E-Mutated Colorectal Cancer. N Engl J Med. https://doi.org/10.1056/NEJMoa1908075

Kopetz S, Guthrie KA, van Morris K, Lenz H-J, Magliocco AM, Maru D, Yan Y, Lanman R, Manyam G, Hong DS, Sorokin A, Atreya CE, Diaz LA, Allegra C, Raghav KP, Wang SE, Lieu CH, McDonough SL, Philip PA, Hochster HS (2021) Randomized Trial of Irinotecan and Cetuximab With or Without Vemurafenib in BRAF-Mutant Metastatic Colorectal Cancer (SWOG S1406). JCO 39:285–294. https://doi.org/10.1200/JCO.20.01994

Kozer N, Barua D, Henderson C, Nice EC, Burgess AW, Hlavacek WS, Clayton AHA (2014) Recruitment of the adaptor protein Grb2 to EGFR tetramers. Biochemistry 53:2594–2604. https://doi.org/10.1021/bi500182x

Kryeziu K, Bruun J, Guren TK, Sveen A, Lothe RA (2019) Combination therapies with HSP90 inhibitors against colorectal cancer. Biochim Biophys Acta Rev Cancer 1871:240–247. https://doi.org/10.1016/j.bbcan.2019.01.002

Lavoie H, Therrien M (2015) Regulation of RAF protein kinases in ERK signalling. Nat Rev Mol Cell Biol 16:281–298. https://doi.org/10.1038/nrm3979

Lee SL, Dempsey-Hibbert NC, Vimalachandran D, Wardle TD, Sutton PA, Williams JHH (2017) Re-examining HSPC1 inhibitors. Cell Stress Chaperones 22:293–306. https://doi.org/10.1007/s12192-017-0774-0

Li J, Qin S, Xu R, Yau TCC, Ma B, Pan H, Xu J, Bai Y, Chi Y, Wang L, Yeh K-H, Bi F, Cheng Y, Le AT, Lin J-K, Liu T, Ma D, Kappeler C, Kalmus J, Kim TW (2015) Regorafenib plus best supportive care versus placebo plus best supportive care in Asian patients with previously treated metastatic colorectal cancer (CONCUR): a randomised, double-blind, placebo-controlled, phase 3 trial. The Lancet Oncology 16:619–629. https://doi.org/10.1016/S1470-2045(15)70156-7

Lin W-C, Iversen L, Tu H-L, Rhodes C, Christensen SM, Iwig JS, Hansen SD, Huang WYC, Groves JT (2014) H-Ras forms dimers on membrane surfaces via a protein-protein interface. Proc Natl Acad Sci U S A 111:2996–3001. https://doi.org/10.1073/pnas.1321155111

Liszkay G, Gogas H, Mandalà M, Arance Fernandez AM, Garbe C, Schadendorf D, Dummer R, Ascierto PA, Robert C, Pickard MD, Sandor V, Gollerkeri A, Flaherty K (2019) Update on overall survival in COLUMBUS: A randomized phase III trial of encorafenib (ENCO) plus binimetinib (BINI) versus vemurafenib (VEM) or ENCO in patients with BRAF V600–mutant melanoma. JCO 37:9512. https://doi.org/10.1200/JCO.2019.37.15_suppl.9512

Lito P, Pratilas CA, Joseph EW, Tadi M, Halilovic E, Zubrowski M, Huang A, Wong WL, Callahan MK, Merghoub T, Wolchok JD, Stanchina E de, Chandarlapaty S, Poulikakos PI, Fagin JA, Rosen N (2012) Relief of profound feedback inhibition of mitogenic signaling by RAF inhibitors attenuates their activity in BRAFV600E melanomas. Cancer Cell 22:668–682. https://doi.org/10.1016/j.ccr.2012.10.009

Lochhead P, Kuchiba A, Imamura Y, Liao X, Yamauchi M, Nishihara R, Qian ZR, Morikawa T, Shen J, Meyerhardt JA, Fuchs CS, Ogino S (2013) Microsatellite instability and BRAF mutation testing in colorectal cancer prognostication. J Natl Cancer Inst 105:1151–1156. https://doi.org/10.1093/jnci/djt173

Loewe S, Muischnek H (1926) Über Kombinationswirkungen. Archiv f. experiment. Pathol. u. Pharmakol 114:313–326. https://doi.org/10.1007/BF01952257

Lopez JS, Banerji U (2017) Combine and conquer: challenges for targeted therapy combinations in early phase trials. Nat Rev Clin Oncol 14:57–66. https://doi.org/10.1038/nrclinonc.2016.96

Loree JM, Pereira AAL, Lam M, Willauer AN, Raghav K, Dasari A, van Morris K, Advani S, Menter DG, Eng C, Shaw K, Broaddus R, Routbort MJ, Liu Y, Morris JS, Luthra R, Meric-Bernstam F, Overman MJ, Maru D, Kopetz S (2018) Classifying Colorectal Cancer by Tumor Location Rather than Sidedness Highlights a Continuum in Mutation Profiles and Consensus Molecular Subtypes. Clin Cancer Res 24:1062–1072. https://doi.org/10.1158/1078-0432.CCR-17-2484

Maeno K, Masuda A, Yanagisawa K, Konishi H, Osada H, Saito T, Ueda R, Takahashi T (2006) Altered regulation of c-jun and its involvement in anchorage-independent growth of human lung cancers. Oncogene 25:271–277. https://doi.org/10.1038/sj.onc.1209018

Maik-Rachline G, Hacohen-Lev-Ran A, Seger R (2019) Nuclear ERK: Mechanism of Translocation, Substrates, and Role in Cancer. Int J Mol Sci 20. https://doi.org/10.3390/ijms20051194

Mani SA, Guo W, Liao M-J, Eaton EN, Ayyanan A, Zhou AY, Brooks M, Reinhard F, Zhang CC, Shipitsin M, Campbell LL, Polyak K, Brisken C, Yang J, Weinberg RA (2008) The epithelial-mesenchymal transition generates cells with properties of stem cells. Cell 133:704–715. https://doi.org/10.1016/j.cell.2008.03.027

Mao M, Tian F, Mariadason JM, Tsao CC, Lemos R, Dayyani F, Gopal YNV, Jiang Z-Q, Wistuba II, Tang XM, Bornman WG, Bollag G, Mills GB, Powis G, Desai J, Gallick GE, Davies MA, Kopetz S (2013) Resistance to BRAF inhibition in BRAF-mutant colon cancer can be overcome with PI3K inhibition or demethylating agents. Clin Cancer Res 19:657–667. https://doi.org/10.1158/1078-0432.CCR-11-1446

Marconcini L, Marchio S, Morbidelli L, Cartocci E, Albini A, Ziche M, Bussolino F, Oliviero S (1999) c-fos-induced growth factor/vascular endothelial growth factor D induces angiogenesis in vivo and in vitro. Proc Natl Acad Sci U S A 96:9671–9676. https://doi.org/10.1073/pnas.96.17.9671

Marcus L, Lemery SJ, Keegan P, Pazdur R (2019) FDA Approval Summary: Pembrolizumab for the Treatment of Microsatellite Instability-High Solid Tumors. Clin Cancer Res 25:3753–3758. https://doi.org/10.1158/1078-0432.CCR-18-4070

Margolis B, Skolnik EY (1994) Activation of Ras by receptor tyrosine kinases. J Am Soc Nephrol 5:1288–1299. https://doi.org/10.1681/ASN.V561288

Mayor-López L, Tristante E, Carballo-Santana M, Carrasco-García E, Grasso S, García-Morales P, Saceda M, Luján J, García-Solano J, Carballo F, Torre C de, Martínez-Lacaci I (2014) Comparative Study of 17-AAG and NVP-AUY922 in Pancreatic and Colorectal Cancer Cells: Are There Common Determinants of Sensitivity? Transl Oncol 7:590–604. https://doi.org/10.1016/j.tranon.2014.08.001

McCullough ML, Zoltick ES, Weinstein SJ, Fedirko V, Wang M, Cook NR, Eliassen AH, Zeleniuch-Jacquotte A, Agnoli C, Albanes D, Barnett MJ, Buring JE, Campbell PT, Clendenen TV, Freedman ND, Gapstur SM, Giovannucci EL, Goodman GG, Haiman CA, Ho GYF, Horst RL, Hou T, Huang W-Y, Jenab M, Jones ME, Joshu CE, Krogh V, Lee I-M, Lee JE, Männistö S, Le Marchand L, Mondul AM, Neuhouser ML, Platz EA, Purdue MP, Riboli E, Robsahm TE, Rohan TE, Sasazuki S, Schoemaker MJ, Sieri S, Stampfer MJ, Swerdlow AJ, Thomson CA, Tretli S, Tsugane S, Ursin G, Visvanathan K, White KK, Wu K, Yaun S-S, Zhang X, Willett WC, Gail MH, Ziegler RG, Smith-Warner SA (2019) Circulating Vitamin D and Colorectal Cancer Risk: An International Pooling Project of 17 Cohorts. J Natl Cancer Inst 111:158–169. https://doi.org/10.1093/jnci/djy087

McPherson RA, Harding A, Roy S, Lane A, Hancock JF (1999) Interactions of c-Raf-1 with phosphatidylserine and 14-3-3. Oncogene 18:3862–3869. https://doi.org/10.1038/sj.onc.1202730

Medico E, Russo M, Picco G, Cancelliere C, Valtorta E, Corti G, Buscarino M, Isella C, Lamba S, Martinoglio B, Veronese S, Siena S, Sartore-Bianchi A, Beccuti M, Mottolese M, Linnebacher M, Cordero F, Di Nicolantonio F, Bardelli A (2015) The molecular landscape of colorectal cancer cell lines unveils clinically actionable kinase targets. Nat Commun 6:7002. https://doi.org/10.1038/ncomms8002

Mehmet A, Olatunji BA, Walid LS, Christina W, Gregory BL, Bassel FE-R (2020) Phase Ib trial of pembrolizumab and XL888 in patients with advanced gastrointestinal malignancies: Results of the dose-escalation phase. JCO 38:830. https://doi.org/10.1200/JCO.2020.38.4_suppl.830

Menezes DL, Taverna P, Jensen MR, Abrams T, Stuart D, Yu GK, Duhl D, Machajewski T, Sellers WR, Pryer NK, Gao Z (2012) The novel oral Hsp90 inhibitor NVP-HSP990 exhibits potent and broad-spectrum antitumor activities in vitro and in vivo. Mol Cancer Ther 11:730–739. https://doi.org/10.1158/1535-7163.MCT-11-0667

Menzies AM, Kefford RF, Long GV (2013) Paradoxical oncogenesis: are all BRAF inhibitors equal? Pigment Cell Melanoma Res 26:611–615. https://doi.org/10.1111/pcmr.12132

Miller DM, Thomas SD, Islam A, Muench D, Sedoris K (2012) c-Myc and cancer metabolism. Clin Cancer Res 18:5546–5553. https://doi.org/10.1158/1078-0432.CCR-12-0977

Mirzaie AZ, Khakpour H, Mireskandari M, Shayanfar N, Fatahi L (2016) Investigating The Frequency of Serrated Polyps/Adenomas and Their Subtypes in Colonic Polyp Samples. Med Arch 70:198–202. https://doi.org/10.5455/medarh.2016.70.198-202

Morata-Tarifa C, Jiménez G, García MA, Entrena JM, Griñán-Lisón C, Aguilera M, Picon-Ruiz M, Marchal JA (2016) Low adherent cancer cell subpopulations are enriched in tumorigenic and metastatic epithelial-to-mesenchymal transition-induced cancer stem-like cells. Sci Rep 6:18772. https://doi.org/10.1038/srep18772

Morrison DK (2012) MAP kinase pathways. Cold Spring Harb Perspect Biol 4. https://doi.org/10.1101/cshperspect.a011254

Mullard A (2012) 2011 FDA drug approvals. Nat Rev Drug Discov 11:91–94. https://doi.org/10.1038/nrd3657

Murphy MJ, Wilson A, Trumpp A (2005) More than just proliferation: Myc function in stem cells. Trends Cell Biol 15:128–137. https://doi.org/10.1016/j.tcb.2005.01.008

Muto T, Bussey HJ, Morson BC (1975) The evolution of cancer of the colon and rectum. Cancer 36:2251–2270. https://doi.org/10.1002/cncr.2820360944

Nagaraju GP, Long T-E, Park W, Landry JC, Taliaferro-Smith L, Farris AB, Diaz R, El-Rayes BF (2015) Heat shock protein 90 promotes epithelial to mesenchymal transition, invasion, and migration in colorectal cancer. Mol Carcinog 54:1147–1158. https://doi.org/10.1002/mc.22185

Nagasawa I, Kunimasa K, Tsukahara S, Tomida A (2017) BRAF-mutated cells activate GCN2-mediated integrated stress response as a cytoprotective mechanism in response to vemurafenib. Biochem Biophys Res Commun 482:1491–1497. https://doi.org/10.1016/j.bbrc.2016.12.062

Nan X, Tamgüney TM, Collisson EA, Lin L-J, Pitt C, Galeas J, Lewis S, Gray JW, McCormick F, Chu S (2015) Ras-GTP dimers activate the Mitogen-Activated Protein Kinase (MAPK) pathway. Proc Natl Acad Sci U S A 112:7996–8001. https://doi.org/10.1073/pnas.1509123112

Nazarian R, Shi H, Wang Q, Kong X, Koya RC, Lee H, Chen Z, Lee M-K, Attar N, Sazegar H, Chodon T, Nelson SF, McArthur G, Sosman JA, Ribas A, Lo RS (2010) Melanomas acquire resistance to B-RAF(V600E) inhibition by RTK or N-RAS upregulation. Nature 468:973–977. https://doi.org/10.1038/nature09626

Nomura Y, Tashiro H, Hisamatsu K (1989) In vitro clonogenic growth and metastatic potential of human operable breast cancer. Cancer Res 49:5288–5293

Oddo D, Sennott EM, Barault L, Valtorta E, Arena S, Cassingena A, Filiciotto G, Marzolla G, Elez E, van Geel, Robin M J M, Bartolini A, Crisafulli G, Boscaro V, Godfrey JT, Buscarino M, Cancelliere C, Linnebacher M, Corti G, Truini M, Siravegna G, Grasselli J, Gallicchio M, Bernards R, Schellens JHM, Tabernero J, Engelman JA, Sartore-Bianchi A, Bardelli A, Siena S, Corcoran RB, Di Nicolantonio F (2016) Molecular Landscape of Acquired Resistance to Targeted Therapy Combinations in BRAF-Mutant Colorectal Cancer. Cancer Res 76:4504–4515. https://doi.org/10.1158/0008-5472.CAN-16-0396

Paraiso KHT, Xiang Y, Rebecca VW, Abel EV, Chen YA, Munko AC, Wood E, Fedorenko IV, Sondak VK, Anderson ARA, Ribas A, Palma MD, Nathanson KL, Koomen JM, Messina JL, Smalley KSM (2011) PTEN loss confers BRAF inhibitor resistance to melanoma cells through the suppression of BIM expression. Cancer Res 71:2750–2760. https://doi.org/10.1158/0008-5472.CAN-10-2954

Paraiso KHT, Haarberg HE, Wood E, Rebecca VW, Chen YA, Xiang Y, Ribas A, Lo RS, Weber JS, Sondak VK, John JK, Sarnaik AA, Koomen JM, Smalley KSM (2012) The HSP90 inhibitor XL888 overcomes BRAF inhibitor resistance mediated through diverse mechanisms. Clin Cancer Res 18:2502–2514. https://doi.org/10.1158/1078-0432.CCR-11-2612

Park Y, Hunter DJ, Spiegelman D, Bergkvist L, Berrino F, van den Brandt PA, Buring JE, Colditz GA, Freudenheim JL, Fuchs CS, Giovannucci E, Goldbohm RA, Graham S, Harnack L, Hartman AM, Jacobs DR, Kato I, Krogh V, Leitzmann MF, McCullough ML, Miller AB, Pietinen P, Rohan TE, Schatzkin A, Willett WC, Wolk A, Zeleniuch-Jacquotte A, Zhang SM, Smith-Warner SA (2005) Dietary fiber intake and risk of colorectal cancer: a pooled analysis of prospective cohort studies. JAMA 294:2849–2857. https://doi.org/10.1001/jama.294.22.2849

Pastushenko I, Blanpain C (2019) EMT Transition States during Tumor Progression and Metastasis. Trends Cell Biol 29:212–226. https://doi.org/10.1016/j.tcb.2018.12.001

Picard D (2019) HSP90 INTERACTORS. https://www.picard.ch/downloads/Hsp90interactors.pdf. Accessed 25 October 2019

Pietrantonio F, Petrelli F, Coinu A, Di Bartolomeo M, Borgonovo K, Maggi C, Cabiddu M, Iacovelli R, Bossi I, Lonati V, Ghilardi M, Braud F de, Barni S (2015) Predictive role of BRAF mutations in patients with advanced colorectal cancer receiving cetuximab and panitumumab: a meta-analysis. Eur J Cancer 51:587–594. https://doi.org/10.1016/j.ejca.2015.01.054

Pietrantonio F, Oddo D, Gloghini A, Valtorta E, Berenato R, Barault L, Caporale M, Busico A, Morano F, Gualeni AV, Alessi A, Siravegna G, Perrone F, Di Bartolomeo M, Bardelli A, Braud F de, Di Nicolantonio F (2016) MET-Driven Resistance to Dual EGFR and BRAF Blockade May Be Overcome by Switching from EGFR to MET Inhibition in BRAF-Mutated Colorectal Cancer. Cancer Discov 6:963–971. https://doi.org/10.1158/2159-8290.CD-16-0297

Pino MS, Chung DC (2010) The chromosomal instability pathway in colon cancer. Gastroenterology 138:2059–2072. https://doi.org/10.1053/j.gastro.2009.12.065

Piotrowska Z, Costa DB, Oxnard GR, Huberman M, Gainor JF, Lennes IT, Muzikansky A, Shaw AT, Azzoli CG, Heist RS, Sequist LV (2018) Activity of the Hsp90 inhibitor luminespib among non-small-cell lung cancers harboring EGFR exon 20 insertions. Ann Oncol 29:2092–2097. https://doi.org/10.1093/annonc/mdy336

Polier S, Samant RS, Clarke PA, Workman P, Prodromou C, Pearl LH (2013) ATP-competitive inhibitors block protein kinase recruitment to the Hsp90-Cdc37 system. Nat Chem Biol 9:307–312. https://doi.org/10.1038/nchembio.1212

Poulikakos PI, Persaud Y, Janakiraman M, Kong X, Ng C, Moriceau G, Shi H, Atefi M, Titz B, Gabay MT, Salton M, Dahlman KB, Tadi M, Wargo JA, Flaherty KT, Kelley MC, Misteli T, Chapman PB, Sosman JA, Graeber TG, Ribas A, Lo RS, Rosen N, Solit DB (2011) RAF inhibitor resistance is mediated by dimerization of aberrantly spliced BRAF(V600E). Nature 480:387–390. https://doi.org/10.1038/nature10662

Prahallad A, Sun C, Huang S, Di Nicolantonio F, Salazar R, Zecchin D, Beijersbergen RL, Bardelli A, Bernards R (2012) Unresponsiveness of colon cancer to BRAF(V600E) inhibition through feedback activation of EGFR. Nature 483:100–103. https://doi.org/10.1038/nature10868

Prahallad A, Heynen, Guus J J E, Germano G, Willems SM, Evers B, Vecchione L, Gambino V, Lieftink C, Beijersbergen RL, Di Nicolantonio F, Bardelli A, Bernards R (2015) PTPN11 Is a Central Node in Intrinsic and Acquired Resistance to Targeted Cancer Drugs. Cell Rep 12:1978–1985. https://doi.org/10.1016/j.celrep.2015.08.037

Prasetyanti PR, Capone E, Barcaroli D, D'Agostino D, Volpe S, Benfante A, van Hooff S, Iacobelli V, Rossi C, Iacobelli S, Medema JP, Laurenzi V de, Sala G (2015) ErbB-3 activation by NRG-1beta sustains growth and promotes vemurafenib resistance in BRAF-V600E colon cancer stem cells (CSCs). Oncotarget 6:16902–16911. https://doi.org/10.18632/oncotarget.4642

Pratt WB, Morishima Y, Osawa Y (2008) The Hsp90 chaperone machinery regulates signaling by modulating ligand binding clefts. J Biol Chem 283:22885–22889. https://doi.org/10.1074/jbc.R800023200

Puszkiel A, Noé G, Bellesoeur A, Kramkimel N, Paludetto M-N, Thomas-Schoemann A, Vidal M, Goldwasser F, Chatelut E, Blanchet B (2019) Clinical Pharmacokinetics and Pharmacodynamics of Dabrafenib. Clin Pharmacokinet 58:451–467. https://doi.org/10.1007/s40262-018-0703-0

Qu X, Yan X, Kong C, Zhu Y, Li H, Pan D, Zhang X, Liu Y, Yin F, Qin H (2019) c-Myb promotes growth and metastasis of colorectal cancer through c-fos-induced epithelial-mesenchymal transition. Cancer Sci 110:3183–3196. https://doi.org/10.1111/cas.14141

Ramalingam S, Goss G, Rosell R, Schmid-Bindert G, Zaric B, Andric Z, Bondarenko I, Komov D, Ceric T, Khuri F, Samarzija M, Felip E, Ciuleanu T, Hirsh V, Wehler T, Spicer J, Salgia R, Shapiro G, Sheldon E, Teofilovici F, Vukovic V, Fennell D (2015) A randomized phase II study of ganetespib, a heat shock protein 90 inhibitor, in combination with docetaxel in second-line therapy of advanced non-small cell lung cancer (GALAXY-1). Ann Oncol 26:1741–1748. https://doi.org/10.1093/annonc/mdv220

Renehan AG, Tyson M, Egger M, Heller RF, Zwahlen M (2008) Body-mass index and incidence of cancer: a systematic review and meta-analysis of prospective observational studies. The Lancet 371:569–578. https://doi.org/10.1016/S0140-6736(08)60269-X

Renouf DJ, Hedley D, Krzyzanowska MK, Schmuck M, Wang L, Moore MJ (2016) A phase II study of the HSP90 inhibitor AUY922 in chemotherapy refractory advanced pancreatic cancer. Cancer Chemother Pharmacol 78:541–545. https://doi.org/10.1007/s00280-016-3102-y

Riss TL, Moravec RA, Niles AL, Duellman S, Benink HA, Worzella TJ, Minor L (2004) Assay Guidance Manual: Cell Viability Assays, Bethesda (MD)

Robert C, Grob JJ, Stroyakovskiy D, Karaszewska B, Hauschild A, Levchenko E, Chiarion Sileni V, Schachter J, Garbe C, Bondarenko I, Gogas H, Mandalá M, Haanen JBAG, Lebbé C, Mackiewicz A, Rutkowski P, Nathan PD, Ribas A, Davies MA, Flaherty KT, Burgess P, Tan M, Gasal E, Voi M, Schadendorf D, Long GV (2019) Five-Year Outcomes with Dabrafenib plus Trametinib in Metastatic Melanoma. N Engl J Med 381:626–636. https://doi.org/10.1056/NEJMoa1904059

Rodina A, Wang T, Yan P, Gomes ED, Dunphy MPS, Pillarsetty N, Koren J, Gerecitano JF, Taldone T, Zong H, Caldas-Lopes E, Alpaugh M, Corben A, Riolo M, Beattie B, Pressl C, Peter RI, Xu C, Trondl R, Patel HJ, Shimizu F, Bolaender A, Yang C, Panchal P, Farooq MF, Kishinevsky S, Modi S, Lin O, Chu F, Patil S, Erdjument-Bromage H, Zanzonico P, Hudis C, Studer L, Roboz GJ, Cesarman E, Cerchietti L, Levine R, Melnick A, Larson SM, Lewis JS, Guzman ML, Chiosis G (2016) The epichaperome is an integrated chaperome network that facilitates tumour survival. Nature 538:397–401. https://doi.org/10.1038/nature19807

Roell KR, Reif DM, Motsinger-Reif AA (2017) An Introduction to Terminology and Methodology of Chemical Synergy—Perspectives from Across Disciplines. Front Pharmacol 8. https://doi.org/10.3389/fphar.2017.00158

Roth AD, Tejpar S, Delorenzi M, Yan P, Fiocca R, Klingbiel D, Dietrich D, Biesmans B, Bodoky G, Barone C, Aranda E, Nordlinger B, Cisar L, Labianca R, Cunningham D, van Cutsem E, Bosman F (2010) Prognostic role of KRAS and BRAF in stage II and III resected colon cancer: results of the translational study on the PETACC-3, EORTC 40993, SAKK 60-00 trial. JCO 28:466–474. https://doi.org/10.1200/JCO.2009.23.3452

Samowitz WS, Sweeney C, Herrick J, Albertsen H, Levin TR, Murtaugh MA, Wolff RK, Slattery ML (2005) Poor survival associated with the BRAF V600E mutation in microsatellite-stable colon cancers. Cancer Res 65:6063–6069. https://doi.org/10.1158/0008-5472.CAN-05-0404

Sanchez J, Carter TR, Cohen MS, Blagg BSJ (2020) Old and New Approaches to Target the Hsp90 Chaperone. Curr Cancer Drug Targets 20:253–270. https://doi.org/10.2174/1568009619666191202101330

Sanz-Garcia E, Argiles G, Elez E, Tabernero J (2017) BRAF mutant colorectal cancer: prognosis, treatment, and new perspectives. Ann Oncol 28:2648–2657. https://doi.org/10.1093/annonc/mdx401

Saturno G, Valenti M, Haven Brandon A de, Thomas GV, Eccles S, Clarke PA, Workman P (2013) Combining trail with PI3 kinase or HSP90 inhibitors enhances apoptosis in colorectal cancer cells via suppression of survival signaling. Oncotarget 4:1185–1198. https://doi.org/10.18632/oncotarget.1162

Schmitz S (2011) Der Experimentator: Zellkultur. Spektrum Akademischer Verlag, Heidelberg

Schopf FH, Biebl MM, Buchner J (2017) The HSP90 chaperone machinery. Nat Rev Mol Cell Biol 18:345–360. https://doi.org/10.1038/nrm.2017.20

Schulte TW, Blagosklonny MV, Ingui C, Neckers L (1995) Disruption of the Raf-1-Hsp90 molecular complex results in destabilization of Raf-1 and loss of Raf-1-Ras association. J Biol Chem 270:24585–24588. https://doi.org/10.1074/jbc.270.41.24585

Shaw E, Farris MS, Stone CR, Derksen JWG, Johnson R, Hilsden RJ, Friedenreich CM, Brenner DR (2018) Effects of physical activity on colorectal cancer risk among family history and body mass index subgroups: a systematic review and meta-analysis. BMC Cancer 18:71. https://doi.org/10.1186/s12885-017-3970-5

Shimada Y, Muneoka Y, Nagahashi M, Ichikawa H, Tajima Y, Hirose Y, Ando T, Nakano M, Sakata J, Kameyama H, Takii Y, Ling Y, Okuda S, Takabe K, Wakai T (2019) BRAF V600E and SRC mutations as molecular markers for predicting prognosis and conversion surgery in Stage IV colorectal cancer. Sci Rep 9:2466. https://doi.org/10.1038/s41598-019-39328-6

Sievers CK, Grady WM, Halberg RB, Pickhardt PJ (2017) New insights into the earliest stages of colorectal tumorigenesis. Expert Rev Gastroenterol Hepatol 11:723–729. https://doi.org/10.1080/17474124.2017.1330150

Smeby J, Sveen A, Merok MA, Danielsen SA, Eilertsen IA, Guren MG, Dienstmann R, Nesbakken A, Lothe RA (2018) CMS-dependent prognostic impact of KRAS and BRAFV600E mutations in primary colorectal cancer. Ann Oncol 29:1227–1234. https://doi.org/10.1093/annonc/mdy085

Sorge RE, Martin LJ, Isbester KA, Sotocinal SG, Rosen S, Tuttle AH, Wieskopf JS, Acland EL, Dokova A, Kadoura B, Leger P, Mapplebeck JCS, McPhail M, Delaney A, Wigerblad G, Schumann AP, Quinn T, Frasnelli J, Svensson CI, Sternberg WF, Mogil JS (2014) Olfactory exposure to males, including men, causes stress and related analgesia in rodents. Nat Methods 11:629–632. https://doi.org/10.1038/nmeth.2935

Sottoriva A, Kang H, Ma Z, Graham TA, Salomon MP, Zhao J, Marjoram P, Siegmund K, Press MF, Shibata D, Curtis C (2015) A Big Bang model of human colorectal tumor growth. Nat Genet 47:209–216. https://doi.org/10.1038/ng.3214

Spreafico A, Delord J-P, Mattos-Arruda L de, Berge Y, Rodon J, Cottura E, Bedard PL, Akimov M, Lu H, Pain S, Kaag A, Siu LL, Cortes J (2015) A first-in-human phase I, dose-escalation, multicentre study of HSP990 administered orally in adult patients with advanced solid malignancies. Br J Cancer 112:650–659. https://doi.org/10.1038/bjc.2014.653

Straussman R, Morikawa T, Shee K, Barzily-Rokni M, Qian ZR, Du J, Davis A, Mongare MM, Gould J, Frederick DT, Cooper ZA, Chapman PB, Solit DB, Ribas A, Lo RS, Flaherty KT, Ogino S, Wargo

JA, Golub TR (2012) Tumour micro-environment elicits innate resistance to RAF inhibitors through HGF secretion. Nature 487:500–504. https://doi.org/10.1038/nature11183

Subramaniam S, Goodman GE, Boatman B, Smith AW, Iriarte D, Gold PJ (2015) A phase Ib study of AUY922 and cetuximab in patients with KRAS wild-type (WT) metastatic colorectal cancer (mCRC). JCO 33:3540. https://doi.org/10.1200/jco.2015.33.15_suppl.3540

Sueda T, Sakai D, Kawamoto K, Konno M, Nishida N, Koseki J, Colvin H, Takahashi H, Haraguchi N, Nishimura J, Hata T, Takemasa I, Mizushima T, Yamamoto H, Satoh T, Doki Y, Mori M, Ishii H (2016) BRAF V600E inhibition stimulates AMP-activated protein kinase-mediated autophagy in colorectal cancer cells. Sci Rep 6:18949. https://doi.org/10.1038/srep18949

Sveen A, Bruun J, Eide PW, Eilertsen IA, Ramirez L, Murumägi A, Arjama M, Danielsen SA, Kryeziu K, Elez E, Tabernero J, Guinney J, Palmer HG, Nesbakken A, Kallioniemi O, Dienstmann R, Lothe RA (2018) Colorectal Cancer Consensus Molecular Subtypes Translated to Preclinical Models Uncover Potentially Targetable Cancer Cell Dependencies. Clin Cancer Res 24:794–806. https://doi.org/10.1158/1078-0432.CCR-17-1234

Takayama T, Katsuki S, Takahashi Y, Ohi M, Nojiri S, Sakamaki S, Kato J, Kogawa K, Miyake H, Niitsu Y (1998) Aberrant crypt foci of the colon as precursors of adenoma and cancer. N Engl J Med 339:1277–1284. https://doi.org/10.1056/NEJM199810293391803

Tejpar S, Stintzing S, Ciardiello F, Tabernero J, van Cutsem E, Beier F, Esser R, Lenz H-J, Heinemann V (2017) Prognostic and Predictive Relevance of Primary Tumor Location in Patients With RAS Wild-Type Metastatic Colorectal Cancer: Retrospective Analyses of the CRYSTAL and FIRE-3 Trials. JAMA Oncol 3:194–201. https://doi.org/10.1001/jamaoncol.2016.3797

Terrell EM, Morrison DK (2019) Ras-Mediated Activation of the Raf Family Kinases. Cold Spring Harb Perspect Med 9. https://doi.org/10.1101/cshperspect.a033746

Testa U, Pelosi E, Castelli G (2018) Colorectal cancer: genetic abnormalities, tumor progression, tumor heterogeneity, clonal evolution and tumor-initiating cells. Med Sci (Basel) 6. https://doi.org/10.3390/medsci6020031

Travers T, López CA, Van QN, Neale C, Tonelli M, Stephen AG, Gnanakaran S (2018) Molecular recognition of RAS/RAF complex at the membrane: Role of RAF cysteine-rich domain. Sci Rep 8:8461. https://doi.org/10.1038/s41598-018-26832-4

Tutuka CSA, Andrews MC, Mariadason JM, Ioannidis P, Hudson C, Cebon J, Behren A (2017) PLX8394, a new generation BRAF inhibitor, selectively inhibits BRAF in colonic adenocarcinoma cells and prevents paradoxical MAPK pathway activation. Mol Cancer 16:112. https://doi.org/10.1186/s12943-017-0684-x

Ursem C, Atreya CE, van Loon K (2018) Emerging treatment options for BRAF-mutant colorectal cancer. Gastrointest Cancer 8:13–23. https://doi.org/10.2147/GICTT.S125940

van Cutsem E, Huijberts S, Grothey A, Yaeger R, Cuyle P-J, Elez E, Fakih M, Montagut C, Peeters M, Yoshino T, Wasan H, Desai J, Ciardiello F, Gollerkeri A, Christy-Bittel J, Maharry K, Sandor V, Schellens JHM, Kopetz S, Tabernero J (2019) Binimetinib, Encorafenib, and Cetuximab Triplet Therapy for Patients With BRAF V600E-Mutant Metastatic Colorectal Cancer: Safety Lead-In Results From the Phase III BEACON Colorectal Cancer Study. JCO 37:1460–1469. https://doi.org/10.1200/JCO.18.02459

van Geel RMJM, Tabernero J, Elez E, Bendell JC, Spreafico A, Schuler M, Yoshino T, Delord J-P, Yamada Y, Lolkema MP, Faris JE, Eskens FALM, Sharma S, Yaeger R, Lenz H-J, Wainberg ZA, Avsar E, Chatterjee A, Jaeger S, Tan E, Maharry K, Demuth T, Schellens JHM (2017) A Phase Ib Dose-Escalation Study of Encorafenib and Cetuximab with or without Alpelisib in Metastatic BRAF-Mutant Colorectal Cancer. Cancer Discov 7:610–619. https://doi.org/10.1158/2159-8290.CD-16-0795

Venderbosch S, Nagtegaal ID, Maughan TS, Smith CG, Cheadle JP, Fisher D, Kaplan R, Quirke P, Seymour MT, Richman SD, Meijer GA, Ylstra B, Heideman DAM, Haan AFJ de, Punt CJA, Koopman M (2014) Mismatch repair status and BRAF mutation status in metastatic colorectal cancer patients: a pooled analysis of the CAIRO, CAIRO2, COIN, and FOCUS studies. Clin Cancer Res 20:5322–5330. https://doi.org/10.1158/1078-0432.CCR-14-0332

Villanueva J, Vultur A, Lee JT, Somasundaram R, Fukunaga-Kalabis M, Cipolla AK, Wubbenhorst B, Xu X, Gimotty PA, Kee D, Santiago-Walker AE, Letrero R, D'Andrea K, Pushparajan A, Hayden JE, Brown KD, Laquerre S, McArthur GA, Sosman JA, Nathanson KL, Herlyn M (2010) Acquired resistance to BRAF inhibitors mediated by a RAF kinase switch in melanoma can be overcome by cotargeting MEK and IGF-1R/PI3K. Cancer Cell 18:683–695. https://doi.org/10.1016/j.ccr.2010.11.023

Vin H, Ojeda SS, Ching G, Leung ML, Chitsazzadeh V, Dwyer DW, Adelmann CH, Restrepo M, Richards KN, Stewart LR, Du L, Ferguson SB, Chakravarti D, Ehrenreiter K, Baccarini M, Ruggieri R, Curry JL, Kim KB, Ciurea AM, Duvic M, Prieto VG, Ullrich SE, Dalby KN, Flores ER, Tsai KY (2013) BRAF inhibitors suppress apoptosis through off-target inhibition of JNK signaling. Elife 2:e00969. https://doi.org/10.7554/eLife.00969

Vogelstein B, Fearon ER, Hamilton SR, Kern SE, Preisinger AC, Leppert M, Nakamura Y, White R, Smits AM, Bos JL (1988) Genetic alterations during colorectal-tumor development. N Engl J Med 319:525–532. https://doi.org/10.1056/NEJM198809013190901

Wagle N, Emery C, Berger MF, Davis MJ, Sawyer A, Pochanard P, Kehoe SM, Johannessen CM, MacConaill LE, Hahn WC, Meyerson M, Garraway LA (2011) Dissecting therapeutic resistance to RAF inhibition in melanoma by tumor genomic profiling. JCO 29:3085–3096. https://doi.org/10.1200/JCO.2010.33.2312

Walter V, Jansen L, Hoffmeister M, Brenner H (2014) Smoking and survival of colorectal cancer patients: systematic review and meta-analysis. Ann Oncol 25:1517–1525. https://doi.org/10.1093/annonc/mdu040

Wan PTC, Garnett MJ, Roe SM, Lee S, Niculescu-Duvaz D, Good VM, Jones CM, Marshall CJ, Springer CJ, Barford D, Marais R (2004) Mechanism of activation of the RAF-ERK signaling pathway by oncogenic mutations of B-RAF. Cell 116:855–867. https://doi.org/10.1016/s0092-8674(04)00215-6

Wang W, Xu S, Yin M, Jin ZG (2015) Essential roles of Gab1 tyrosine phosphorylation in growth factor-mediated signaling and angiogenesis. Int J Cardiol 181:180–184. https://doi.org/10.1016/j.ijcard.2014.10.148

Wang L, Zhang L, Li L, Jiang J, Zheng Z, Shang J, Wang C, Chen W, Bao Q, Xu X, Jiang Z, Zhang J, You Q (2019) Small-molecule inhibitor targeting the Hsp90-Cdc37 protein-protein interaction in colorectal cancer. Sci Adv 5:eaax2277. https://doi.org/10.1126/sciadv.aax2277

Wang L, Jiang J, Zhang L, Zhang Q, Zhou J, Li L, Xu X, You Q (2020) Discovery and Optimization of Small Molecules Targeting the Protein-Protein Interaction of Heat Shock Protein 90 (Hsp90) and Cell Division Cycle 37 as Orally Active Inhibitors for the Treatment of Colorectal Cancer. J Med Chem 63:1281–1297. https://doi.org/10.1021/acs.jmedchem.9b01659

Wang CY, Guo ST, Wang JY, Yan XG, Farrelly M, Zhang YY, Liu F, Yari H, La T, Lei FX, Jin L, Zhang XD, Jiang CC (2016) Reactivation of ERK and Akt confers resistance of mutant BRAF colon cancer cells to the HSP90 inhibitor AUY922. Oncotarget 7:49597–49610. https://doi.org/10.18632/oncotarget.10414.

Wasserstein RL, Lazar NA (2016) The ASA Statement on p -Values: Context, Process, and Purpose. The American Statistician 70:129–133. https://doi.org/10.1080/00031305.2016.1154108

Wasserstein RL, Schirm AL, Lazar NA (2019) Moving to a World Beyond " p < 0.05". The American Statistician 73:1–19. https://doi.org/10.1080/00031305.2019.1583913

Weber CK, Slupsky JR, Kalmes HA, Rapp UR (2001) Active Ras induces heterodimerization of cRaf and BRaf. Cancer Res 61:3595–3598

Wolff WI, Shinya H (1973) Polypectomy via the fiberoptic colonoscope. Removal of neoplasms beyond reach of the sigmoidoscope. N Engl J Med 288:329–332. https://doi.org/10.1056/NEJM197302152880701

Yaeger R, Cercek A, O'Reilly EM, Reidy DL, Kemeny N, Wolinsky T, Capanu M, Gollub MJ, Rosen N, Berger MF, Lacouture ME, Vakiani E, Saltz LB (2015) Pilot trial of combined BRAF and EGFR inhibition in BRAF-mutant metastatic colorectal cancer patients. Clin Cancer Res 21:1313–1320. https://doi.org/10.1158/1078-0432.CCR-14-2779

Yaeger R, Yao Z, Hyman DM, Hechtman JF, Vakiani E, Zhao H, Su W, Wang L, Joelson A, Cercek A, Baselga J, Stanchina E de, Saltz L, Berger MF, Solit DB, Rosen N (2017) Mechanisms of Acquired Resistance to BRAF V600E Inhibition in Colon Cancers Converge on RAF Dimerization and Are Sensitive to Its Inhibition. Cancer Res 77:6513–6523. https://doi.org/10.1158/0008-5472.CAN-17-0768

Yao Z, Torres NM, Tao A, Gao Y, Luo L, Li Q, Stanchina E de, Abdel-Wahab O, Solit DB, Poulikakos PI, Rosen N (2015) BRAF Mutants Evade ERK-Dependent Feedback by Different Mechanisms that Determine Their Sensitivity to Pharmacologic Inhibition. Cancer Cell 28:370–383. https://doi.org/10.1016/j.ccell.2015.08.001

Yao Z, Yaeger R, Rodrik-Outmezguine VS, Tao A, Torres NM, Chang MT, Drosten M, Zhao H, Cecchi F, Hembrough T, Michels J, Baumert H, Miles L, Campbell NM, Stanchina E de, Solit DB, Barbacid M, Taylor BS, Rosen N (2017) Tumours with class 3 BRAF mutants are sensitive to the inhibition of activated RAS. Nature 548:234–238. https://doi.org/10.1038/nature23291

Yun J, Rago C, Cheong I, Pagliarini R, Angenendt P, Rajagopalan H, Schmidt K, Willson JKV, Markowitz S, Zhou S, Diaz LA, Velculescu VE, Lengauer C, Kinzler KW, Vogelstein B, Papadopoulos N (2009) Glucose deprivation contributes to the development of KRAS pathway mutations in tumor cells. Science 325:1555–1559. https://doi.org/10.1126/science.1174229

Zhang W, Liu HT (2002) MAPK signal pathways in the regulation of cell proliferation in mammalian cells. Cell Res 12:9–18. https://doi.org/10.1038/sj.cr.7290105

Zhang W, Heinzmann D, Grippo JF (2017) Clinical Pharmacokinetics of Vemurafenib. Clin Pharmacokinet 56:1033–1043. https://doi.org/10.1007/s40262-017-0523-7

Zoratto F, Rossi L, Verrico M, Papa A, Basso E, Zullo A, Tomao L, Romiti A, Lo Russo G, Tomao S (2014) Focus on genetic and epigenetic events of colorectal cancer pathogenesis: implications for molecular diagnosis. Tumour Biol 35:6195–6206. https://doi.org/10.1007/s13277-014-1845-9

8 Theses

1 The HSP90 inhibitors 17-AAG and HSP990 are active in all examined BRAF-mutated colorectal cancer cell lines with high potency at nanomolar concentrations in two-dimensional-monolayer cell culture conditions, as well as in three-dimensional anchorage-independent culture conditions.

2 The BRAF inhibitors vemurafenib and dabrafenib and the HSP90 inhibitors 17-AAG and HSP990 in combination act additively in the examined BRAFV600-mutated colorectal cancer cell lines in two-dimensional-monolayer cell culture conditions with the exception of some slightly antagonistic effects in HT-29 cells and some slightly synergistic effects in RKO cells.

3 The BRAF inhibitors vemurafenib and dabrafenib and the HSP90 inhibitors 17-AAG and HSP990 in combination act clearly synergistic in BRAFV600-mutant COLO 201 cells and slightly synergistic or at least additively in BRAFV600-mutant HT-29 cells in the three-dimensional anchorage-independent culture conditions at nanomolar concentrations.

4 Combination treatment of the BRAF inhibitor dabrafenib and the HSP90 inhibitor HSP990 inhibits tumour growth in BRAFV600-mutated HT-29 xenografts in mice.

5 The combination regimen of the BRAF inhibitor dabrafenib and the HSP90 inhibitor HSP990 is relatively well tolerated by mice since mice recovered quickly from diarrhoea and weight loss after HSP990 application.

Appendix

Table 3: *Clinical trials in BRAFV600mut CRC patients.*

inhibitor	compounds	ref	N	CR/PR [%]	SD [%]	PD [%]	PFS [month]	OS [month]
placebo	-	(Grothey et al. 2013)	255	0.4	15	80	1.7	5.0
BRAFi	R		505	1	43	50	1.9	6.4
BRAFi	E	(Gomez-Roca et al. 2014)	18	0	67	22	4.0	
BRAFi	V	(Kopetz et al. 2015)	21	24	33	43	2.1	7.7
BRAFi	V	(Hyman et al. 2015)	10	0	50	26	4.5	9.3
BRAFi + EGFRi	V + C		27	4	67	23	3.7	7.1
BRAFi + EGFRi	V + P	(Yaeger et al. 2015)	15	13	53	33	3.2	7.6
BRAFi + MEKi	D + T	(Corcoran et al. 2015)	43	12	56	23	3.5	
BRAFi + MEKi	D + T	(Atreya et al. 2015)	20	10	80	10		
BRAFi + MEKi + EGFRi	D + T + P		35	26	57	14		
BRAFi + EGFRi + CT	V + C + IRI	(Hong et al. 2016)	19	32	47	11	7.7	
BRAFi + MEKi	E + C	(van Geel et al. 2017)	26	19	58	15	3.4	
BRAFi + MEKi + PI3Ki	E + C + AL		28	18	75	4	4.2	
BRAFi + EGFRi	D + P	(Corcoran et al. 2018)	20	10	80	10	3.5	13.2
BRAFi + MEKi + EGFRi	D + T + P		91	21	65	9	4.2	9.1
BRAFi + MEKi + EGFRi	E + B + C	(van Cutsem et al. 2019)	29	41	45	0	5.5	15.3
EGFRi + CT	C+IRI/ FOLFIRI	(Kopetz et al. 2019)	107	2	29	34	1.5	5.4
BRAFi + EGFRi	E + C		113	20	54	7	4.2	8.4
BRAFi + MEKi + EGFRi	E + B + C		111	26	42	10	4.3	9.0
EGFRi + CT	C + IRI	(Kopetz et al. 2021)	50	4	17	53	2	5.9
BRAFi + EGFRi + CT	V + C + IRI		49	16	50	16	4.2	9.6

Abbreviations: alpelisib (AL), binimetinib (B), cetuximab (C), complete response (CR), chemo therapy (CT), dabrafenib (D), encorafenib (E), folinic acid + irinotecan (FOLFIRI), inhibitor (-i) irinotecan (IRI), number of patients (N), overall survival (OS), panitumumab (P), progressive disease (PD), progression free survival (PFS), partial response (PR), regorafenib (R), reference (ref), stable disease (SD), vemurafenib (V)

Table 4: *BRAFi resistance mechanisms, non-mutational and mutational alterations.*

MAPK/ERK pathway	Cross-talking pathways
- RASwt amplification (Mao et al. 2013; Yaeger et al. 2017) - BRAFwt, BRAFV600 amplification (Corcoran et al. 2010; Oddo et al. 2016) - increased BRAFV600/BRAFwt/CRAF homo/heterodimerisation (Lito et al. 2012; Yaeger et al. 2017) - kinase switch between A/B/CRAF (Villanueva et al. 2010) - alternatively spliced BRAFV600 isoforms dimerising RAS independently (Poulikakos et al. 2011) - feedback activation of EGFR (Corcoran et al. 2012; Prahallad et al. 2012) - EGFR amplification (Mao et al. 2013) - HGF secreting microenvironment (Straussman et al. 2012) - up-regulation of other RTKs, especially HER2/3 (Herr et al. 2018; Prasetyanti et al. 2015), PDGFR (Nazarian et al. 2010), IGF1R (Villanueva et al. 2010), HGFR (Pietrantonio et al. 2016) - GAB1/2, SHP2 up-regulation (Herr et al. 2018; Prahallad et al. 2015)	- AKT over-expression, up-regulation of PI3K/AKT/mTOR pathway (Mao et al. 2013) - CRC: WNT activation (Chen et al. 2018) - Malignant melanoma: WNT inactivation (Biechele et al. 2012) - down-regulation of proapoptotic BMF (Boussemart et al. 2014) - EIF4F complex accumulation, increased translation (Boussemart et al. 2014) - ATF4 up-regulation, integrated stress response (Nagasawa et al. 2017) - AMPK up-regulation, increased autophagy (Sueda et al. 2016) - COT over-expression (Johannessen et al. 2010)
- KRAS/NRASmut (Oddo et al. 2016) - EGFRmut (Oddo et al. 2016) - MEK1/2mut (Emery et al. 2009; Emery et al. 2017; Oddo et al. 2016)	- PTEN loss, PI3Kmut (Mao et al. 2013; Paraiso et al. 2011)

Colours: non-mutational (grey), mutational (white)
Abbreviations: colorectal cancer (CRC), mutated (mut), receptor tyrosine kinase (RTK), wild type (wt), protein names (please see section Abbreviations, pages III-V)

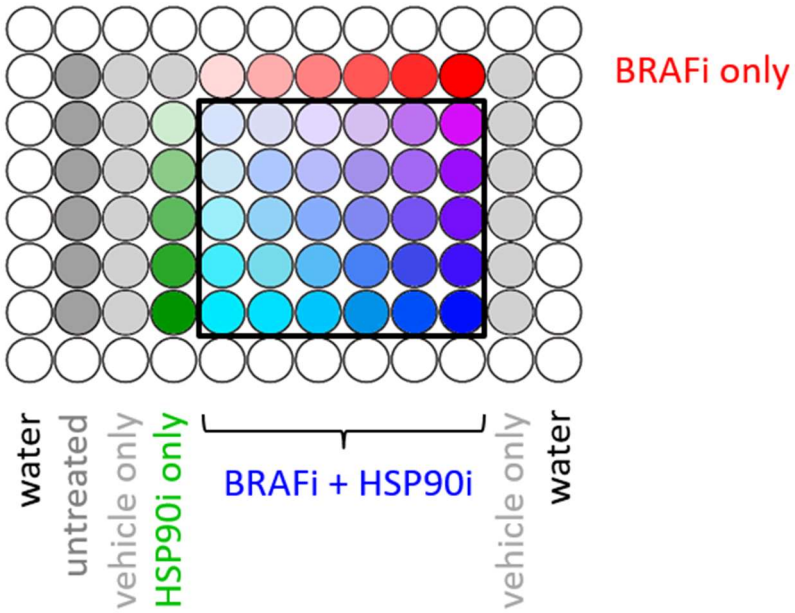

Figure 9: *Treatment scheme for cells cultures in 96-well plates to conduct the 2D resazurin assay. Abbreviations: BRAF inhibitor (BRAFi), HSP90 inhibitor (HSP90i)*

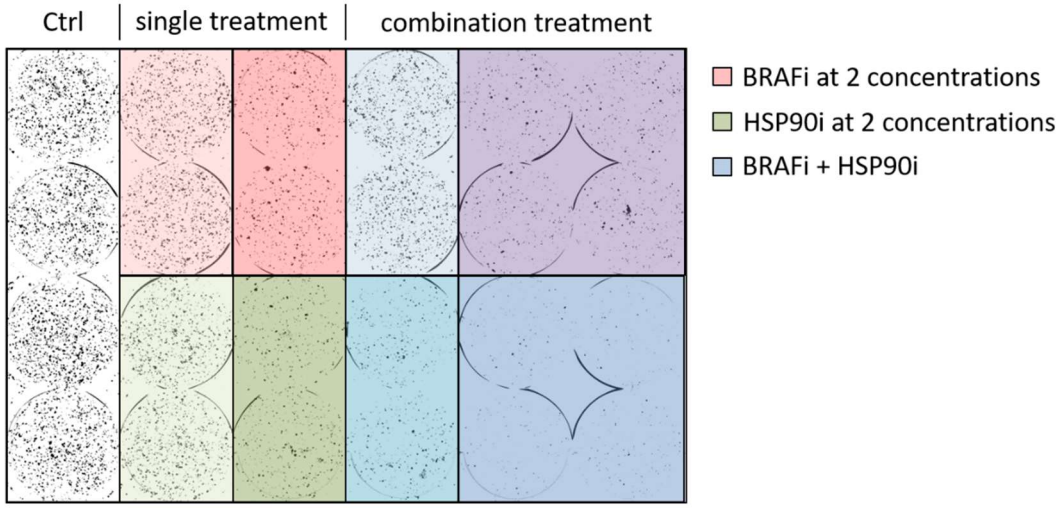

Figure 10: *Treatment scheme for 24-well plates utilised for the 3D anchorage-independent growth soft agar assay. Abbreviations: BRAF inhibitor (BRAFi), control (Ctrl), HSP90 inhibitor (HSP90i)*

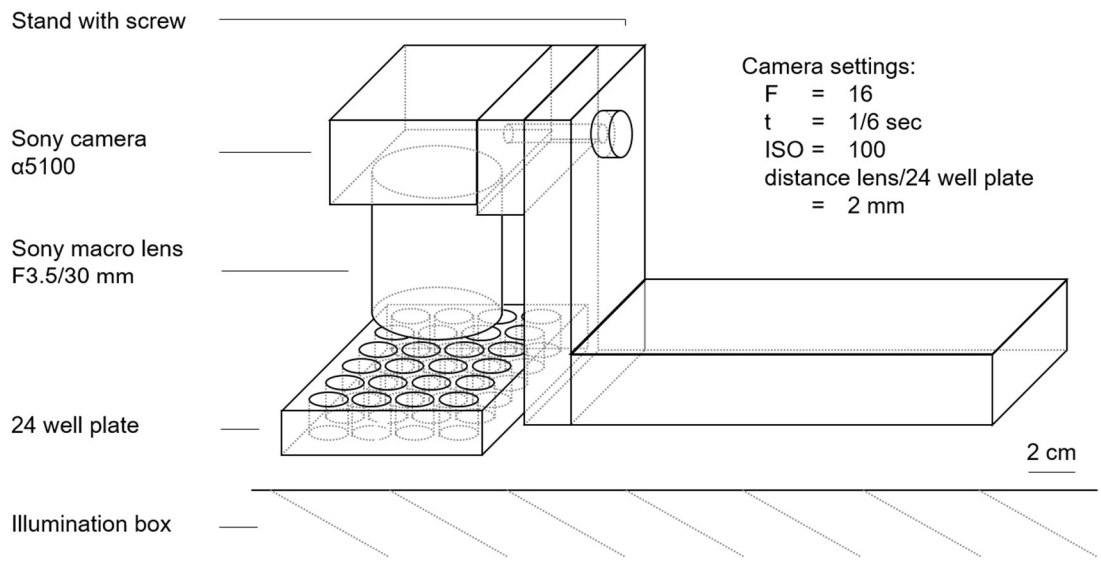

Figure 11: *Image acquisition conditions for colonies formed in the soft agar anchorage-independent growth assay. Abbreviations: Focal length (F), exposure time (t), sensitivity (ISO)*

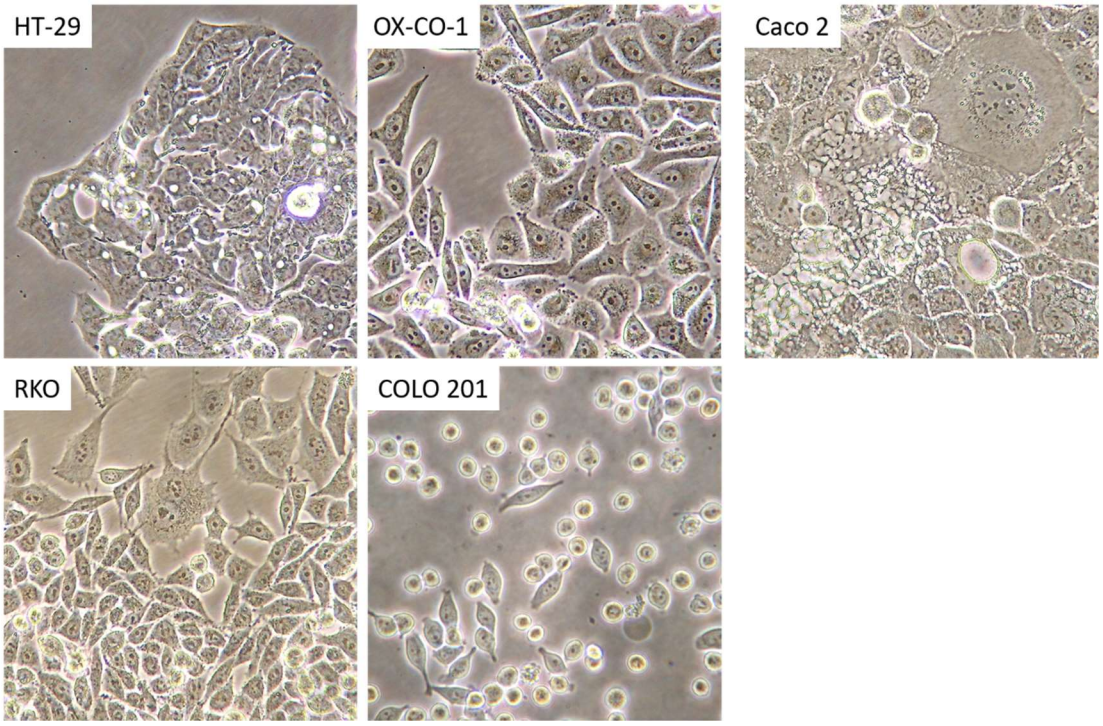

Figure 12: *Colorectal cancer cell lines used in 2D cell culture experiments.*

```
//preparation 1: manually load images of 24 wells and one scale to ImageJ
//preparation 2: set global scale in mm, close scale image
run("Images to Stack", "name=Stack title=[] use"); //creates stack of all 24 images
run("Duplicate...", "duplicate"); //duplicates stack to keep one non-binarized stack for comparison
selectWindow("Stack-1");
run("Make Montage...", "columns=6 rows=4 scale=0.25 first=1 last=24 increment=1 border=0 font=12");
//creates a montage consisting of 24 images in 6 columns and 4 rows
selectWindow("Stack");
run("8-bit"); //runs image binarization
waitForUser( "Pause","Some \n Dialog"); //set threshold for binarization manually:  Image -> Adjust -> Threshold, then press <ok> in user dialog
run("Fill Holes", "stack"); //fills white pixels within colonies; run("Watershed", "stack"); //separates confluent colonies
myPicWidth = getWidth();
print(myPicWidth);
toScaled(myPicWidth);
myPicWidth = myPicWidth/2;
print(myPicWidth);

for (myslice=1; myslice<25; myslice++) {
                        run("Specify...", "width=13 height=13 x=myPicWidth y=myPicWidth slice=myslice oval constrain centered scaled");
                        run("Analyze Particles...", "  circularity=0.00-1.00 display exclude clear add slice");
                        sliceLabel = getInfo("slice.label");
                        myFileName = "D:\\Medizin\\Dissertation\\data\\0Soft-Agar-Assays_results\\0output\\"+sliceLabel+".xls";
                        saveAs("Results", myFileName);
                        print(myFileName);
                        roiManager("Delete");
}
//creates a defined selection, extracts colony size in mm² from selection and saves data as excel sheet for each image within the stack

run("Make Montage...", "columns=6 rows=4 scale=0.25 first=1 last=24 increment=1 border=0 font=12");
//creates a montage consisting of 24 images in 6 columns and 4 rows
selectWindow("Stack-1");
run("Close");
selectWindow("Stack");
run("Close");
//save binarized and non binarized montage manually
```

Figure 13: *Macro module for image analysis in ImageJ; written with the support of Dr. Marc Lewitzky.*

```
' first: run macro "GetSheets"
' imports all sheets from a directory into one single map
Sub GetSheets()
Path = "myPath"
' insert directory
Filename = Dir(Path & "*.xls")
  Do While Filename <> ""
  Workbooks.Open Filename:=Path & Filename, ReadOnly:=True
     For Each Sheet In ActiveWorkbook.Sheets
     Sheet.Copy After:=ThisWorkbook.Sheets(1)
  Next Sheet
     Workbooks(Filename).Close
     Filename = Dir()
  Loop
End Sub
```

```
' second: run macro "Sort_Active_Book"
' sorts all imported sheets according to their title
Sub Sort_Active_Book()
Dim i As Integer
Dim j As Integer
Dim iAnswer As VbMsgBoxResult
' prompts the user to choose sorting direction
   iAnswer = MsgBox("Sort Sheets in Ascending Order?" & Chr(10) _
     & "Clicking No will sort in Descending Order", _
     vbYesNoCancel + vbQuestion + vbDefaultButton1, "Sort Worksheets")
   For i = 1 To Sheets.Count
      For j = 1 To Sheets.Count - 1
' if the answer is Yes, then sort in ascending order.
         If iAnswer = vbYes Then
            If UCase$(Sheets(j).Name) > UCase$(Sheets(j + 1).Name) Then
               Sheets(j).Move After:=Sheets(j + 1)
            End If
' if the answer is No, then sort in descending order.
         ElseIf iAnswer = vbNo Then
            If UCase$(Sheets(j).Name) < UCase$(Sheets(j + 1).Name) Then
               Sheets(j).Move After:=Sheets(j + 1)
            End If
         End If
      Next j
   Next i
End Sub
```

Figure 14: *Macro module for MS Excel to import and sort sheets; written by Dr. Marc Lewitzky.*

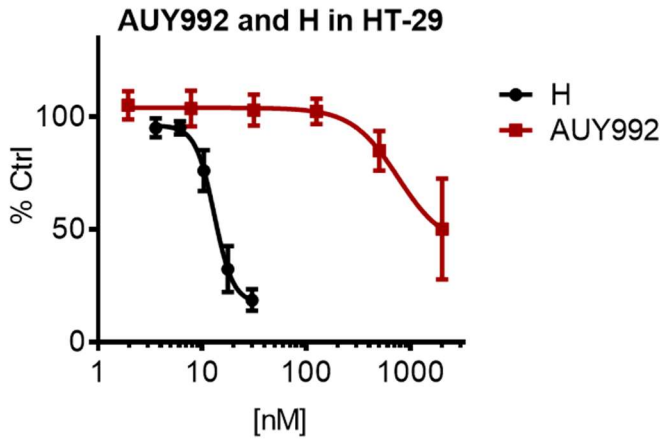

Figure 15: *Single treatment of HT-29 cells with AUY992 and HSP990 (H) for 72 h using resazurin assay. Normalized data between background (0%) and vehicle-treated control (Ctrl) (100%). Means and standard deviations of at least three independent experiments.*

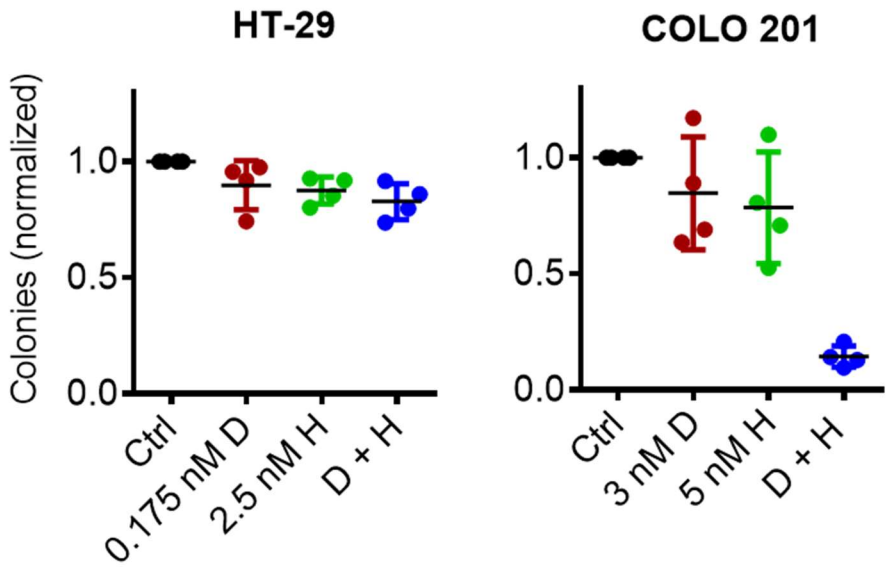

Figure 16: *Dabrafenib (D) and HSP990 (H) combination treatment at low concentrations of HT-29 cells in comparison to COLO 201 cells in 3D soft agar anchorage-independent growth assay. Results of four independent experiments are shown. Vehicle-treated control (Ctrl).*

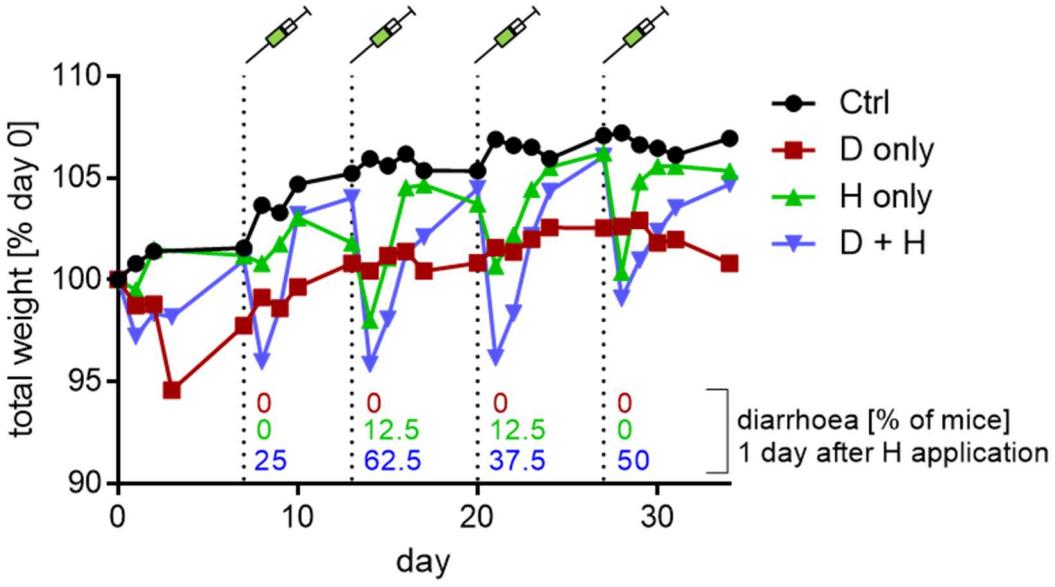

Figure 17*: Total weight of mice during treatment, normalized to day 0. Dabrafenib (D) was applied daily, except on weekends, and HSP990 (H) as indicated by the dotted lines. Means of eight mice each are shown. Vehicle-treated control (Ctrl).*

Danksagung

Mein Dank gilt all denjenigen, die zum Gelingen meiner Dissertation beigetragen haben.

Allen voran danke ich Herrn Prof. Stephan M. Feller, meinem Doktorvater. Mit seiner freundlichen, weitsichtigen und toleranten Supervision begleitete, unterstütze und förderte er mich und meine Promotion in seiner Arbeitsgruppe Tumorbiologie. Außerdem gilt mein Dank insbesondere Herrn Dr. Marc Lewitzky, welcher mir stets mit Rat und Tat zur Seite stand und für Fragen aller Art ein offenes Ohr und eine hilfreiche Antwort parat hatte. Der häufige Austausch mit Herrn Prof. Stephan M. Feller und Herrn Dr. Marc Lewitzky, auf fachlicher wie auf privater Ebene, hat mich auch nachhaltig geprägt, nicht nur wissenschaftliche Literatur, sondern auch alltägliche Aspekte kritisch und zielorientiert zu hinterfragen.

Zudem danke ich Herrn Dr. Thomas Müller, dem Gruppenleiter der Arbeitsgruppe Experimentelle Onkologie, Klinik für Innere Medizin IV, Universitätsklinikum Halle für die freundliche Zusammenarbeit und für die Durchführung der Xenotransplantatversuche. Auch Herrn Prof. Hüttelmaier, dem Direktor des Instituts für molekulare Medizin der medizinischen Fakultät der Martin-Luther-Universität Halle-Wittenberg, gilt mein Dank, dass ich die photometrischen Messungen in seiner Arbeitsgruppe molekulare Zellbiologie durchführen durfte. Ebenso danke ich Herrn Prof. Wienke, dem stellvertretenden Direktor des Instituts für medizinische Epidemiologie, Biometrie und Informatik der medizinischen Fakultät der Martin-Luther-Universität Halle-Wittenberg, für seine überaus hilfreiche Beratung und Durchsicht bezüglich der statistischen Auswertung.

Die Arbeit im Labor war eine sehr schöne Zeit, an die ich mich sehr gern zurückerinnere und an deren angenehmen Atmosphäre die gesamte Arbeitsgruppe einen großen Anteil hatte. Also vielen Dank an Frau Mandy Bühnemann, Frau Dr. Ilka Böhme, Herrn Dr. Tobias Gruber, Frau Dr. Katharina Mandel, Herrn Dr. Terumasa Sowa und Frau Dr. Guadalupe Soledad Lopez Alvarez.

Im Rahmen des halleschen Promotionskollegs Medizin (HaPKoM) standen mir eine Vielzahl an hilfreichen und interessanten Veranstaltungen zur Verfügung. Also auch vielen Dank an die Organisatoren des HaPKoM.

Nicht zuletzt danke ich meinen Eltern und Geschwistern für die liebevolle Unterstützung, sowie meiner Großmama, Helga Trusch, und meiner Frau, Luisa Klose, zusätzlich für die sprachliche und grammatikalische Durchsicht meiner Arbeit.

Erklärung über frühere Promotionsversuche und Selbstständigkeitserklärung mit Unterschrift

Erklärungen

(1) Ich erkläre, dass ich mich an keiner anderen Hochschule einem Promotionsverfahren unterzogen bzw. eine Promotion begonnen habe.

(2) Ich erkläre, die Angaben wahrheitsgemäß gemacht und die wissenschaftliche Arbeit an keiner anderen wissenschaftlichen Einrichtung zur Erlangung eines akademischen Grades eingereicht zu haben.

(3) Ich erkläre an Eides statt, dass ich die Arbeit selbstständig und ohne fremde Hilfe verfasst habe. Alle Regeln der guten wissenschaftlichen Praxis wurden eingehalten; es wurden keine anderen als die von mir angegebenen Quellen und Hilfsmittel benutzt und die den benutzten Werken wörtlich oder inhaltlich entnommenen Stellen als solche kenntlich gemacht.

Datum, Unterschrift